

**CONTROLS ON SEDIMENT GENERATION FROM  
FOREST ROADS IN A PACIFIC MARITIME WATERSHED**

by

Elizabeth Baird  
BSc, Simon Fraser University, 2008

THESIS SUBMITTED IN PARTIAL FULFILLMENT OF  
THE REQUIREMENTS FOR THE DEGREE OF

MASTER OF SCIENCE

In the  
Faculty of Environment

© Elizabeth Baird 2011

SIMON FRASER UNIVERSITY

Spring 2011

All rights reserved. However, in accordance with the *Copyright Act of Canada*, this work may be reproduced, without authorization, under the conditions for *Fair Dealing*. Therefore, limited reproduction of this work for the purposes of private study, research, criticism, review and news reporting is likely to be in accordance with the law, particularly if cited appropriately.

# APPROVAL

**Name:** Elizabeth Baird  
**Degree:** Master of Science  
**Title of Thesis:** Controls on sediment generation from forest roads in a Pacific Maritime watershed

**Examining Committee:**

**Chair:** Margaret Schmidt  
Associate Professor, Department of Geography

---

**Ilja van Meerveld**  
Senior Supervisor  
Assistant Professor, Department of Geography

---

**Jeremy Venditti**  
Supervisor  
Assistant Professor, Department of Geography

---

**R. Dan Moore**  
External Examiner  
Professor, Department of Geography  
University of British Columbia

**Date Defended/Approved:** April 21, 2011



SIMON FRASER UNIVERSITY  
LIBRARY

## Declaration of Partial Copyright Licence

The author, whose copyright is declared on the title page of this work, has granted to Simon Fraser University the right to lend this thesis, project or extended essay to users of the Simon Fraser University Library, and to make partial or single copies only for such users or in response to a request from the library of any other university, or other educational institution, on its own behalf or for one of its users.

The author has further granted permission to Simon Fraser University to keep or make a digital copy for use in its circulating collection (currently available to the public at the "Institutional Repository" link of the SFU Library website <[www.lib.sfu.ca](http://www.lib.sfu.ca)> at: <<http://ir.lib.sfu.ca/handle/1892/112>>) and, without changing the content, to translate the thesis/project or extended essays, if technically possible, to any medium or format for the purpose of preservation of the digital work.

The author has further agreed that permission for multiple copying of this work for scholarly purposes may be granted by either the author or the Dean of Graduate Studies.

It is understood that copying or publication of this work for financial gain shall not be allowed without the author's written permission.

Permission for public performance, or limited permission for private scholarly use, of any multimedia materials forming part of this work, may have been granted by the author. This information may be found on the separately catalogued multimedia material and in the signed Partial Copyright Licence.

While licensing SFU to permit the above uses, the author retains copyright in the thesis, project or extended essays, including the right to change the work for subsequent purposes, including editing and publishing the work in whole or in part, and licensing other parties, as the author may desire.

The original Partial Copyright Licence attesting to these terms, and signed by this author, may be found in the original bound copy of this work, retained in the Simon Fraser University Archive.

Simon Fraser University Library  
Burnaby, BC, Canada

## **ABSTRACT**

Twenty four large scale rainfall simulation experiments were completed on the Queen Charlotte Mainline Forest Road South, Haida Gwaii, BC, in order to determine the controls on sediment production from forest roads. Precipitation intensity was the dominant control on the amount of sediment produced from the road section; antecedent precipitation conditions and truck speed were not important. For most experiments only a small fraction of sediment (<30%) was directly caused by traffic. The results of seven small scale experiments revealed that the amount of sediment produced by a road section varied spatially. Turbidity measurements along the Honna River showed that sediment concentrations decreased and sediment fluxes either remained constant or decreased at locations progressively down-stream, suggesting the main sediment sources are located in higher reaches in the watershed and that sediment plumes are diluted further downstream. The contribution from forest roads to the total sediment flux was ~10%.

**Keywords:** Haida Gwaii; forest roads; sediment; turbidity; rainfall simulations; water quality

## **ACKNOWLEDGEMENTS**

I would like to thank the many people and organizations that supported this project. Thank you to BC Ministry of Forest and Range for providing equipment and extensive in kind-support, I would like to thank Bill Floyd, Research Hydrologist, and Larry Duke, Engineering Officer, in particular for their personal support and involvement with the project. I would like to acknowledge Island Timberlands, BC Timber Sales and the Village of Queen Charlotte for providing funds towards a MITACS BC internship and NSERC for additional funding through a Discovery grant. Senninger Irrigation Inc. and the Burnaby Fire Department generously donated equipment used in the construction of the rainfall simulator.

I would like to thank Ilja Tromp-van Meerveld for her guidance, encouragement and assistance throughout the project, as well as her numerous edits of this document. I would also like to apologize for any and all injuries obtained while helping me with my fieldwork. It was a great experience working with you.

Thank you also to the resource and tech. support team in the Department of Geography; all site location maps were produced by John Ng.

I would finally like to thank my family who helped and supported me throughout this project. You were are all wonderful and I couldn't have done it without you.

# TABLE OF CONTENTS

Approval.....	ii
Abstract .....	iii
Acknowledgements .....	iv
Table of Contents.....	v
List of Figures .....	vii
List of Tables.....	x
<b>1 INTRODUCTION .....</b>	<b>1</b>
1.1 Problem statement .....	1
1.2 Background.....	2
1.2.1 Sediment generation from forest roads.....	2
1.2.2 Controls on sediment generation from forest roads.....	8
1.2.3 Moving sediment to streams.....	13
1.2.4 Effects of sediment on streams and water quality .....	13
1.2.5 Potential management techniques .....	16
1.3 Research questions and hypotheses .....	18
1.4 Study Site .....	19
<b>2 RAINFALL SIMULATIONS .....</b>	<b>25</b>
2.1 Introduction.....	25
2.2 Study Sites.....	27
2.3 Methods.....	30
2.3.1 Sprinkler design.....	30
2.3.2 Sediment concentrations.....	47
2.3.3 Splash .....	47
2.3.4 Traffic.....	49
2.3.5 Data Analysis .....	49
2.4 Results and discussion.....	63
2.4.1 Non-truck related sediment mass .....	63
2.4.2 Mass due to traffic .....	69
2.4.3 Total mass .....	76
2.4.4 Ditchflow measurements .....	81

2.4.5	Small scale results .....	85
<b>2.5</b>	<b>Conclusions .....</b>	<b>86</b>
<b>3</b>	<b>TURBIDITY MONITORING .....</b>	<b>89</b>
<b>3.1</b>	<b>Introduction .....</b>	<b>89</b>
<b>3.2</b>	<b>Study Site .....</b>	<b>91</b>
<b>3.3</b>	<b>Methods.....</b>	<b>91</b>
3.3.1	Turbidity measurements .....	91
3.3.2	Discharge measurements .....	99
3.3.3	Turbidity data processing .....	104
3.3.4	Data analysis .....	105
<b>3.4</b>	<b>Results and discussion.....</b>	<b>106</b>
3.4.1	Turbidity exceedance graphs .....	106
3.4.2	Individual turbidity events.....	112
3.4.3	Estimated monthly sediment fluxes.....	114
3.4.4	Multiple linear regression.....	129
<b>3.5</b>	<b>Conclusions .....</b>	<b>131</b>
<b>4</b>	<b>SEDIMENT VOLUME .....</b>	<b>133</b>
<b>4.1</b>	<b>Introduction.....</b>	<b>133</b>
<b>4.2</b>	<b>Methods.....</b>	<b>133</b>
4.2.1	Road derived sediment .....	138
<b>4.3</b>	<b>Results and discussion.....</b>	<b>139</b>
4.3.1	WQEE Results.....	139
4.3.2	Total road derived sediment .....	141
4.3.3	Comparison to measured sediment flux in the Honna River .....	142
<b>4.4</b>	<b>Conclusions .....</b>	<b>145</b>
<b>5</b>	<b>SUMMARY AND CONCLUSIONS .....</b>	<b>146</b>
<b>5.1</b>	<b>Rainfall Simulation .....</b>	<b>146</b>
<b>5.2</b>	<b>River Monitoring.....</b>	<b>147</b>
<b>5.3</b>	<b>Total road derived sediment volume .....</b>	<b>148</b>
	<b>Works Cited .....</b>	<b>150</b>

## LIST OF FIGURES

Figure 1.1	A forest road prism showing the cut-slope, road surface and fill-slope with a ditch along one side.....	3
Figure 1.2	The location of the Honna Watershed in relation to the Village of Queen Charlotte and Sandspit.....	20
Figure 1.3	Climate normals (1971 - 2000) for Sandspit (data from Environment Canada <a href="http://www.climate.weatheroffice.gc.ca/climate_normals/index_e.html">http://www.climate.weatheroffice.gc.ca/climate_normals/index_e.html</a> ) and measured precipitation in the Honna Watershed from September 2009 to June 2010 .....	22
Figure 1.4	Measured cumulative precipitation in the Honna Watershed between August 1 <sup>st</sup> 2009 and July 1 <sup>st</sup> 2010. For the location of the two rain gauges see Figure 1.2.....	23
Figure 2.1	Location of large and small scale rainfall simulation trials .....	28
Figure 2.2	Road profile at the location of the large scale rainfall simulation trials .....	29
Figure 2.3	Intensity-duration-frequency graph for precipitation in the Honna Watershed based on precipitation data from 1990-2002 with frequent data gaps, and SandspitA based precipitation data from 1972-2004 (reviewed and adjusted by Environment Canada) .....	32
Figure 2.4	Plan view of large scale sprinkler apparatus .....	35
Figure 2.5	Oblique view of the large scale sprinkler set up.....	36
Figure 2.6	Small scale sprinkler set up .....	37
Figure 2.7	Inferred sprinkler intensity across the road. The sprinkler rainfall intensity along the midway and beside sprinkler transects is given in Figure 2.8 .....	40
Figure 2.8	Comparison of the measured and inferred sprinkler intensity as a function of distance across the road for nozzle 6. See Figure 2.7 for the location of the transects for which the sprinkler intensities were inferred .....	41
Figure 2.9	Drop size distribution of natural and simulated precipitation based on drop diameter (a) and drop volume (b).....	42
Figure 2.10	Gutter flow rates for the large scale trials. The equations describe the outflow rate during the first 30, 10, and 5 minutes of trials using nozzle 6, 11, and 22 respectively .....	45
Figure 2.11	Small scale experiment flow rates .....	47
Figure 2.12	Blue dye splashed from a water filled pothole is carried mainly down the road by tires. Lateral splash is mainly within 2.0 m of the pothole.....	48
Figure 2.13	Sediment concentrations in the gutter outflow during low intensity trials. The times that a loaded logging truck passed the site are indicated by a star. The equation represents the best fit line for the background concentrations.....	51
Figure 2.14	Sediment concentrations in the gutter and weir outflow during medium intensity trials. The times that a loaded logging truck passed the site are indicated by a star. The equation represents the best fit line for the background concentrations.....	54



Figure 2.15	Sediment concentrations in the gutter and weir outflow during high intensity trials. The times that a loaded logging truck passed the site are indicated by a star. The equation represents the best fit line for the background concentrations.....	56
Figure 2.16	Sediment concentrations during small scale trials. The equation represents the best fit line for the background concentrations .....	58
Figure 2.17	The relations between total background mass and trial duration for the large scale trials. None of the relations are significant at the 95% confidence interval. Error bars represent the maximum possible error .....	65
Figure 2.18	Clockwise hysteretic relation between flow rate and background sediment concentration..	66
Figure 2.19	The relation between background mass ( $M_B$ ) and precipitation intensity (I) for the large scale trials. Functional analysis relations are shown by the dashed lines while linear regression relations are shown by the solid lines.....	67
Figure 2.20	The relation between background mass and ( $M_B$ ) precipitation (P) for the large scale trials. Functional analysis relations are shown by the dashed lines while linear regression relations are shown by the solid lines .....	67
Figure 2.21	The relation between steady state gutter outflow ( $F$ ) and total non-truck related mass ( $M_B$ ) generated during a large scale trial. The functional analysis relation is shown by a dashed line while the linear regression relation is shown by a solid line .....	70
Figure 2.22	The relation between steady state gutter outflow ( $F$ ) and steady state sediment concentration ( $C$ ) during large scale trials. The functional analysis relation is shown by a dashed line while the linear regression relation is shown by a solid line .....	70
Figure 2.23	Total background mass during large scale trials as a function of the antecedent precipitation index (API). None of the relations are significant at the 95% confidence interval .....	71
Figure 2.24	First hour background mass during large scale trials as a function of the antecedent precipitation index (API). None of the relations are significant at the 95% confidence interval.....	72
Figure 2.25	The relation between antecedent traffic intensity and the mass of background sediment generated in the first hour of a large scale trial. Only nozzle 11 trials are significant at the 95% confidence interval .....	73
Figure 2.26	The relation between mass due to traffic and number of truck passages during a trial. None of the relations are significant at the 95% confidence interval.....	77
Figure 2.27	The relation between mass per truck (m) and precipitation intensity (I) .....	77
Figure 2.28	The relation between sediment mass due to a truck passage and time in the trial. The relations are significant at the 95% confidence interval for nozzle 6 trials only .....	78
Figure 2.29	The relation between mass per truck passage and truck speed. None of the relations are significant at the 95% confidence interval .....	78
Figure 2.30	Mass of sediment generated by the first truck passage during a trial compared to 3, 5 and 10 day antecedent precipitation indexes. None of the relations are significant at the 95% confidence interval .....	79
Figure 2.31	The relation between total sediment mass (M) generated during a trial and precipitation intensity (I) and depth (P). Functional analysis relations are shown by the dashed lines while linear regression relations are shown by the solid lines.....	82
Figure 2.32	The relation between total sediment mass generated during a trial and number of truck passages. None of the relations are significant at the 95% confidence interval .....	82
Figure 2.33	The relation between antecedent traffic and the total sediment mass generated during a large scale trial. Only nozzle 11 trials are significant at the 95% confidence interval .....	83

Figure 2.34	The relation between the total mass of sediment and precipitation intensity for the small scale trials. The relation is not significant at the 95% confidence interval.....	85
Figure 2.35	The relation between the total mass of sediment and precipitation depth for the small scale trials. The relation is not significant at the 95% confidence interval.....	86
Figure 2.36	The relation between the total mass of sediment and road surface slope for the small scale trials. The relation is not significant at the 95% confidence interval.....	86
Figure 3.1	Location of turbidity monitoring equipment .....	92
Figure 3.2	Turbidity monitoring sites showing the location of the equipment .....	93
Figure 3.3	Turbidity-suspended sediment concentration relation for the portable turbidity probe.....	98
Figure 3.4	Rating curves for the water level recorders installed in the lower reach of the Honna River and the Honna North West and the Environment Canada gauging station rating curve.....	100
Figure 3.5	Contributing area-discharge relation for the Honna Watershed .....	100
Figure 3.6	Relation between instantaneous discharge derived from the depth-averaged-velocity equation ( $Q_{\text{Wolman}}$ ) and the contributing area-discharge relation ( $Q_{\text{area}}$ ) (top) and between the rating curve based discharge ( $Q_{\text{rating}}$ ) and the contributing area and depth-averaged-velocity based discharge (bottom).....	103
Figure 3.7	Summary of the percent time a certain turbidity value was exceeded at the Drinking Water Intake.....	107
Figure 3.8	Summary of the percent time a specific turbidity value was exceeded in Tributary 1 upstream and downstream of the road crossing.....	108
Figure 3.9	Turbidity exceedance graphs.....	110
Figure 3.10	August 27, 2009 event.....	115
Figure 3.11	Clockwise hysteretic relation between suspended sediment concentration and discharge.....	126
Figure 3.12	Suspended sediment mass fluxes.....	128
Figure 3.13	Observed and predicted peak turbidity values.....	131
Figure 4.1	Sample photos of WQEE assessment at Site 33 .....	136
Figure 4.2	Locations of stream crossings assessed in the Honna Watershed with the hazard score (size of circle) representing the predicted amount of sediment contributed to nearby streams ..	137
Figure 4.3	WQEE hazard ratings for stream crossings of the QC Mainline between km 3 and km 10, assessed in October 2009 .....	140
Figure 4.4	Sediment laden road surface runoff passing through ditch blocks along the Queen Charlotte Mainline Forest Road South.....	140
Figure 4.5	Comparison of WQEE and rainfall simulation (RS) based yearly sediment yield estimates .....	142

## LIST OF TABLES

Table 1.1	Studies showing controls on and sources of sediment generated from forest roads .....	8
Table 1.2	Studies, using various methods, which measured sediment from forest roads.....	9
Table 2.1	Overview of the large scale rainfall simulation trials .....	26
Table 2.2	Overview of the small scale rainfall simulation trials .....	27
Table 2.3	Measured drop size distribution statistics.....	43
Table 2.4	Published median drop diameters for natural precipitation .....	43
Table 2.5	Overview of the calculated background mass and mass from traffic for the large scale trials .....	62
Table 3.1	Overview of turbidity monitoring data .....	90
Table 3.2	Linear regression relations between portable and deployed turbidity probe measurements.	97
Table 3.3	Percent of time specific turbidity values were exceeded.....	109
Table 4.1	Total fine sediment generation hazard rating (independent of stream size) .....	134
Table 4.2	Sample form showing required WQEE data gathered for a road crossing .....	135
Table 4.3	Total sediment derived from the road surface for all crossings between km 3 and km 10.	143
Table 4.4	Total road derived sediment reaching the Honna River .....	145

# 1 INTRODUCTION

## 1.1 *Problem statement*

Forest roads have the potential to produce large amounts of sediment (Luce and Black, 1999; Luce and Black, 2001; Reid and Dunne, 1984). In some instances forest roads have been shown to supply the majority of sediment to streams in forested areas (Reid and Dunne, 1984), especially in areas where mass failures are infrequent (Bilby et al., 1989). Roads can serve as chronic sources of sediment in coastal watersheds (Floyd, 2008). In fact soil disturbance and associated erosion is considered the most important effect of road building in forested regions (Spinelli and Marchi, 1996). Sediment generated from forest roads can impact aquatic ecology and water quality, including drinking water quality, in nearby streams (Ramos-Scharron and MacDonald, 2007). Degradation of stream ecology and water quality due to sediment from forest roads is the most studied effect of road building in forested areas, with the majority of studies focusing on temperate forests (Spinelli and Marchi, 1996). However, current datasets, literature and models addressing road hydrology are restricted to a few study sites. We therefore still do not understand sediment production from forest roads very well. Watersheds containing forest roads whose aquatic ecology is particularly important or whose streams are being developed as drinking water sources, such as the Honna River on Graham Island, Haida Gwaii, British Columbia, the site of this study, will benefit from a better understanding of the specific local controls on sediment generation from forest roads. This project aimed to provide a better understanding of the timing and triggers of sediment production from forest roads in the Honna River watershed and the factors that control it. The influence of rainfall intensity, rainfall amount, rainfall duration and road

use intensity on sediment production was studied through controlled experiments using a large mobile rainfall simulator. Turbidity was monitored continuously upstream and downstream of two road crossings and at several locations along the Honna River to determine sediment transport under natural rainfall conditions. The roads and streams were surveyed to determine their connectivity and identify areas with high potential to produce sediment. Multiple linear regression was used to predict sediment production from forest roads in the Honna Watershed. Since the Honna River is currently being developed as a drinking water source for the Village of Queen Charlotte, this study also comments on the effectiveness of road management techniques to improve water quality in this watershed.

## **1.2 Background**

### **1.2.1 Sediment generation from forest roads**

A forest road prism generally consists of a cut-slope, road surface, and fill-slope with ditches along one or both sides (Figure 1.1). Road surfaces are covered with aggregate material and are out-sloped, in-sloped or crown-sloped in order to direct water towards ditches. Cross drains collect water running along the road surface and transfer in-slope ditch water to out-slope ditches. Berms and ditches can be used to route and collect water before it becomes highly erodible.

In order to understand what factors control sediment generation from forest roads, we must understand the factors that influence the ability to move sediment from roads, potential sources of sediment, and sediment availability; areas that actively contribute sediment to the stream channel network need to be specified in order to successfully

manage sediment (Croke et al., 2005). While sediment may be derived from many sources and several factors affect sediment availability, in temperate forests overland flow is mainly responsible for erosion of forest road material. The ability to transport sediment from a road segment, therefore, depends on the amount and distribution of overland flow, which depends on rainfall characteristics as well as road attributes (Bilby et al., 1989).

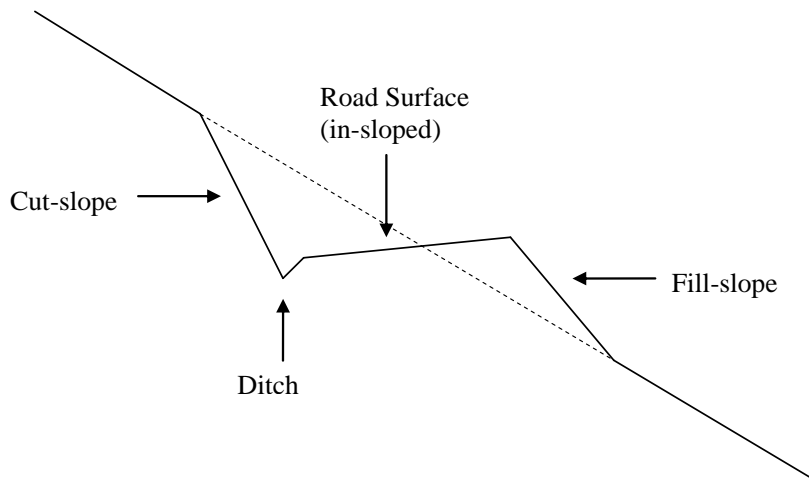


**Figure 1.1 A forest road prism showing the cut-slope, road surface and fill-slope with a ditch along one side**

Forest roads change natural drainage patterns by altering the amount and distribution of overland flow (Croke et al., 2005). During initial road construction vegetation is removed from the road prism, the underlying soil is disturbed and loosened, and preferential flow pathways may develop (Spinelli and Marchi, 1996). Vegetation removal exposes soil to erosive precipitation and flow; loosened soil is more easily eroded, and preferential flow paths concentrate run-off, increasing its ability to entrain and transport sediment. Following construction, infiltration capacities of forest roads are generally lower than those of the surrounding landscape (Spinelli and Marchi, 1996).

Forest road surface infiltration capacities have been estimated to be as low as 0.1 to 0.8 mm/h, much lower than most rainfall intensities during moderate storms (Reid and Dunne, 1984). Reduced infiltration capacities cause infiltration excess overland flow on forest roads even for low intensity storms (Croke et al., 2005). Forest roads can also intercept subsurface flow and redirect it overland (Spinelli and Marchi, 1996). Increased amounts of overland flow can lead to increased erosion from road surfaces, cut-slopes, fill-slopes and/or along ditches depending on flow pathways and sediment availability (Spinelli and Marchi, 1996). Altered overland flow pathways can also lead to changes in nearby stream channel networks through adjustment of road-stream connectivity (Croke et al., 2005). For example, concentrated overland flow draining onto the forest floor may instigate the development of small channels and gullies transporting run-off quickly to streams creating flashier stream responses (Croke et al., 2005).

The potential sediment sources in a forest road prism include the road surface, cut-slopes, fill-slopes, and/or ditches (Spinelli and Marchi, 1996). Potential controls on the amount of sediment available from cut-slopes, fill-slopes and ditches are soil texture, vegetative cover, road maintenance, and gradient. Silty soils produce the highest amount of sediment as silt is most easily dislodged and transported by overland flow. Larger particles (sand sized) are eroded at a slower rate than finer particles (silt sized) as they are moved in traction and saltation, while finer particles are carried in suspension by overland flow. However, very fine soils with high clay content are less erodible due to particle aggregation (Luce and Black, 1999). If large particles (> 2 mm) are present on the cut-slope, fill-slope or ditches, an armor layer may develop which can reduce the amount of sediment available for erosion. The presence of vegetation on cut-slopes and

fill-slopes as well as in ditches also greatly reduces the amount of coarse sediment available for erosion. The effects of vegetation on availability of finer sediment, however, are not as well documented (Luce and Black, 1999).

Road maintenance along cut-slopes and fill-slopes is often not essential. However, cleaning ditches is often necessary. Removal of vegetation and disturbance of soil and armor layers following road maintenance generally leads to a temporary increase in the amount of sediment available for erosion (Luce and Black, 2001). Arnáez et al. (2004) found the cut-slope had the largest erosion rate and cut-slope gradient had the largest control on sediment generation from a road prism. This was attributed to mass wasting and freeze-thaw processes along the cut-banks continuously supplying loose material for transport. In addition gradient, plant cover density, and stone cover density of the cut-slope area also controlled erosion rates. Road usage in this study area, however, was considered low, and was dominated by light vehicles (not logging trucks). Runoff coefficients were also higher on the cut-slope than the road surface or fill-slope, which is often not the case. Where off-road sediment sources were generally coarse grained, Reid and Dunne (1984) found the cut slope, fill slope, and ditches contributed a small amount of sediment compared to the road surface. However, texture of the road surface also affected this relation. Although some roads have been shown to generate the majority of their sediment from the cut-slope, fill-slope and/or ditches, this project focused on sediment generated directly from the road surface, not other portions of the road prism.

Forest roads in the Honna Watershed have cut-slopes and fill-slopes that are short and have a low gradient. The ditches are well maintained and vegetated, preventing these features from being a significant source of sediment to nearby streams. Visual



observations prior to this study also suggested the main source of sediment from the road prisms in the Honna Watershed was the road surface (Bill Floyd, Ministry of Forest and Range, Personal Communication).

Controls on the amount of sediment available from forest road surfaces are related to surface type, surface dimensions, surface gradients, and traffic density (Akay et al., 2008). Similar to cut-slopes, fill-slopes and ditches, the texture of the material on the road surface strongly affects sediment yields. Coarser surfaces generally produce much less sediment than finer surfaces and larger particles can form an armoring layer (Luce and Black, 1999). Longer road segments tend to yield more sediment as they have a greater sediment supply to draw on and concentrate more water, while steeper road segments can transport larger particles due to increased flow energy, leading to greater sediment yields (Bilby et al., 1989).

Traffic can impact the amount of sediment produced from a forest road in many ways. Fine sediment on road surfaces is generally derived from the breakdown of surface material as vehicles pass and/or the forcing upward of fine-grained sediment from the road bed as traffic pushes the surface material into the bed (Reid and Dunne, 1984). Fine sediment derived from truck crushing reduces the infiltration capacity of the road surface, leading to augmented overland flow and increased erosion. Traffic also causes cross-slope flattening, which directs water down the road surface slightly as it travels to side ditches, causing the distance required for water to flow off the road to increase and create more opportunity for erosion (Foltz, 1996). Roads with high traffic intensity or those whose surfaces are not well maintained may progress from cross-slope flattening to rut

development. Overland flow concentrated in ruts will have a higher shear stress giving it more ability to erode and carry sediment, augmenting erosion (Foltz, 1996).

The type of material on a road surface also affects sediment generation. Improving aggregate quality can decrease the formation of cross-slope flattening and rutting. Good quality aggregate can also resist crushing by traffic, limiting the amount of sediment available for transport (Rodgers et al., 2009; Foltz, 1996). Roads with marginal quality aggregate require more frequent maintenance, resulting in the disturbance of armor layers and increased erosion (Foltz, 1996). The importance of aggregate quality has been shown to increase as traffic and rainfall increases (Foltz, 1996). Good quality aggregate, however, is not always locally available and high transport costs often make importing higher quality aggregate uneconomic.

As discussed above, different processes have been deemed important in controlling erosion and sediment availability in each section of the road prism and many of these processes are likely acting simultaneously but to different degrees. Although the above relations have been shown empirically (Table 1.1) and empirical models predicting soil loss have been developed (e.g. the Universal Soil Loss Equation), physically based models are not well developed and tend to be highly parameterized, making it difficult to apply them in unstudied areas. We therefore still do not understand sediment generation from forest roads very well and cannot predict sediment yield from forest roads in unstudied watersheds with adequate certainty. The many different combinations of potential factors controlling sediment generation from forest roads result in large variations in sediment yield between road segments, even within the same watershed. It may be possible, therefore, to substantially reduce sediment generation from forest roads

by targeting the few sections with the greatest sediment production (Luce and Black, 1999) and greatest connectivity with nearby streams (Section 1.2.3).

<b>Author</b>	<b>Year</b>	<b>Area of greatest erosion</b>	<b>Major controls</b>
Amann	2004	Entire prism	Total runoff volume
Arnaez et al.	2004	Cut-slope	-
Bilby et al.	1989	-	Traffic (number of axles since the last storm)
Croke et al.	2006	Road surface	Road usage and traffic intensity
Fahey and Coker	1992	Road surface	-
Luce and Black	2001	Ditch	Time since ditch grading
Reid and Dunne	1984	Road surface	Traffic intensity

## **1.2.2 Controls on sediment generation from forest roads**

Pioneering work on quantifying sediment generated from forest roads was done by Reid and Dunne in 1984. Since then, several studies, using various methods, have been completed on the subject (Table 1.2). Despite the increasing number of studies, there is no agreement on the dominant controls and physical processes affecting the amount of sediment generated from forest roads (Luce, 2002).

### **1.2.2.1 Rainfall amount and intensity**

In theory, precipitation intensity and amount determine the sediment transport capacity of road prism runoff (Bilby et al., 1989). Reid and Dunne (1984), however, found only a poor relation between sediment concentration and ditch discharge, which was assumed to be a measure of precipitation intensity and amount. Croke et al. (2006) did not find a significant relation between sediment concentration in road surface runoff samples and rainfall intensity. Amann (2004) compared road and hydrologic variables with total sediment production from forest road segments and found hill-slope gradient

and cut-slope height did not yield significant correlations with total sediment production unless total runoff volume was also considered. However, precipitation amount was not a significant variable in itself. In all of these studies the road surface was the dominant supplier of sediment.

<b>Author</b>	<b>Date</b>	<b>Location</b>	<b>Type of Study</b>	<b>Duration of study</b>
Akay et al.	2008	Kahramanmaras, Turkey	GIS Models and observational studies	Annual sediment yields
Amann	2004	Oregon, USA	Natural rainfall	Four runoff producing storms
Arnáez et al.	2003	Northeastern Spain	Simulated rainfall	28 simulations
Beschta	1978	Oregon Coast Range, USA	Paired catchment	15 years
Bilby	1985	Western Washington, USA	Stream monitoring	2 years
Bilby et al.	1989	Western Washington, USA	Stream and traffic monitoring	2 years
Croke et al.	2006	Southeaster New South Wales, Australia	Large scale simulated rainfall	Hours
Fahey and Coker	1992	Eastern Marlborough Sounds, New Zealand	Runoff plots, natural rainfall	2 to 3 years
Foltz	1996	Oregon, USA	Runoff plots, natural rainfall	Winter months for 4 years
Jordán and Martínez-Zavala	2008	Southern Spain	Runoff plots, simulated rainfall	30 simulations
Luce and Black	1999	Western Oregon, USA	74 plots, natural rainfall	Variable
Ramos-Scharrón and MacDonald	2007	St John, US Virgin Islands	Runoff plots and stream suspended sediment concentrations	8 months
Reid and Dunne	1984	Washington, USA	Road culvert suspended sediment, natural rainfall	1 year
Sheridan et al.	2006	Victoria, Australia	Road culvert suspended sediment, natural rainfall	1 year
Sheridan et al.	2008	Victoria, Australia	Runoff plots, small scale simulated rainfall and monitoring	1 year

Bilby et al. (1989) suggest precipitation variables, including total precipitation, may not be significantly related to sediment concentrations due to the supply-limited nature of appropriate sized sediment, which is more likely true for the road surface than other areas of the road prism. Perhaps the extremely low infiltration capacities of forest road surfaces allows most storms to be equally capable of producing overland flow, and sediment supply issues outweigh variations in storm intensity and duration, suggesting the amount of overland flow is rarely a limiting factor. In areas where precipitation events are generally of low intensity, rainfall duration and intensity could have a more prominent role in controlling the amount of sediment generated from forest roads than at previously studied sites.

During individual precipitation events, soil erosion and sediment concentrations are greatest near the beginning of storms (Hairsine and Rose, 1992). Arnáez et al. (2004) found sediment concentrations were greatly reduced after the first few minutes of precipitation due to the exhaustion of loose surface material available for erosion and the development of a thin layer of flow that protected against splash, similar to erosion from bare soils (Proffitt and Rose, 1991).

### **1.2.2.2 Traffic**

Several studies have shown a strong relation between traffic volume or intensity and sediment generated from forest roads. For example, Reid and Dunne (1984) found road use explained 68% of the variance in forest road erosion, while Croke et al. (2005) found 95% of the variation in sediment concentration was accounted for by road use alone. Bilby et al. (1989) found the total number of axles since the last storm, total axles during the storm, and time since ditch flow began were the variables most related to

sediment concentrations in ditch flow. However, under extremely heavy traffic (>100 axles/day) this relation broke down and the variables became independent. The deterioration of this relation was explained as the result of accumulated fine sediments buffering the road surface from further abrasion and sediment production (Bilby et al., 1989). Although these studies present a range of empirical relations, no physical processes were quantified or calibrated.

Luce and Black (2001) found the effects of traffic on sediment yield during precipitation events persisted on a time scale of tens of minutes following truck passage. Although longer term observations suggest effects may persist for longer time periods, no other studies have looked at this. Bilby et al. (1989) suggested that traffic during dry weather, not just during precipitation events, is responsible for creating sediment eroded from road surfaces, and that construction techniques and the type of road surfacing material can influence the amount of sediment each road segment produces in response to traffic. Fransen et al. (2001) suggested variations in permeability affect sediment yield based on observations of highly permeable schist and rhyolite pumice roads producing an order of magnitude less sediment than roads constructed of compacted granite with low permeability. If road surface material and buffering effects influence the amount of sediment eroded from a road surface, then relations derived from one watershed may not be easily applied to another road section even if they have similar climate and vegetation. Therefore, it is possible that sediment yield will be significantly different in the Honna River watershed compared to other watersheds in the Pacific North-West.

### **1.2.2.3 Road construction and maintenance**

Akay et al. (2008) found forest roads produced the largest amount of sediment during the first two years following their construction. The decline in sediment generation following construction was attributed to the re-establishment of vegetative cover along the cut-slope, fill-slope, and ditch area which reduced the amount of sediment available for erosion. Road maintenance, which is necessary to keep conditions suitable for travel and prevent failure of drainage systems resulting in severe erosion, can create road conditions similar to those following initial construction (Fahey and Coker, 1992; Luce and Black, 2001). Luce and Black (1999) found cleaning ditches and removal of cut-slope vegetation dramatically increased sediment production from the road prism. They also found grading only the road surface did not always produce an increase in sediment yield, while grading of the ditch, cut slope and road surface substantially increased sediment yields for up to three years. Recovery following ditch grading was mainly attributed to re-armoring versus re-vegetating of the ditch and fill-slope. The majority of sediment in their study catchment, however, was derived from the cut-slope and fill-slope, not from the road surface itself, which is not always the case. Thus construction and maintenance practices may have different effects in other watersheds especially those that derive most of their sediment from the road surface.

The above findings suggest specific features of the road, including age, maintenance schedule, and material type and texture of the entire prism all play a role in determining how much sediment will be produced for a given rainfall event. Any study trying to understand sediment generation from forest roads should therefore consider all these aspects. However, due to time constraints, this study did not look at the effects of road maintenance.

### **1.2.3 Moving sediment to streams**

Connectivity between a road and nearby streams is a measure of the probability that runoff from a specific source area will reach the stream edge (Croke et al., 2005); not all sediment generated from a forest road will reach nearby streams. Areas that actively contribute sediment to the stream channel network need to be specified in order to successfully manage sediment (Croke et al., 2005). Once sediment is generated from a forest road, it can be carried by flow in either a dispersive or advective (channelized) pathway. Advective pathways are generally associated with culvert pipes while dispersive pathways are associated with miter drains and push outs. Overland flow traveling in channel systems has little opportunity to deposit finer grained sediment (carried as wash load), while dispersive pathways may provide conditions allowing deposition. Most fine sediments are carried as washload until flow infiltrates into the soil (Croke et al., 2005). Flow traveling in a dispersive pathway is more likely to infiltrate prior to reaching a nearby stream, as advective pathways generally travel 2 to 3 times further from the road prism prior to infiltration (Croke et al., 2005). Roads closer to nearby streams are more likely to have highly connected flow paths as there is less distance over which flow can infiltrate and deposit sediment (Bilby et al., 1989). There is currently, however, a gap in understanding changes in sediment fluxes as runoff moves across the landscape to streams (Croke et al., 2005).

### **1.2.4 Effects of sediment on streams and water quality**

The effect of road derived sediment on nearby streams is largely dependent on whether sediment is deposited on the stream bed or carried in suspension (Bilby et al., 1989). The probability that sediment is deposited on a stream bed is dependent on the



local shear stress divergence, influenced by particle size, flow rate at the time the sediment enters the stream, and the hydraulic properties of the channel (Bilby, 1985). Road derived sediment entering small tributary streams is often filtered and partially deposited before reaching larger rivers (Bilby et al., 1989); coarser sediments (sand sized and larger) are preferentially stored in small tributaries, especially in tributaries heavily loaded with woody debris. In fact, storage of more than 50% of road derived sediment is expected in small tributaries in some watersheds during normal precipitation events (Bilby et al., 1989). Increased sediment deposition in streams can infiltrate and cover existing river bed habitat, reduce suitable areas for organism growth, and alter invertebrate populations (Beschta, 1978; Ramos-Scharron and MacDonald, 2007). For example, increased sedimentation in small mountain streams may clog gravel used as fish spawning areas and reduce survival rates following spawning (Phillips et al., 1975; Beschta, 1978; Tappel and Bjornn, 1983). Preferred salmon spawning gravels, however, tend to be located at the top of riffles in areas of the stream with relatively high flow velocities. Sediment derived from nearby roads tends to be too fine to be deposited in these areas (Bilby, 1985).

Smaller particles (silt sized and smaller), which remain in suspension and are more likely to reach higher order streams, are thought to pose the greatest threat to aquatic environments (Fahey and Coker, 1992; Ramos-Scharron and MacDonald, 2007), though their effects are generally more subtle than those observed for coarser (sand sized and larger) deposited sediment (Bilby, 1985). Wash load and suspended sediment reduces the amount of light available for photosynthesis (Ramos-Scharron and MacDonald, 2007), and can irritate fish gills (Bilby, 1985; Marquis, 2005). Perhaps due to the subtle

consequences of fine sediment, few studies have confirmed adverse effects of sediment from forest roads on nearby stream environments (Fransen et al., 2001). Stream ecosystems are sometimes viewed as being quite resilient to infrequent storm events (the primary generators of significant sediment) as these events will not necessarily have long term effects (Fransen et al., 2001). However, other studies have suggested both deposited and suspended road derived sediment can have long term negative impacts on aquatic ecology and water quality (Beschta, 1978; Bilby, 1985; Marquis, 2005; Ramos-Scharron and MacDonald, 2007).

Fine sediment can act as a vector for pathogens in drinking water because it reduces the effectiveness of water treatment by shielding pathogens from both chemical (e.g. chlorination) and physical (e.g. ultraviolet irradiation) disinfection (Marquis, 2005). Health Canada has set the maximum turbidity<sup>1</sup> of potable water entering a distribution system to no more than 1 Nephelometric Turbidity Unit (NTU) (Marquis, 2005). Watersheds with sensitive ecosystems or drinking water facilities should therefore carefully monitor the sediment concentrations in their rivers and manage sediment production from forest roads where it has the potential to reach streams.

Water quality guidelines in British Columbia for induced suspended sediment and turbidity in rivers are based on increases over background levels (Pike et al., 2010):

- Induced suspended sediment concentrations should not exceed background levels by more than 25 mg/L at any one time for a duration of 24 hours, or exceed 5

---

<sup>1</sup> Turbidity refers to the degree to which transparency of a liquid is lost due to the presence of suspended particulates and is thus an indirect measure of the concentration of suspended solids.

mg/L from background levels at any one time for a duration of 30 days, in all waters during clear flows.

- Induced suspended sediment concentrations should not exceed background levels by more than 25 mg/L at any time when background levels are 25-100 mg/L during high flows or in turbid waters.
- When background concentrations exceed 100 mg/L, suspended sediment should not be increased by more than 10% of the measured background levels at any one time.
- For raw drinking water with treatment for particulates, turbidity should not increase from background turbidity by more than 5 NTU when background levels are less than or equal to 50 NTU, or should not change from background turbidity by more than 10% when background levels are greater than 50 NTU.
- For raw drinking water without treatment for the removal of particulates: turbidity should not increase from background turbidity by more than 1 NTU when background levels are less than or equal to 5 NTU, or should not change from background turbidity by more than 5 NTU at any time when background levels are greater than 5 NTU.

### **1.2.5 Potential management techniques**

Luce and Black (2001) stated that reducing unnecessary ditch grading will “unequivocally” decrease the amount of sediment produced from the road prism. Bilby et al. (1989) suggested ditch vegetation is only effective at settling out larger (sand sized and larger) sediment and the most effective method of removing fine particles (silt sized

and smaller) from ditch flow is by infiltration through the soil, implying the most effective management technique would be to allow ditches to drain directly onto the forest floor in a way that promotes infiltration. This might include increasing the frequency of cross culverts in order to reduce the amount of water drained at one site (Bilby et al., 1989). Luce and Black (1999) and Reid and Dunne (1984), however, found decreasing the road segment lengths contributing runoff to culverts was only effective for high gradient reaches and not for low gradient areas and only for areas far away from streams.

Settling ponds along ditch lines are no longer recommended, as they do not effectively remove fine sediment from the flow and trapped sediment can be remobilized under certain flow conditions. Although peak sediment concentrations were lowered, Bilby et al. (1989) found prolonged periods of elevated turbidity occurred after certain storm events in catchments with settling ponds along ditches due to the remobilization of previously captured sediment. These structures are also not practical in areas with very high rainfall as they fill and overflow quickly. Silt fences, check dams and sediment socks are also not always effective for similar reasons.

Best management practices involve covering exposed soil along ditch lines and cut and fill slopes as quickly as possible (Thurton, 2009). Grass seeding, hydroseeding, mulching, rip rap and geotextiles have all been used successfully in coastal British Columbia (Bill Floyd, Ministry of Forest and Range, Personal Communication).

Although hauling restrictions and/or road closures during wet weather are frequently considered in management plans, they may not always significantly reduce the amount of sediment delivered to streams. Bilby et al. (1989) suggest traffic during dry

weather is also responsible for creating sediment washed from road surfaces during precipitation events and Luce and Black (1999) state such restrictions provide “little and uncertain benefits” to roads with recently bladed ditches. Furthermore, decommissioned roads sometimes still produce significant amounts of sediment (Dobson Engineering Ltd., 1996).

Resurfacing road sections that produce the most sediment with thicker ballast and harder rock can be effective, as it reduces the amount of soil piping below the road and limits the supply of fine sediment to the road surface from below (Bilby et al., 1989). Rock surfacing of ditches, especially in areas with highly erodible native soils may also provide significant decreases in sediment yield (Luce and Black, 2001). These methods, however, may not be cost effective as appropriate ballast and surfacing material may not be locally available and transport costs are high.

### ***1.3 Research questions and hypotheses***

This study examines the controls on the amount of sediment generated from forest roads in a Pacific Maritime watershed during different rainfall and traffic conditions, as well as how much road derived sediment contributes to the overall sediment budget in a nearby river. Specifically this study determines the relation between rainfall intensity and total sediment produced from a forest road section in the Honna Watershed as well as the relation between rainfall amount and total sediment produced from a forest road section in the Honna Watershed. It also determines the relation between the number of logging truck passages during a rainfall event and the total amount of sediment produced from a forest road section in the Honna Watershed, and how long sediment concentrations in

road surface runoff water remain elevated following truck passage. This project also determines if forest roads increase sediment concentrations in the Honna River.

Based on theory presented by Bilby et al. (1989), sediment production from the studied road section is expected to increase with rainfall intensity and amount. Based on the findings of Reid and Dunne (1984) and Croke et al. (2005), the number of logging trucks passing the road section during a rainfall event is expected to increase the amount of sediment produced. Similar to the findings of Luce and Black (2001), elevated sediment concentrations in road surface runoff are expected to persist on the time scale of tens of minutes following truck passage during rainfall events. Sediment concentrations downstream from where the road crosses the river are expected to be significantly higher than sediment concentrations upstream of the road crossing and forest roads are expected to significantly increase sediment concentrations in the Honna River, similar to findings in a watershed on Vancouver Island (Floyd, 2008).

#### **1.4 Study Site**

This research was conducted in the Honna watershed, located on Graham Island, Haida Gwaii, 4 km northwest of the Village of Queen Charlotte and approximately 30 km northwest of the Community of Sandspit (Figure 1.2). The watershed is approximately 52 km<sup>2</sup> and contains 97 km of streams and 92 km of unpaved forest road (Dobson Engineering Ltd., 1996). Approximately 10 km of this road, the Queen Charlotte Mainline Forest Road South, was maintained and used for active hauling by logging trucks during the period of study (September 2009 – August 2010). Six km of the Mainline parallels the Mainstem of the Honna River and is located just meters from the Honna River (Figure 1.2). The average slope of this road section is 3%. The Honna



Figure 1.2 The location of the Honna Watershed in relation to the Village of Queen Charlotte and Sandpit

Watershed extends from sea level to 1000 m in elevation with a gently rolling north-south valley along the Honna River. The watershed's western portion is mountainous and steeper slopes can be found to the east (Dobson Engineering Ltd., 1996).

The Honna Watershed is located within the hypermaritime subzone of the Coastal Western Hemlock biogeoclimatic zone (Meidinger and Pojar, 1991). The Coastal Western Hemlock biogeoclimatic zone is one of Canada's wettest and most productive forest regions (Egan et al., 1999). Western Hemlock and Western Red Cedar are abundant in these zones, with Yellow Cedar common in some areas; on Haida Gwaii Sitka Spruce is also in places a climax species (Egan et al., 1999; Meidinger and Pojar, 1991).

Temperatures in the Coastal Western Hemlock zone are moderated by the Pacific Ocean resulting in cool summers and mild wet winters (Meidinger and Pojar, 1991). Long term climate data is not available for the Village of Queen Charlotte, but climate normals are expected to follow the same trends as Sandspit (23 km to the east), although the Honna Watershed receives more precipitation due to orographic effects. The meteorological station in Sandspit meets World Meteorological Organization standards. On average Sandspit experiences 222 days of detectable precipitation (>0.2 mm) in a year and a daily average temperature of 8.3 °C, with colder wetter months during the winter season and warmer drier months during the summer (Figure 1.3). Long term average precipitation at Sandspit between October 1<sup>st</sup> and May 31<sup>st</sup> is 1154 mm. Total precipitation during the study period (October 1<sup>st</sup> 2009 to May 31<sup>st</sup> 2010) was 999 mm suggesting the study period did not experience unusual weather, although December 2009 was drier than normal and October and November 2009 as well as January and March



2010 were wetter than normal (Figure 1.3). Precipitation was measured in a wetland near km 10 of the Queen Charlotte Mainline Forest Road South (Grapple 10) and near Stanley Lake (Figure 1.2). Twenty four percent more precipitation was recorded at the higher elevation gauge, suggesting a non-uniform precipitation distribution throughout the watershed (Figure 1.4). Total precipitation during the study period (October 1<sup>st</sup> 2009 to May 31<sup>st</sup> 2010) near Grapple 10 was 1980 mm and near Stanley Lake was 2212 mm, which is consistent with higher precipitation expected in the Honna Watershed compared to Sandspit (999mm). Discharge was measured in the lower reaches of the Honna River between September 2009 and June 2010 (Figure 1.2).

The watershed has a siltstone and mudstone dominated lithology, including Cretaceous Bearskin Bay formation mudstone and shale, with small sections of Cretaceous Haida Formation sandstone and siltstone and middle Jurassic Yakoun Group

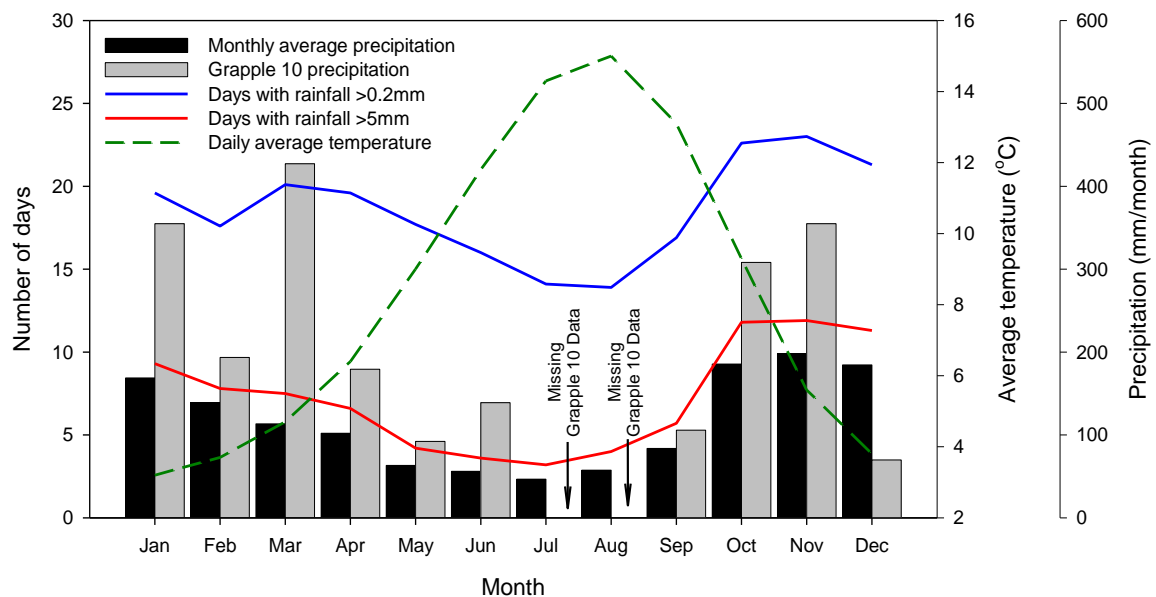


**Figure 1.3 Climate normals (1971 - 2000) for Sandspit (data from Environment Canada [http://www.climate.weatheroffice.gc.ca/climate\\_normals/index\\_e.html](http://www.climate.weatheroffice.gc.ca/climate_normals/index_e.html)) and measured precipitation in the Honna Watershed from September 2009 to June 2010**

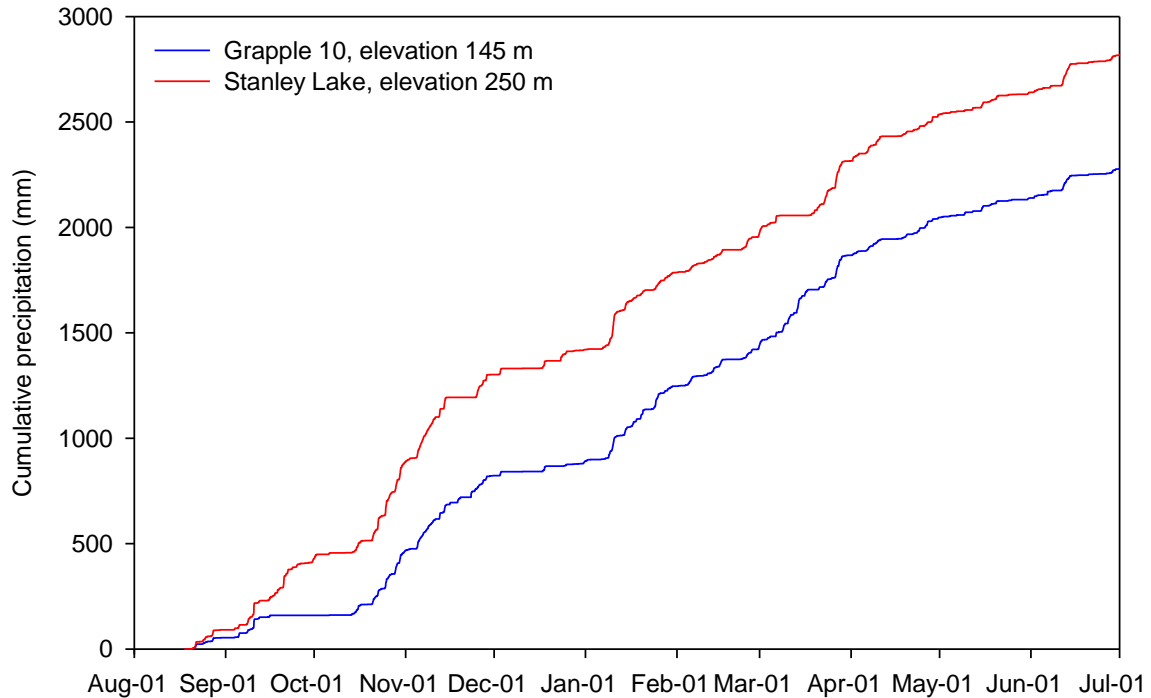


**Figure 1.4 Measured cumulative precipitation in the Honna Watershed between August 1<sup>st</sup> 2009 and July 1<sup>st</sup> 2010. For the location of the two rain gauges see Figure 1.2**

agglomerate, flow breccia, sandstone, conglomerate and minor shales in the eastern and northern portions of the watershed. Small sections of Triassic or Jurassic Sandilands Formation shale and fine-grained sandstone can be found to the north. The west of the watershed is largely underlain by upper Cretaceous Tarundl formation black shale. There are also some areas with upper Cretaceous Honna Formation conglomerates, sandstones and minor mudstone and shales, with small sections of upper Cretaceous Skidegate Formation thin-bedded sandstone and siltstone with mudstone and shale to the west. The western portion of the watershed also extends over a small section of Eocene to Oligocene volcanic rocks including intercalated mafic to felsic lava flows and pyroclastic rocks (Haggart, 2004). Siltstone and mudstone are considered a relatively unstable road bed material. Aggregate material more resistant to erosion, however, is not readily

available on the Island. The section of the Queen Charlotte Mainline Forest Road South which parallels the Mainstem of the Honna River runs through Skidegate Formation mudstone and shale.

Although the Queen Charlotte Mainline Forest Road South passes through moderate terrain and has small or no cut-slopes, it is frequently located just meters away from the Honna River, leading to high connectivity potential between the road and river. In response to an increase in demand for domestic water, the Village of Queen Charlotte has invested in a new water intake and treatment plant on the Honna River. One of the water quality concerns is that potentially high turbidity levels can impact the water treatment process. A number of hydrology related projects have been done on the Honna River (Bruce and Chatwin, 1987; Bruce and Chatwin, 1988; Dobson Engineering Ltd., 1996). However, now that the watershed is developed as a drinking water source, additional research is needed to identify specific sources of sediment and to determine mitigation strategies to prevent or limit forest road related sediment from entering the stream.

## **2 RAINFALL SIMULATIONS**

### ***2.1 Introduction***

Although previous studies have been conducted along the Queen Charlotte Mainline Forest Road South (Bruce and Chatwin, 1987; Bruce and Chatwin, 1988) and work has been done to improve storm water management, there has been no continuous monitoring of sediment derived from the roads or transported by the Honna River, or any studies to examine the controls on sediment generation from the Queen Charlotte Mainline Forest Road South. In this study rainfall simulation experiments were performed to determine the controls on sediment generation from this forest road. In particular, the aim was to address the influence of rainfall intensity, rainfall amount, traffic intensity and truck speed on total sediment production from the road, as well as how long sediment concentrations in road surface runoff remained elevated following truck passage. These results would allow us to determine what management strategies would be effective to control sediment production from forest roads in the Honna Watershed, as well as serve as a baseline for comparison once management strategies are implemented.

Often several years of field monitoring are required to observe a representative sample of natural rainfall events, encompassing typical critical storms. Without extensive monitoring data, few conclusive results related to rainfall phenomena can be reached (Meyer, 1994). To rapidly and efficiently study the wide spectrum of rainfall and traffic scenarios in the Honna Watershed, rainfall simulations were required. Rainfall simulation allows controlled, repeatable, and adaptable experiments to determine erosion and runoff characteristics in a timely manner (Meyer, 1994).

Despite the time efficiency, cost efficiency and experimental control provided by rainfall simulation experiments, there are a few disadvantages. Rainfall simulations are

<b>Table 2.1 Overview of the large scale rainfall simulation trials</b>							
<b>Trial #</b>	<b>Duration h:mm</b>	<b>Traffic</b>	<b>Date</b>	<b>Temporal Uniformity Coefficient (%)</b>	<b>Sprinkler Intensity† (mm/hour)</b>	<b>Return Interval (Figure 2.3) (years)</b>	<b>Runoff Ratio</b>
<b>Nozzle 6</b>							
1	2:30	N	30-Aug-09	N/A	6.5*	1.5	0.8
2	2:56	Y	31-Aug-09	87	7.3	2.0	0.7
3	5:00	Y	01-Sep-09	N/A	6.5*	2.5	0.9
4	3:00	Y	03-Sep-09	N/A	6.5*	2.0	0.8
5	1:03	N	05-Sep-09	50‡	7.3	1.5	0.9
6	5:00	N	06-Sep-09	79	4.7	1.5	1.2
7	2:05	N	07-Sep-09	N/A	6.5*	1.5	0.8
8	3:00	Y	09-Sep-09	N/A	6.5*	2.0	0.8
9	5:00	Y	14-Sep-09	80	6.5	2.5	0.9
22	4:00	N	8-Oct-09	87	7.3	3.0	0.9
23	3:00	Y	19-Oct-09	N/A	6.5*	2.0	0.9
<b>Nozzle 11</b>							
10	2:30	Y	17-Sep-09	91	14.9	15	1.1
11	4:00	N	19-Sep-09	91	16.6	>15	1.0
12	4:00	Y	22-Sep-09	93	16.7	>15	1.0
13	2:30	Y	24-Sep-09	88	11.8	10	1.4
14	2:00	N	26-Sep-09	91	17.4	>15	0.9
15	2:30	Y	28-Sep-09	90	14.7	15	1.1
16	2:30	Y	29-Sep-09	89	14.9	15	1.1
21	3:00	N	7-Oct-09	91	18.1	>15	0.9
<b>Nozzle 22</b>							
17	1:28	Y	01-Oct-09	93	52.2	>15	1.0
18	1:15	Y	02-Oct-09	92	40.4	>15	1.1
19	2:00	N	03-Oct-09	86	40.5	>15	1.1
20	2:00	N	06-Oct-09	95	39.9	>15	1.1
24	2:00	Y	23-Oct-09	85	50.0	>15	0.9

† Experiments with nozzle 6 are considered low intensity experiments throughout the remainder of the text. Experiments with nozzles 11 and 22 are considered medium and high intensity experiments respectively.

\* Assigned average value

‡ Because of the variable intensity due to rainfall during the trial, this trial is not used in any of the analyses

Table 2.2 Overview of the small scale rainfall simulation trials							
Trial #	Duration h:mm	Slope (o)	Date	Temporal Uniformity Coefficient (%)	Sprinkler Intensity (mm/hour)	Return Interval (Figure 2.3) (years)	Runoff Ratio
<b>Nozzle 6</b>							
S1	0:18	3	20-Nov-09	80	6.6	1.0	1.2
S2	0:56	2	20-Nov-09	70	4.2	<1	0.7
S3	0:39	2	21-Nov-09	87	4.9	<1	0.6
S4	0:54	3	21-Nov-09	78	5.3	1.0	1.0
S5	0:44	3	21-Nov-09	85	7.9	1.5	0.7
S6	0:36	2	22-Nov-09	88	8.6	1.5	0.6
S7	0:55	3	22-Nov-09	86	19.5	>10	0.3

usually expensive, have a limited application size, and do not exactly reproduce natural rain events (Renard, 1985). For this project costs were reduced by building the apparatus ourselves and boundary effects were minimized by doing trials at a large scale (tens of meters).

Twenty four large scale rainfall simulation trials were conducted at km 8 of the Queen Charlotte Mainline Forest Road South between August 30<sup>th</sup> and October 23<sup>rd</sup>, 2009 (Table 2.1 and Figure 2.1). Seven additional small scale rainfall simulations were conducted at various locations between km 3 and km 7 and along a well maintained spur road at km 3 between November 20<sup>th</sup> and 22<sup>nd</sup>, 2009 to determine the spatial variability in sediment generation (Table 2.2 and Figure 2.1).

## 2.2 Study Sites

The large scale rainfall simulations were conducted along a 30m section of the Queen Charlotte Mainline Forest Road South north of km 8 (Figure 2.1). This location was selected because it is representative of road surfaces with the potential to contribute sediment to the Honna River (Bruce and Chatwin, 1987; Bruce and Chatwin, 1988).

Inspection of the road confirmed it was representative of the Mainline. The specific road section was chosen based on its proximity to the river, facilitating pumping of water for

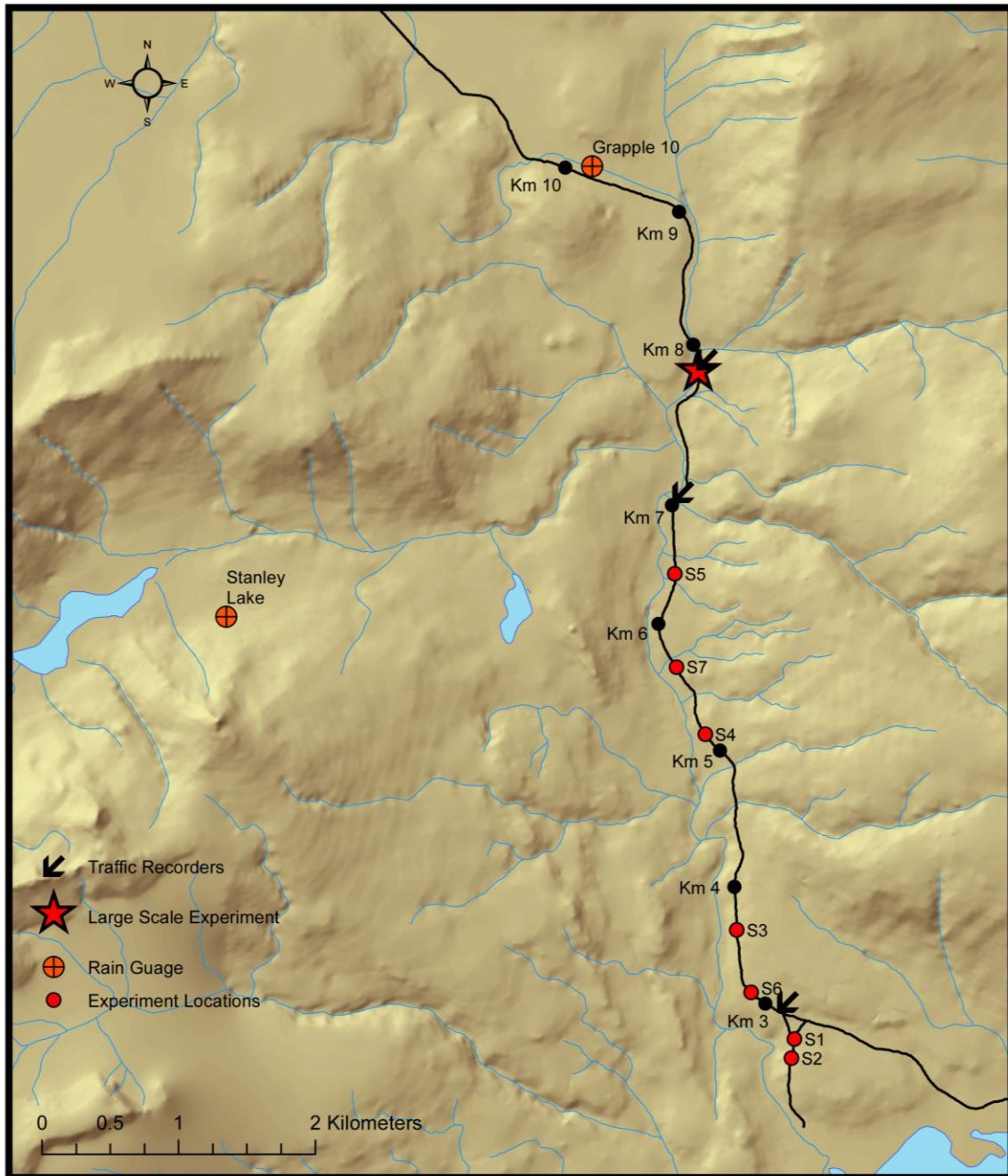


**Figure 2.1 Location of large and small scale rainfall simulation trials**

the sprinklers, as well as its relatively wide shoulder allowing safe sprinkler set up. The section also had a characteristic slope for the area (2% towards the south), was crown sloped facilitating sample collection, and was straight enough to allow adequate visibility of the sprinkler system for logging truck drivers. The east ditch along the road section was deep and narrow while the west ditch was wide and shallow (Figure 2.2).

Five small scale rainfall simulations were conducted between km 3 and km 7 of the Queen Charlotte forest road South and two additional simulations were conducted

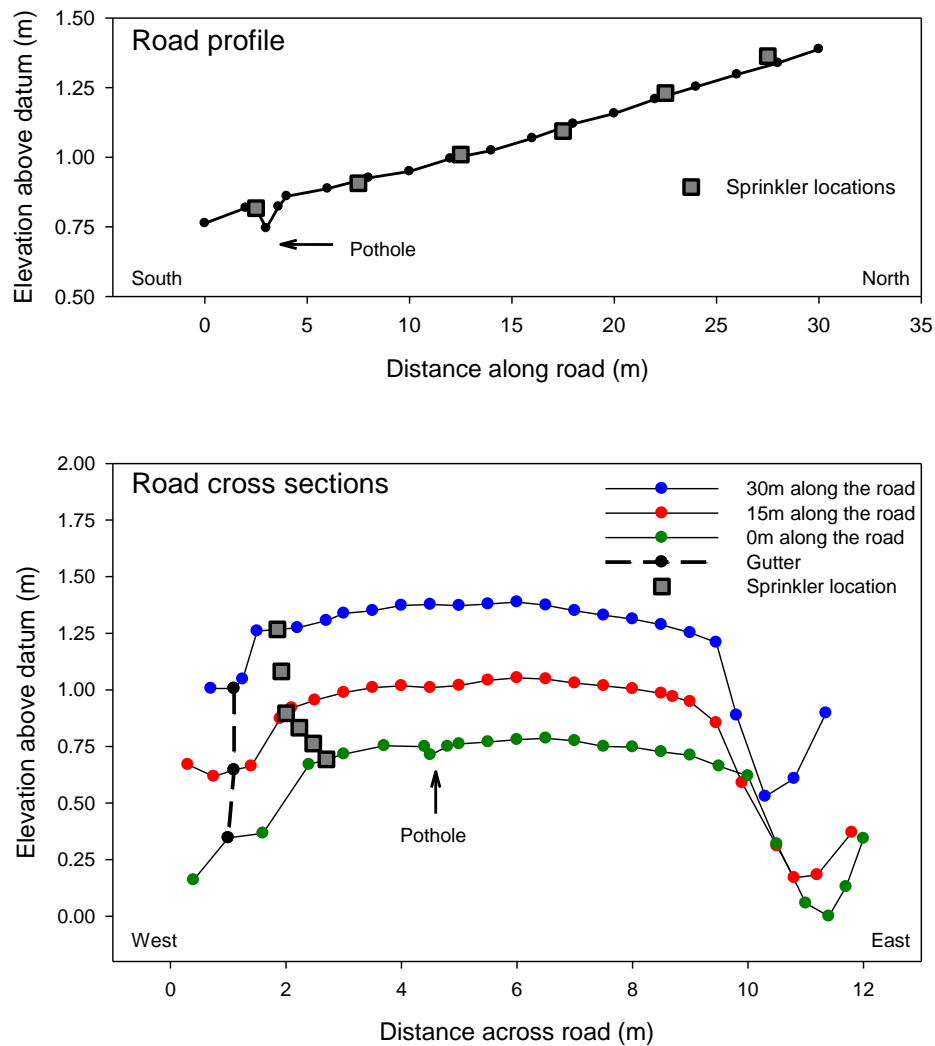


**Figure 2.2 Road profile at the location of the large scale rainfall simulation trials**



along a well maintained spur road that is frequently used by local traffic and occasionally used by larger trucks (Figure 2.1). Small scale sprinkler trial locations were chosen to have representative road surfaces for the kilometer section in which they were located. Simulation locations were off to one side of the road to permit local traffic passage during the trials, but were never located on the road shoulder and always at least partially encompassed a large truck tire track. The local slopes for small scale trial locations ranged from 3.5 to 5%. The slopes of the overall road section of the small scale trials were similar to that of the large scale trial location. Small scale trials were restricted to locations south of km 7 to avoid rainfall simulations on frozen road surfaces.

## **2.3 Methods**

### **2.3.1 Sprinkler design**

While rainfall simulators can never perfectly replicate natural events, they are able to provide useful data, which can be compared to natural precipitation, if several features of the simulated rain are considered (Meyer, 1994). As rill erosion is likely important, a main consideration of the rainfall simulator is the range of precipitation intensities it can produce. If simulation intensities are too low no rill erosion will occur. If they are too high, experiments represent natural conditions that are too rare to be useful for planning (Meyer, 1994).

Hourly precipitation data for the Honna watershed were available from the Ministry of Forest and Range Wildfire Management Branch, Victoria BC, from June 1990 to April 2002, with frequent data gaps particularly in the fall and winter months. In 1998 the rain gauge was moved approximately 2 km east of the watershed but was likely still representative of the local weather. Intensity duration curves were determined for the

2, 5, and 10 year return interval storms based on the available data (Figure 2.3). The most intense storms in the area occur in the fall and winter months, suggesting the frequent data gaps during these time periods would result in minimum intensity-duration values being calculated. Rainfall intensity-duration-frequency data based on 33 years of rainfall (1972 – 2004) were available for the airport in the nearby community of Sandspit (Environment Canada station SandspitA BC 1057050), located approximately 23 km to the east of the Village of Queen Charlotte. These data have been reviewed, adjusted, and quality assured by Environment Canada. Comparing the Honna watershed intensity-duration-frequency data with the Sandpit curves, as well as with published intensity duration values for southern Graham Island (Murray, 1964), shows the Honna data is reasonable, despite the frequent data gaps in winter (Figure 2.3). Assuming the majority of sediment is generated during intense events and that road use policy in the Honna Watershed is based on the 2-, 5- or 10-year return period events, rainfall intensities between 5 and 15 mm/hour are of most interest for this study. These intensities are well below the minimum rainfall intensities of many common rainfall simulators, but agree reasonably well with the rainfall intensities of the chosen rainfall simulator (5-50 mm/h) (Table 2.1)

Although previous studies indicate the amount and distribution of overland flow is usually the main control on sediment transport from forest road surfaces (Bilby et al., 1989), splash erosion may be an important process as well. As the ability of rain drops to erode by splashing is closely related to their kinetic energy (Hudson, 1993), it was important to replicate the kinetic energy of natural rainfall, or account for the difference in kinetic energy between the natural and simulated rainfall. The kinetic energy of a rain

drop depends on its size and velocity. In natural rain events, drop velocity is related to drop size, and drop size distribution varies with intensity. Kinetic energy of natural rainfall is therefore expected to increase with intensity according to the empirical equation  $E = 30 - \frac{124}{I}$  (Hudson, 1993), where E is the kinetic energy of the event in  $J/m^2/mm$  of rain, and I is the intensity in mm/hour. Natural rain drops commonly vary in size from near zero to approximately 7 mm in diameter, with a median between 1 mm and 3 mm, depending on storm intensity (Meyer, 1994). Although no studies on drop size distributions are known for the study site, orographic rain is generally composed of small and medium sized drops (0.1–1.5 mm) (Blanchard, 1953). In order to assess the comparability between the kinetic energy of the rainfall simulator and natural rain in the area, size distributions were measured for both natural and simulated rain drops (Figure 2.9).

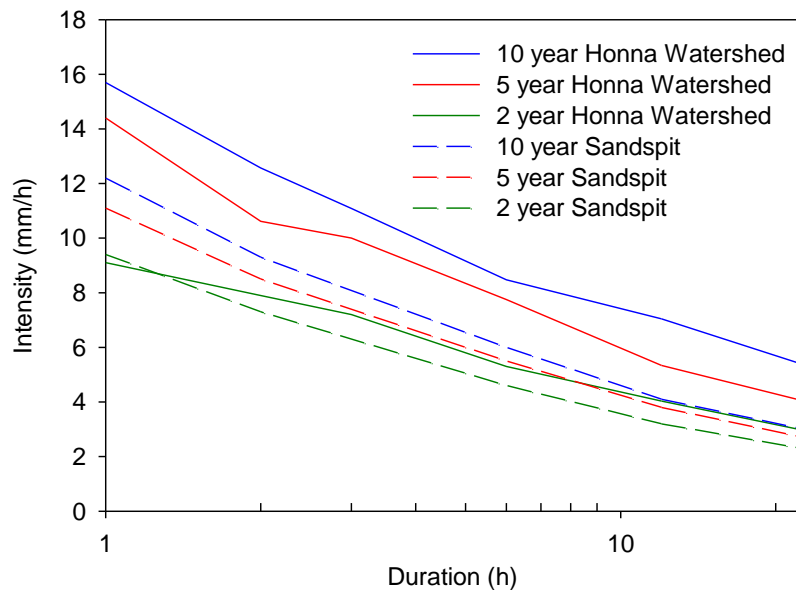


**Figure 2.3 Intensity-duration-frequency graph for precipitation in the Honna Watershed based on precipitation data from 1990-2002 with frequent data gaps, and SandspitA based precipitation data from 1972-2004 (reviewed and adjusted by Environment Canada)**

The rainfall simulator needed to be capable of simulating multiple intensities, the experimental area needed to be large (tens of meters), and the simulator needed to be portable. A drop style simulator was therefore not practical, so a pressurized nozzle simulator was used. Nozzles which produce drops large enough to approximate natural rainfall require large orifices (>3 mm). Because even at low pressure large nozzle openings produce simulated rainfall that is more intense than natural rainfall, some interruption of the spray is necessary (Hudson, 1993). Senninger Irrigation Inc. developed an inverted rotating-plate irrigation nozzle, the i-Wob®, which allows low intensity spraying while still maintaining a large drop size. No literature is available on the i-Wob's ability to simulate natural precipitation, but system design information suggests it is an appropriate alternative to complex computer controlled spray interruption simulators. A study on the Rotator Series R-30 and Spinner Series S-30 rotating-plate nozzles manufactured by the Nelson Corporation showed the sprinkler heads produced drops up to 6 mm in diameter and represented natural rainfall well (DeBoer et al., 2001). The sprinkler heads that produced the widest drop size distributions were those with the largest nozzle diameters and a larger number of grooves on the rotating plate. No information was given on the simulated precipitation intensities of the Rotator or Spinner series nozzles (DeBoer et al., 2001). The i-Wob is similar to the Rotator and Spinner nozzles and markets its ability to produce large drops while maintaining low precipitation intensities.

### **2.3.1.1 Large scale rainfall simulation set up**

Six Senninger Irrigation Inc. i-Wob sprinkler heads artificially rained on a 30 m section of the Queen Charlotte Mainline Forest Road South near km 8. Water was drawn

directly from the Honna River through a 5 cm semi-rigid suction hose with a basket strainer encased in a Marineland Aquarium Products fiberglass bonded filter sleeve (uncompressed thickness of 1 cm) using a Honda WH20X high pressure water pump. Water was then carried through 3.8 cm canvas fire hoses to the sprinkler heads, which were connected to the fire hose using 3.8 cm ABS fittings (Figure 2.4). Individual hose sections were connected using 3.8 cm ABS fittings as well. Sprinkler heads, consisting of a 0.6 m section of reinforced flex tubing, a 100 kPa pressure regulator, a standard 9 groove i-Wob sprinkler head and an i-Wob 0.2 kg threaded weight, were elevated 3 m above the road surface using rigid metal piping and surveying tripods, counter balanced by 40 L buckets filled with water (Figure 2.5).

The large scale trials were conducted using three different nozzle aperture diameters, resulting in different precipitation intensities, with and without traffic from logging trucks and with various antecedent precipitation conditions. Experiments with nozzle 6 are designated low intensity experiments. Experiments with nozzle 11 and 22 are designated medium and high intensity experiments respectively.

A 30 m long, 10 cm wide metal gutter was buried next to the road shoulder along the west side of the road to catch and route road surface runoff from the western half of the road surface (Figure 2.4). Water was routed to the south end of the gutter for sampling. The road side edge of the gutter was folded to a height of 3 cm to reduce the depth required to bury it. During gutter installation special care was taken to disturb as little of the shoulder/ditch material as possible. Loose dirt removed during gutter installation was used to fill small gaps between the gutter and the surrounding ditch surface. Natural rain events between gutter installation and sprinkler trials allowed the

development of an armoring layer on material that was disturbed during gutter installation. Prior to the first rainfall simulation trial there was no noticeable difference between the material used to seal the gutter and the surrounding surface. Blue dye added to runoff water during trials indicated all runoff from the western half of the road was being caught by the gutter.

A 60° v-notch weir was installed in the east ditch opposite the southern most sprinkler. An Odyssey capacitance water level logger and bucket measurements were used to measure discharge. Large rainfall events and wet antecedent conditions were required for flow to occur. Weir grab samples were collected concurrently with gutter samples when possible to compare water flowing in ditches to that collected in the gutter.

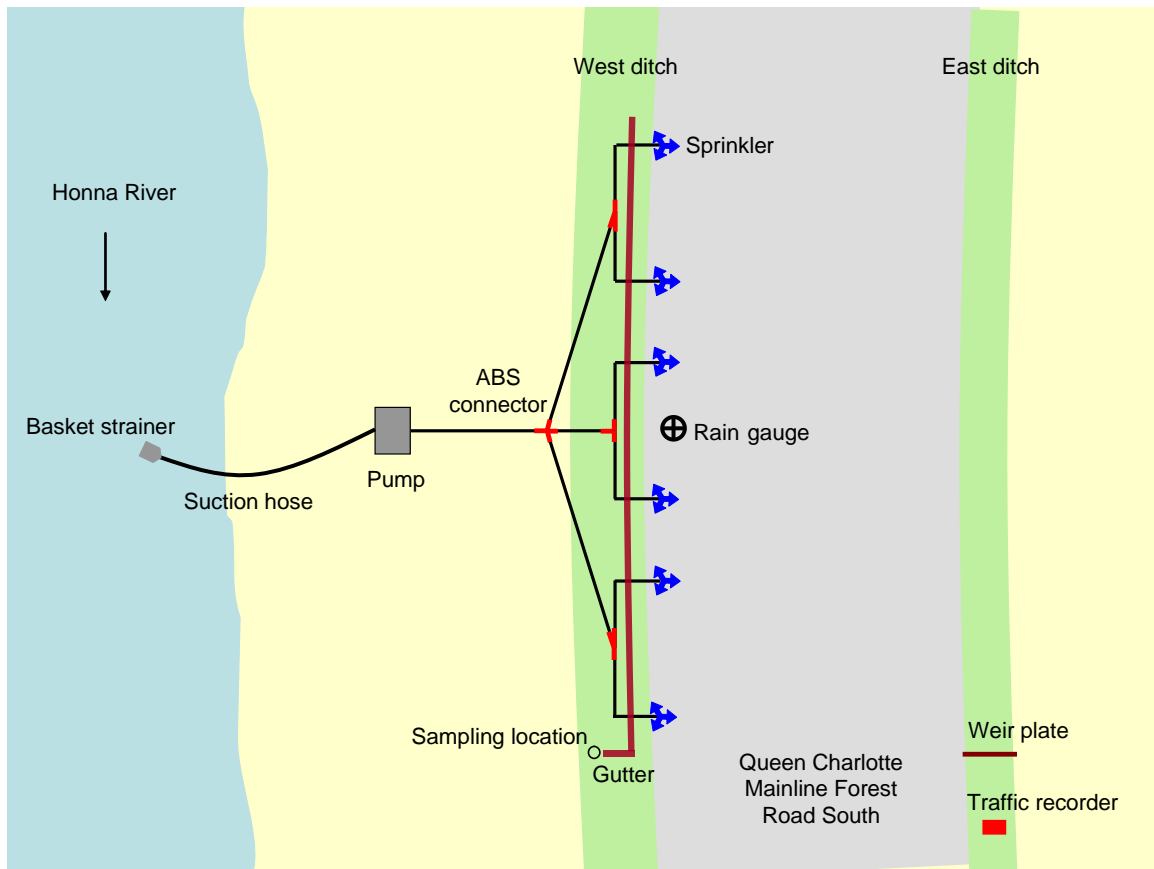


**Figure 2.4 Plan view of large scale sprinkler apparatus**

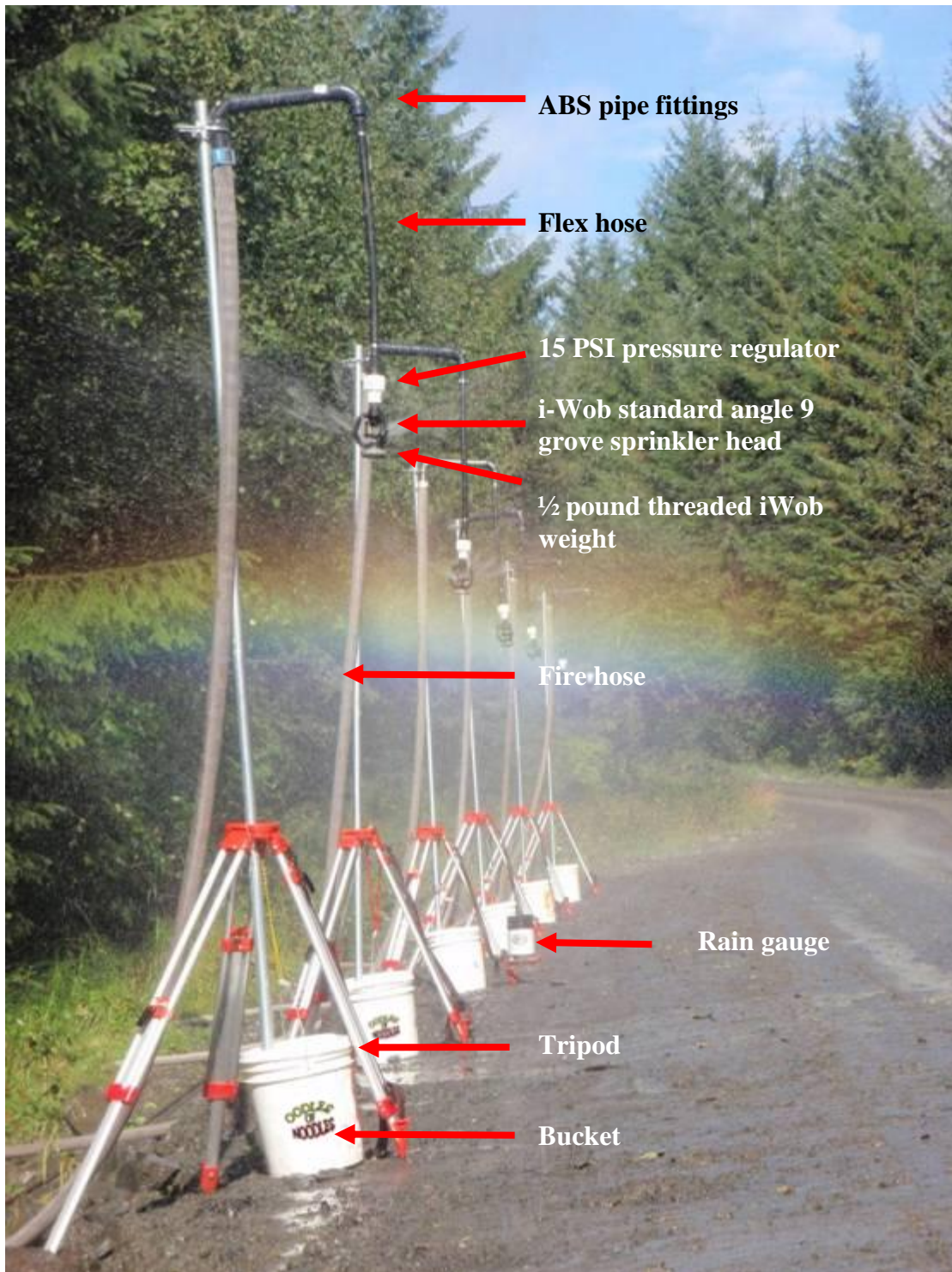


Figure 2.5 Oblique view of the large scale sprinkler set up

### 2.3.1.2 Small scale rainfall simulation set up

A single sprinkler head was used for the small scale experiments and water was pumped from a 300 liter tank, transported in the back of a truck. A 1 m diameter section of road adjacent to the sprinkler head was isolated from the rest of the road surface using a 10 cm high thin metal barrier. The metal barrier was pounded into the road surface where possible, and sealed with a clay mixture around the outside of the barrier to prevent inflow from areas outside the barrier and leakage of surface runoff from within the barrier. Blue dye was applied around the plot during each trial to confirm there was no leakage under the metal barrier. A 2.5 cm diameter plastic hose was installed at the lowest location of the section to collect the water (Figure 2.6).

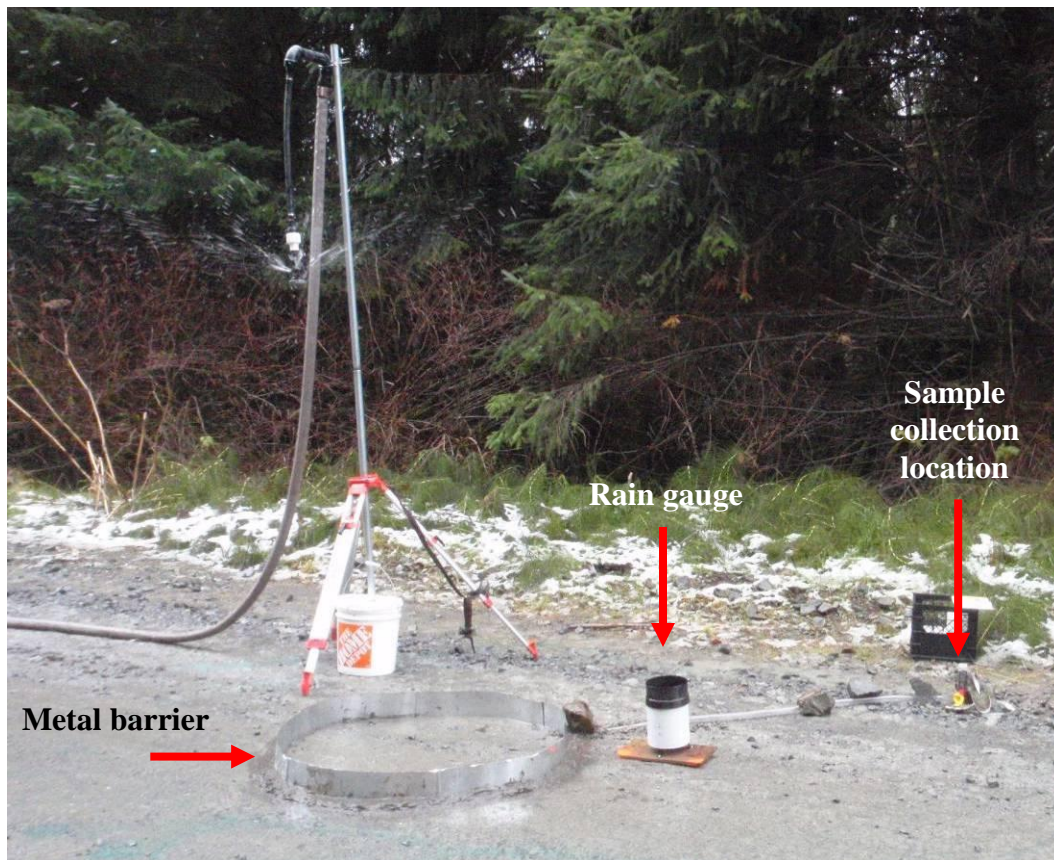


Figure 2.6 Small scale sprinkler set up



### 2.3.1.3 Sprinkler intensity and uniformity

Sprinkler rainfall intensity was measured during large scale trials 2, 5, 6, 9-22, and 24 and during all small scale trials using an Onset RG3-M 0.2 mm Data Logging Rain Gauge (Onset, Bourne MA, USA). For large scale trials the rain gauge was deployed directly between the 3<sup>rd</sup> and 4<sup>th</sup> sprinkler head (Figure 2.4) while for small scale trials it was deployed outside the metal barrier (Figure 2.6). Rainfall intensity was determined at 5 minute intervals throughout each of these trials. The mean rainfall intensity for all but the first and last 5 minute interval of the trial was used as the trial's intensity (Table 2.1 and Table 2.2). The first and last 5 minute intervals were removed to eliminate intervals occurring only partially during a trial.

Large scale trials 1, 3, 4, 8, 7 and 23 had no precipitation data available and were assigned a sprinkler intensity of 6.5 mm/h, equal to the mean intensity of the other trials using nozzle 6 with the exception of trial 5 (which included natural rainfall). Although sprinkler intensity varied between trials using the same nozzle, this variation was relatively small for trials using nozzle 6 (standard deviation: 1.24 mm/h, coefficient of variation: 19%) and therefore the mean of the available data was assumed to be a reasonable estimate.

A temporal uniformity coefficient,  $C_U$  (Harrison and Perry, 2007), was calculated to assess sprinkler intensity stability throughout the large and small scale trials:

$$C_U = \frac{\sum_2^{n-1} |P_i - \bar{P}|}{\sum_2^{n-1} P_i}$$

where  $P_i$  is the precipitation intensity in a 5 minute interval,  $\bar{P}$  is the average precipitation intensity during the trial (excluding the first and last 5-minute intervals) and  $n$  equals the number of 5 minute intervals during the trial. All trials with precipitation data, except trial 5, had a temporal uniformity greater than 70%, indicating that the rainfall simulator produced precipitation of reasonably constant intensity (Table 2.1 and Table 2.2). Trial 5 had a variable precipitation intensity due to the addition of natural rain during the experiment. Because of its variable precipitation intensity, trial 5 is not used in any of the analyses.

In situ measurements of spatial variability in sprinkler rainfall intensity during large scale trials were limited by frequent traffic through the study site. Spatial uniformity was assessed during one low intensity trial using an array of small funnel (6.3 cm diameter) rain gauges. Spatial variability around a single nozzle was assessed more extensively at a non-road location following the trials. Radial sprinkling intensity from a single number 6 or 22 nozzle was best described by a 3<sup>rd</sup> order polynomial, while that from a number 11 nozzle was best described by a 4<sup>th</sup> order polynomial. The best fit polynomials from a single sprinkler head were used to infer the spatial distribution of sprinkler rainfall intensity throughout the large scale study site (Figure 2.7). The inferred sprinkler intensity distribution for nozzle 6 matched the in situ measurements well (Figure 2.8).

Due to the limited area of the small scale trials, rain gauges would have effected the trial results. The spatial variation in rainfall intensity was therefore not assessed for the small scale trials. However, the study sites were located almost directly below the sprinkler head where spatial variability in sprinkler intensity was minimal (Figure 2.8).

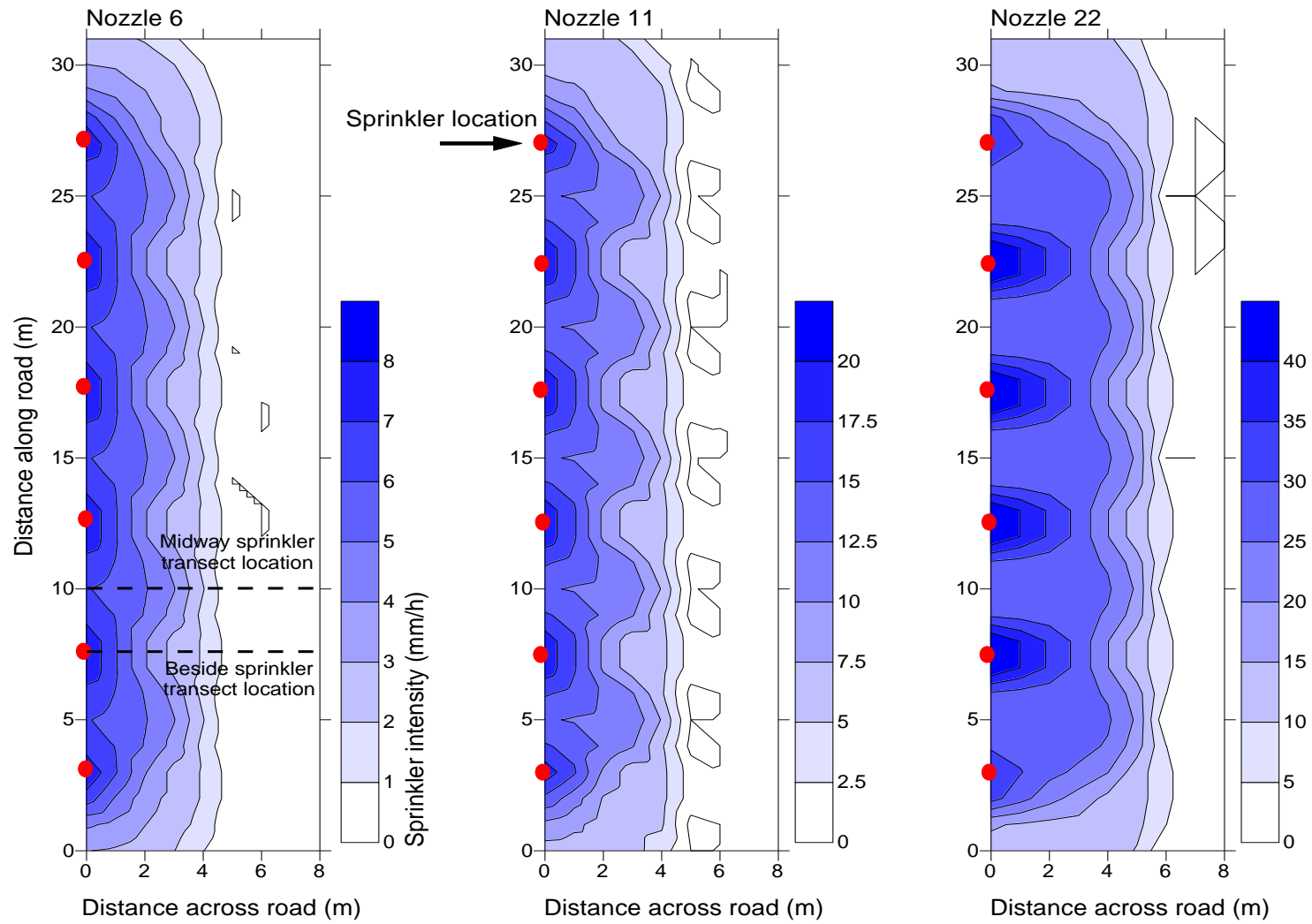


**Figure 2.7 Inferred sprinkler intensity across the road. The sprinkler rainfall intensity along the midway and beside sprinkler transects is given in Figure 2.8**

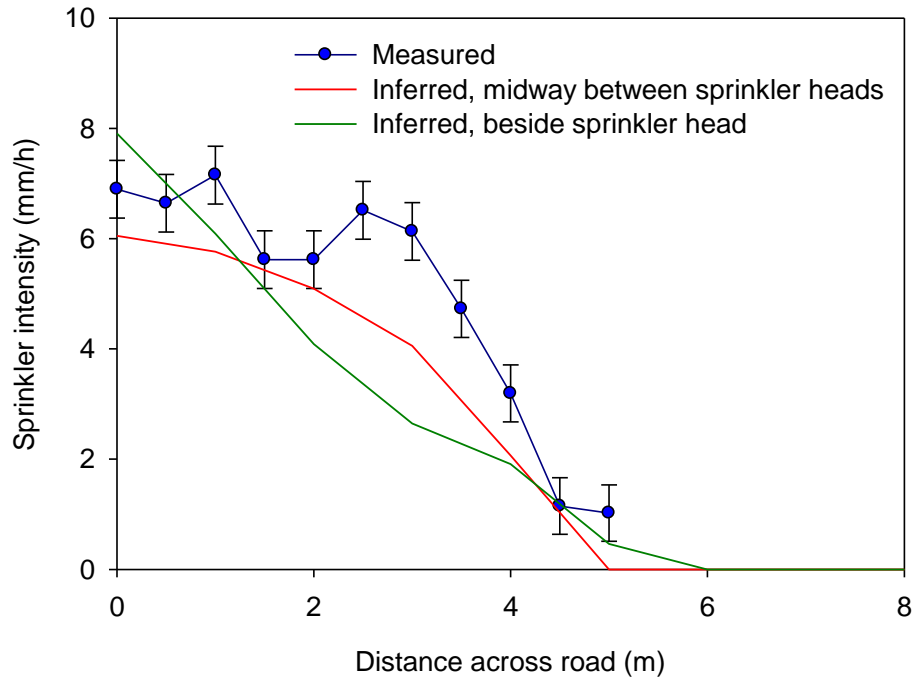


**Figure 2.8 Comparison of the measured and inferred sprinkler intensity as a function of distance across the road for nozzle 6. See Figure 2.7 for the location of the transects for which the sprinkler intensities were inferred**

#### 2.3.1.4 Drop size distribution

The drop size distributions of natural and simulated rain were measured using the oil method (Eigel and Moore, 1983). One part STP fuel oil treatment and two parts mineral oil were combined and used to fill 25 mm deep Petri dishes. The Petri dishes were manually exposed to precipitation for 5 seconds, and photographs were taken within 30 seconds of initial exposure to precipitation to prevent drop distortion from the bottom of the dish. Photographed drops were later counted and measured.

Drop sizes were measured during three natural rainfall events between October 31<sup>st</sup> and November 25<sup>th</sup>, 2009. Five minute precipitation intensities during drop collection were 2.6 mm/h for all three events. Drop sizes were also measured during 5 large scale experiments and later also using a single sprinkler head. The simulator produced drops

ranging from 0.1 mm to 7 mm in diameter, with higher intensity (nozzle 22) trials producing the largest drops (Table 2.3). Lower intensity (nozzle 6) trials produced a smaller number of large drops. Natural precipitation produced the smallest proportion of large drops. The drop size frequency distributions show a good agreement between simulated and natural rain fall (Figure 2.9 and Table 2.4).

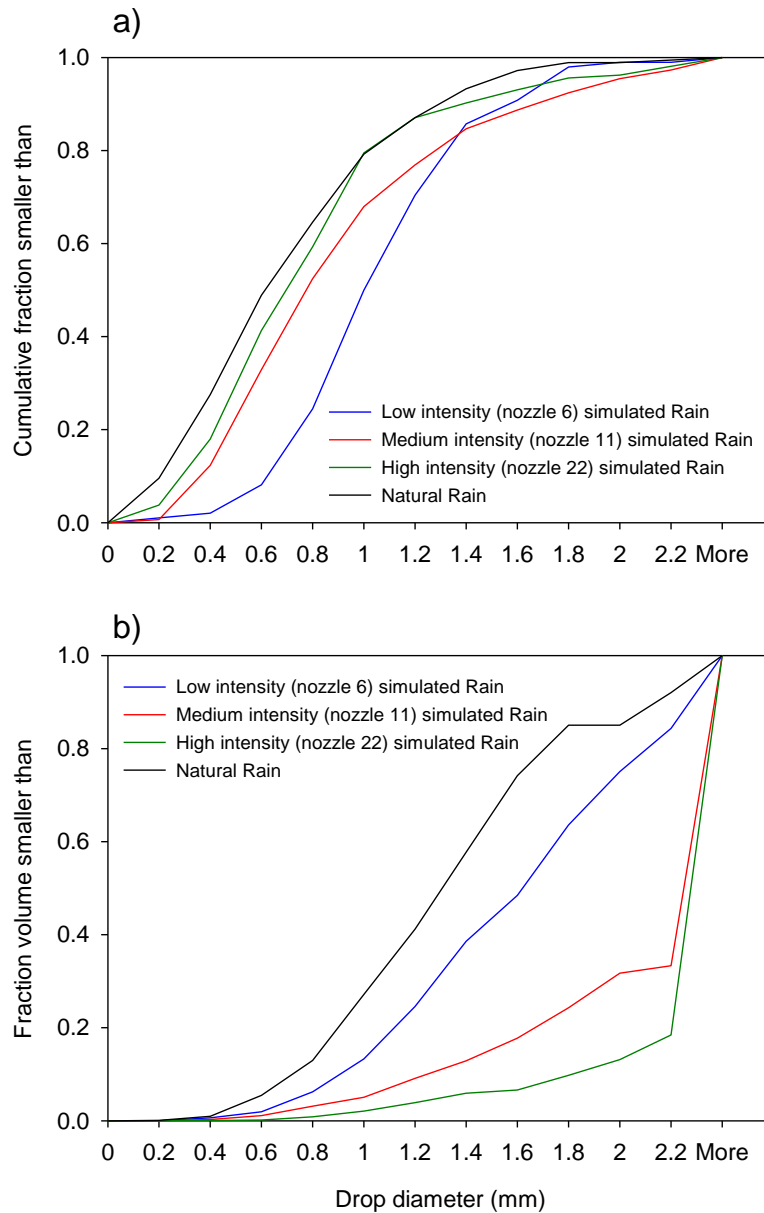


**Figure 2.9 Drop size distribution of natural and simulated precipitation based on drop diameter (a) and drop volume (b)**

<b>Table 2.3 Measured drop size distribution statistics</b>				
<b>Nozzle</b>	<b>Maximum drop diameter (mm)</b>	<b>Minimum drop diameter (mm)</b>	<b>Median drop diameter (mm)</b>	<b>Rainfall intensity (mm/h)</b>
Natural rain	2.3	0.2	0.7	2.6
6	3.3	0.1	0.9	7.3
11	7.0	0.1	0.9	14.8
22	6.0	0.2	1.1	40.4

<b>Table 2.4 Published median drop diameters for natural precipitation</b>				
<b>Author</b>	<b>Location</b>	<b>Measurement method</b>	<b>Median drop diameter (mm)</b>	<b>Intensity (mm/h)</b>
Mason and Andres (1960)	London, England	Filter paper	0.9	1
Mason and Andres (1960)	London, England	Filter paper	1.3	10
Smith et al. (2009)	Princeton, New Jersey	Joss-Waldvogel (JW) disdrometer	2.2	26
Smith et al. (2009)	Princeton, New Jersey	JW disdrometer	1.3	4.6
Tokay et al. (2008)	Roi-Namur, Republic of Marshal Islands	JW disdrometer	1.6	20.6
Tokay et al. (2008)	Wallops Island, Virginia	JW disdrometer	1.7	18.2
Harikumar (2010)	Kochi, India	JW disdrometer	0.7	5
Harikumar (2010)	Kochi, India	JW disdrometer	1.3	30
Fernández-Raga et al. (2010)	Soutelo, Portugal	Optical disdrometer	0.4	< 1
Niu and Jia (2010)	Guyuan, China	PARSIVEL disdrometer	1.1	5
Niu and Jia (2010)	Guyuan, China	PARSIVEL disdrometer	1.3	30

The drop size frequency distributions were different at different distances away from a single sprinkler head, with larger drops dominating at larger distances. However, when multiple sprinkler heads were used in an array, such as during the large scale experiments, this variation in drop size distribution with location was not observed.

### **2.3.1.5 Flow Rates**

Instantaneous discharge from the gutter running along the west side of the road was determined periodically throughout the large scale trials by measuring the time required to fill a container of a known volume. Gutter outflow rates increased logarithmically from the start of a trial up to a certain point when a steady rate was observed.

A logarithmic trend line was fit to all nozzle 6 outflow data (except trial 5) from the beginning of the experiment up to 30 minutes into the experiment (Figure 2.10). The trend line was used to determine continuous outflow for all nozzle 6 trials (except trial 5) up to 30 minutes into the experiment. A value of 0.1 times the flow rate was used to represent the error in outflow during this time. The mean outflow rate for each individual trial from 30 minutes (inclusive) to the end of the trial was used to represent continuous outflow during the steady state period. The standard deviation of the measured outflow values for each individual trial during this period was used to represent the error. Trials without outflow data were assigned the average outflow rate of all available data from nozzle 6 trials (except trial 5). The standard deviation of all available outflow values was used as an approximation of error for these trials.

Outflow data for medium intensity trials 10 – 15 were not used due to inaccurate flow measurements. Following trial 15, modifications at the south end of the gutter allowed more accurate measurements at higher gutter discharge. Outflow data from trials 16 and 21 were used to represent all nozzle 11 trials. A logarithmic trend line was fit to outflow data from the first 11 minutes of the experiment, and used to determine continuous outflow for the beginning of all nozzle 11 trials (Figure 2.10). A value of 0.1

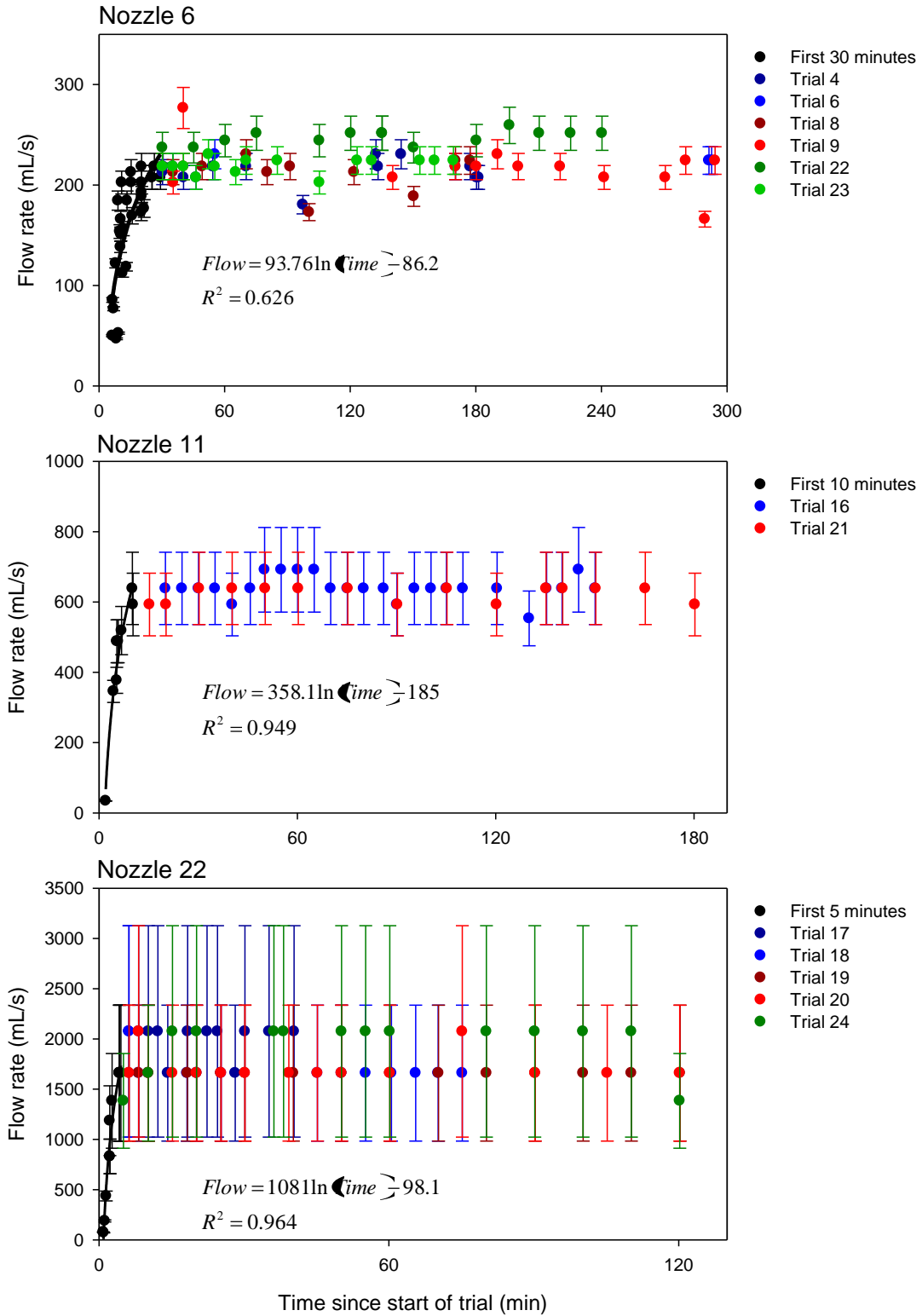


**Figure 2.10 Gutter flow rates for the large scale trials. The equations describe the outflow rate during the first 30, 10, and 5 minutes of trials using nozzle 6, 11, and 22 respectively**



times the flow rate was used to represent the error in discharge for this time period. The mean outflow rate for trials 16 and 21 from 11 minutes (inclusive) to the end of the experiment was used to represent continuous outflow for the steady state period of each of these trials and the average of trial 16 and 21 was used for all other nozzle 11 trials. Errors were calculated in the same way as for nozzle 6.

A logarithmic trend line was also fit to all nozzle 22 outflow data from the beginning of the experiment to 5 minutes into the experiment (Figure 2.10). The trend line was used to determine continuous outflow for all nozzle 22 trials up to 5 minutes into the experiment. The mean outflow rate for each individual trial from 5 minutes (inclusive) to the end of the experiment was used to represent continuous outflow during this time. Errors were calculated similarly as for the nozzle 6 trials.

Small scale trial outflow rates were determined by measuring the time required to collect samples of a known volume from the outflow tube. No initial increase in outflow was detected for the small scale trials (Figure 2.11). The mean outflow rates were used to represent continuous outflow throughout the experiment for trials S1 to S5. The standard deviation of the measured outflow values for each individual trial was used to represent the error. Uncertainty in sample volumes from trials S6 and S7 resulted in uncertain outflow rates. These trials were therefore assigned the average value of all available outflow data from trials S1 to S5. The standard deviation of all available outflow data was used as an approximation of the error for trials S6 and S7.

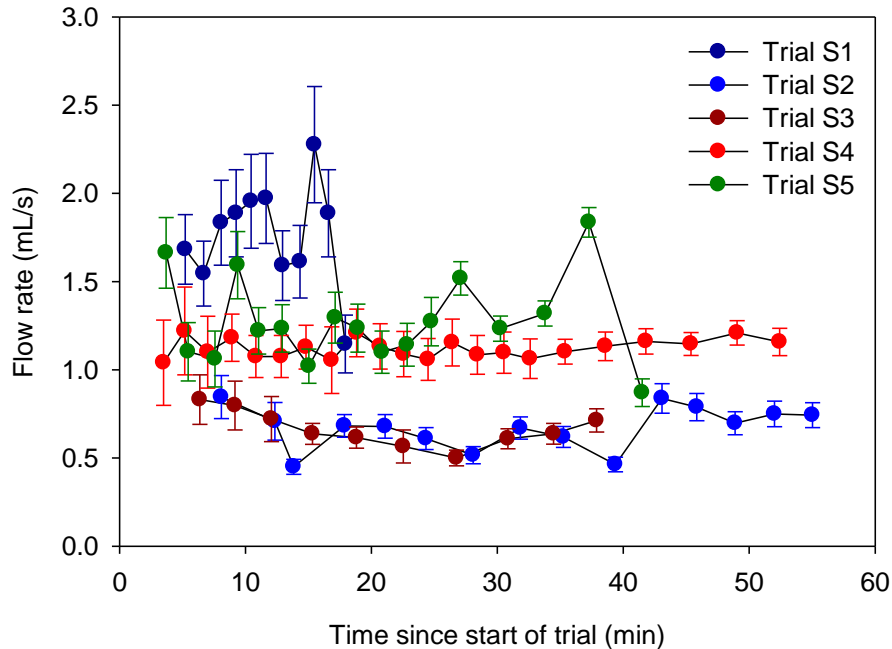


**Figure 2.11 Small scale experiment flow rates**

### 2.3.2 Sediment concentrations

Grab samples were collected from the gutter outflow throughout each trial, and occasionally from the weir during the large scale trials. During the small scale trials, grab samples were taken from the hose. Samples were passed through 1.6  $\mu\text{m}$  Whatman GF/A glass microfibre filters, dried at 200  $^{\circ}\text{C}$  for 20 minutes, and weighed to determine the sediment concentration.

### 2.3.3 Splash

Splash from logging truck tires was proposed as a potentially important method of moving road surface sediment to ditches and streams. In order to determine if splash was significant, blue dye was placed across a wet road surface and added to water filled pot holes prior to the passage of loaded logging trucks. The majority of dye was carried along the road by tires, but minor amounts of splashed blue dye were evident up to 1.5 m

perpendicular to tire treads and up to 4.0 m from potholes. Most splashed dye from potholes, however, was confined to within 2.0 m of the edge of the pothole (Figure 2.12). As tire tracks were usually more than 1.0 m from the road shoulder, very little splash actually reached ditches or bridge edges.

To confirm that splash, even from puddles or potholes, was of minor importance in transporting sediment to ditches or streams, Petri dishes were placed at 20 cm intervals perpendicular to the road surface starting at the road shoulder adjacent to potholes while loaded logging trucks passed. Although some splash was collected in petri dishes up to 60 cm away from the road shoulder, the amount was below the detection limit of 0.0001 g/cm<sup>2</sup>. Because of the minor amounts of splash reaching the ditches and/or streams, no other investigations into tire splash were completed.



**Figure 2.12 Blue dye splashed from a water filled pothole is carried mainly down the road by tires. Lateral splash is mainly within 2.0 m of the pothole**

### **2.3.4 Traffic**

A TrafX vehicle counter was installed at the south end of the large scale sprinkler site to keep track of the number of vehicles passing during and prior to rainfall simulation trials (Figure 2.4). Individual vehicle passages were also recorded manually during the large scale trials and when possible their speed was estimated by timing their passage between two points a known distance apart. GPS units were carried by two logging trucks during several passes through the large scale trial site to confirm traffic speed measurements. Vehicles were classified as loaded logging trucks, empty logging trucks and work trucks, or personal vehicles. Personal vehicles were narrow enough to only influence the eastern half of the road surface and did not affect runoff entering the gutter. Logging trucks and work trucks were wide enough to have at least one tire track on the western half of the road influencing the water reaching the gutter for sampling. TrafX vehicle counters were also installed at km 3 and km 7 of the Mainline road (Figure 2.2).

### **2.3.5 Data Analysis**

#### **2.3.5.1 Determination of background sediment concentrations**

Sediment concentrations in the gutter and hose outflow were assumed to be zero at the start of the trials (time zero). Large scale trials without traffic saw an initial increase in sediment concentration at the start of the experiment followed by a decrease to a steady state concentration. Sediment concentrations in the absence of loaded logging trucks passing during a trial are termed background concentrations. During large scale trials with traffic, background concentrations had additional peaks in sediment concentration following the passage of loaded logging trucks. Empty logging trucks did not produce an increase in sediment concentrations at the gutter outlet, except at very high precipitation intensities (>40 mm/h). Smaller vehicles did not produce a measurable

increase in sediment concentration in gutter outflow and were narrow enough to only affect the eastern portion of the road. Small scale trials were not subject to traffic and all sediment was considered background.

Visual inspection of large scale gutter sediment concentration data revealed that it took approximately 5 minutes for elevated sediment levels to reach the gutter outflow during low intensity rainfall simulation trials and an additional 30 minutes for sediment concentrations to return to background levels following the passage of a loaded logging truck. During medium intensity trials it took 3 minutes for truck related sediment to reach the outflow and an additional 17 minutes for sediment concentrations to return to background levels. During high intensity trials it took 1 minute for truck related sediment to reach the outflow and an additional 14 minutes for sediment concentrations to return to background levels (Figure 2.13 - Figure 2.15).

The influence of sediment pulses caused by the passage of loaded logging trucks was removed from the measured sediment concentrations to obtain the background concentrations. For nozzle 6 trials, samples collected between 5 and 35 minutes after the passage of a loaded logging truck were removed from the concentration time series and a power trend line was fit to the remaining data starting 10 minutes (inclusive) after the trial began. A power trend line was chosen over an exponential trend line because of the better fit for the majority of trials. Background sediment concentrations during truck disturbances were estimated from this power trend line. The error for calculated sediment concentrations was set equal to the measured sediment concentration error for each point. The concentration increase due to truck passage was then calculated as the difference between the measured concentration and the estimated background concentration. For

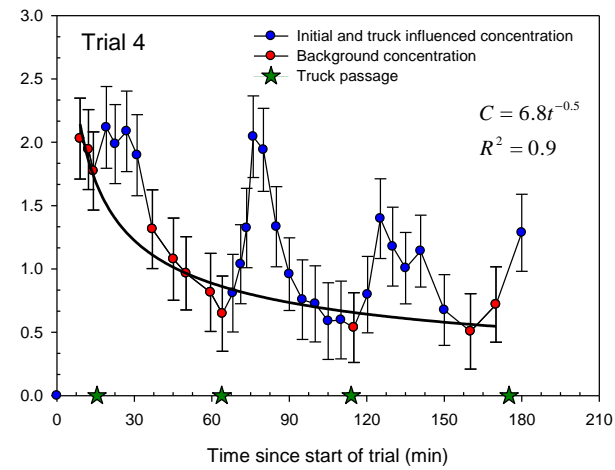
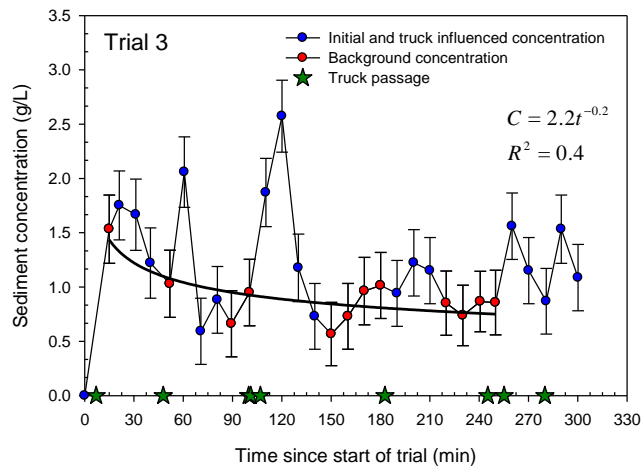
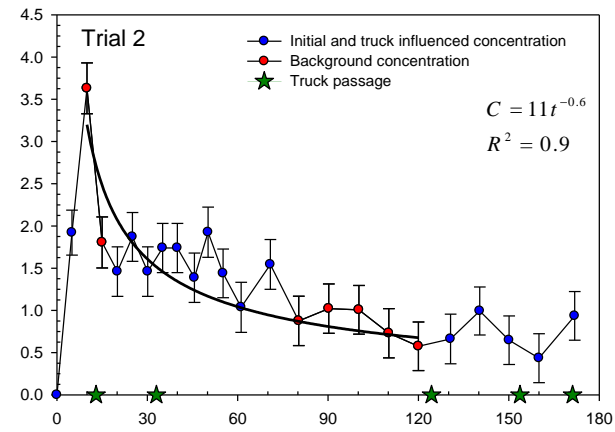
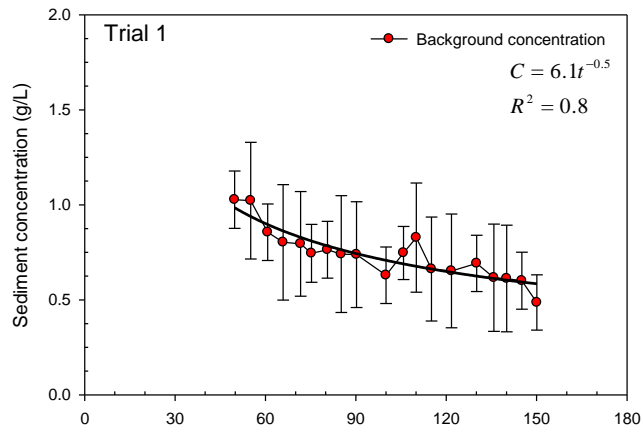


**Figure 2.13 a. Sediment concentrations in the gutter outflow during low intensity trials. The times that a loaded logging truck passed the site are indicated by a star. The equation represents the best fit line for the background concentrations**

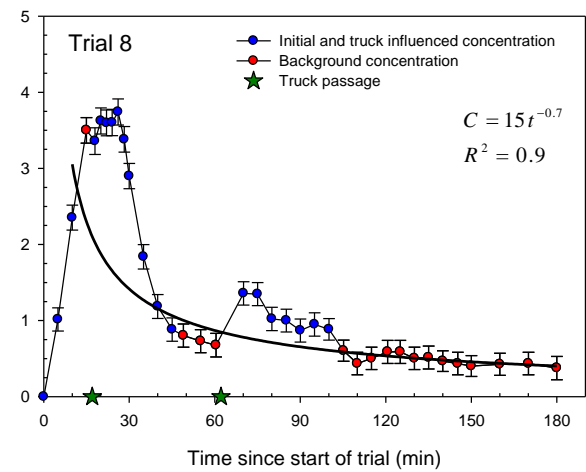
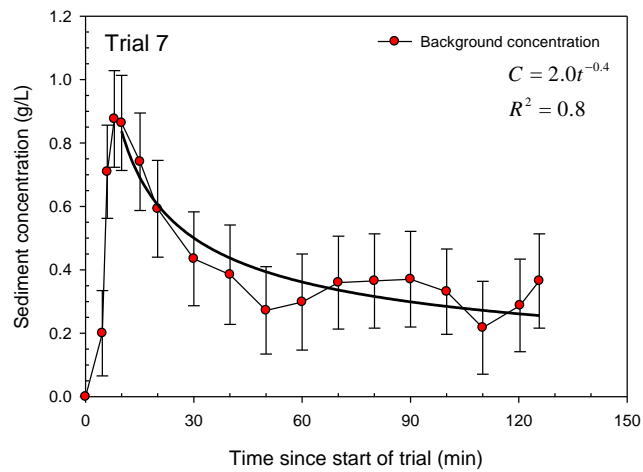
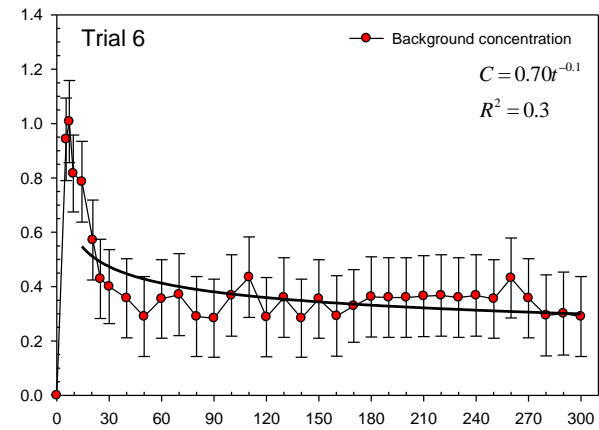
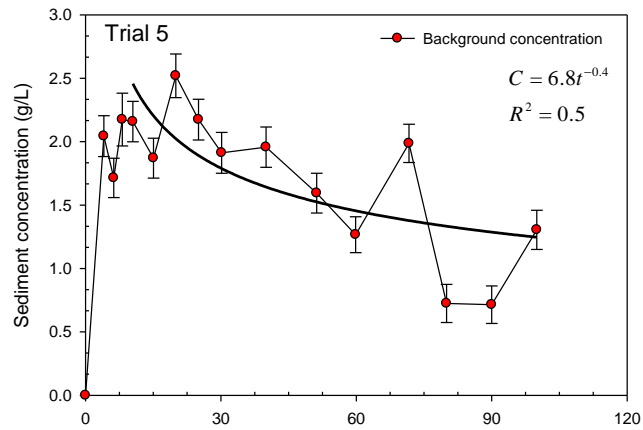


**Figure 2.13 b. Sediment concentrations in the gutter outflow during low intensity trials continued. The times that a loaded logging truck passed the site are indicated by a star. The equation represents the best fit line for the background concentrations**

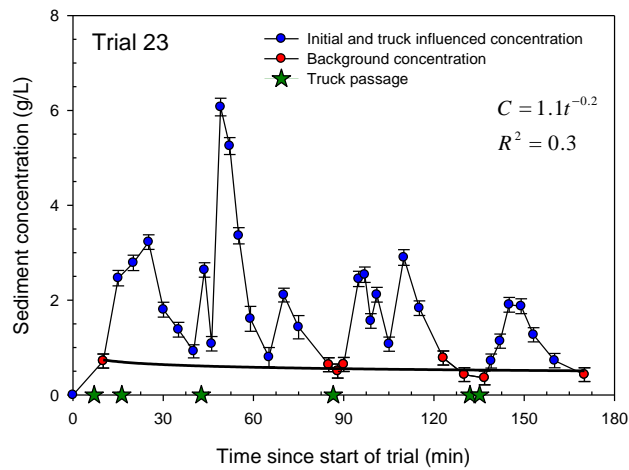
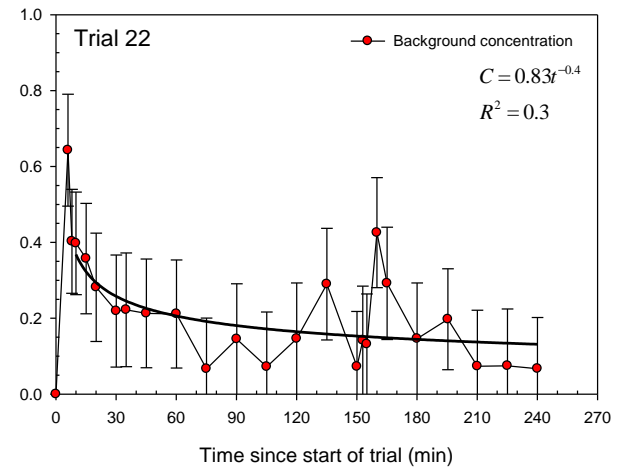
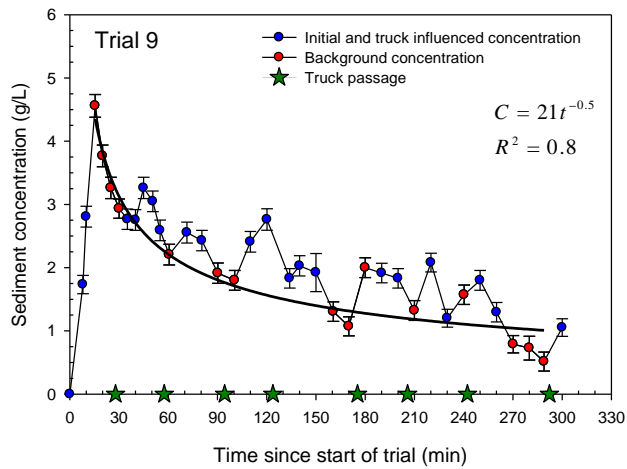
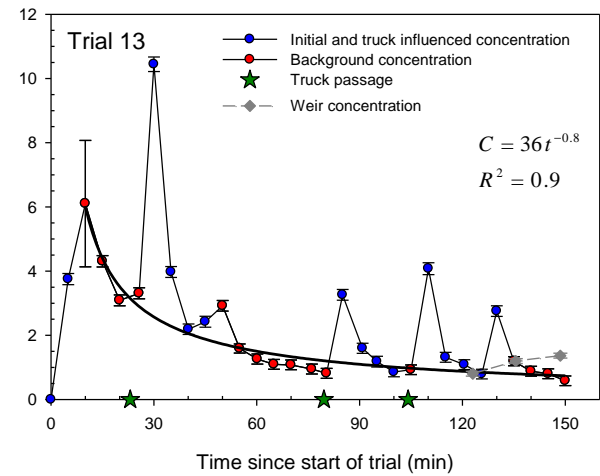
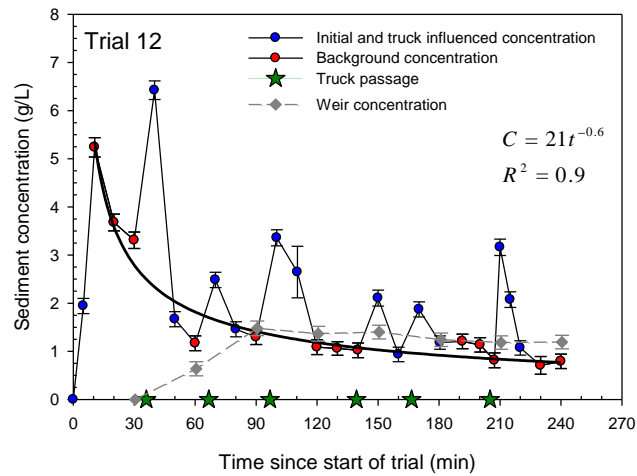
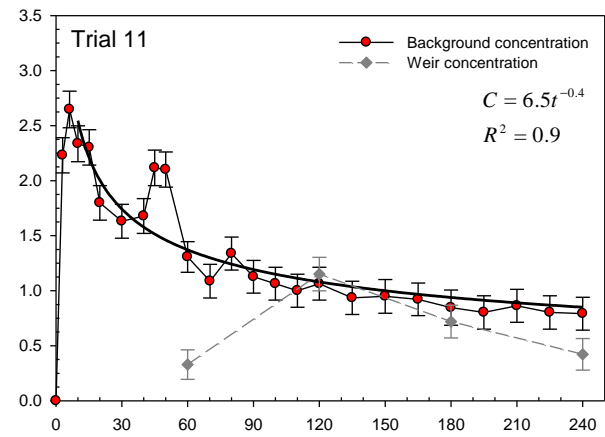
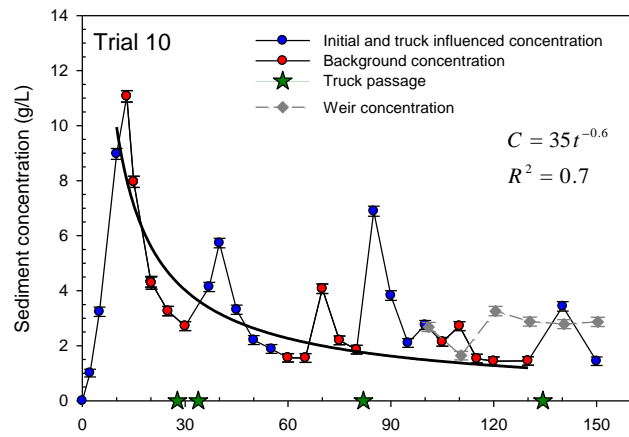
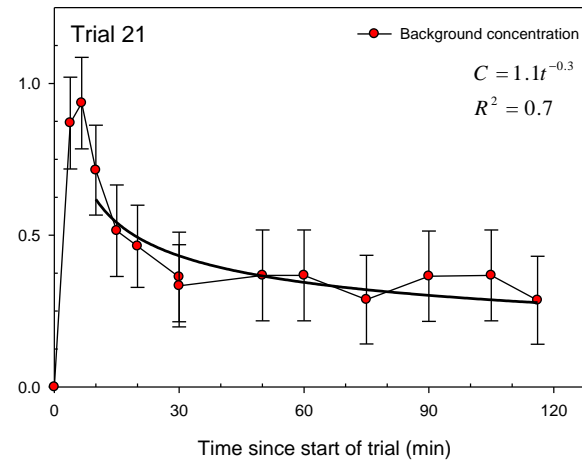
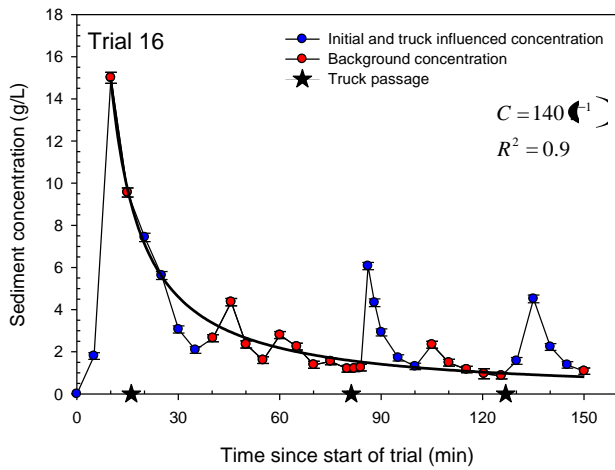
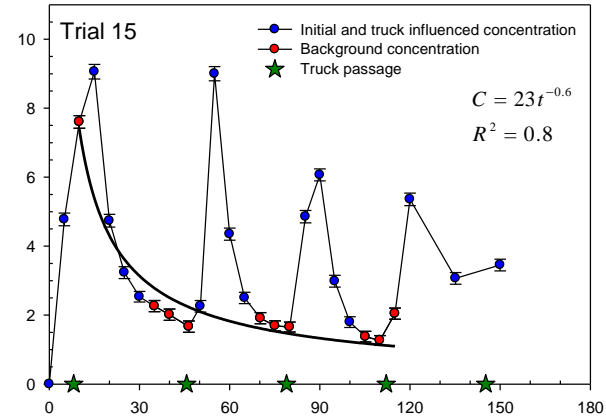
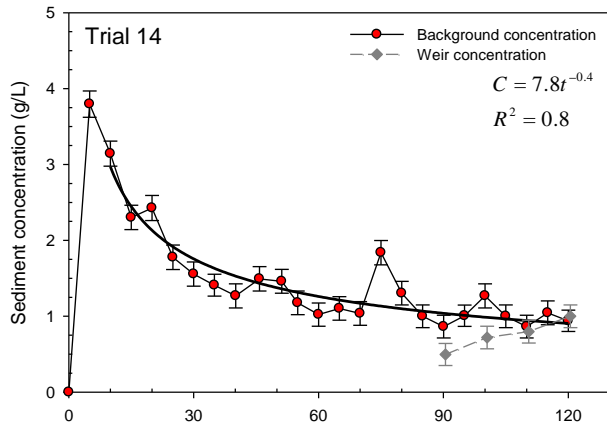


Figure 2.13 c. Sediment concentrations in the gutter outflow during low intensity trials continued. The times that a loaded logging truck passed the site are indicated by a star. The equation represents the best fit line for the background concentrations





**Figure 2.14 a. Sediment concentrations in the gutter and weir outflow during medium intensity trials. The times that a loaded logging truck passed the site are indicated by a star. The equation represents the best fit line for the background concentrations**



**Figure 2.14 b. Sediment concentrations in the gutter and weir outflow during medium intensity trials continued. The times that a loaded logging truck passed the site are indicated by a star. The equation represents the best fit line for the background concentrations**

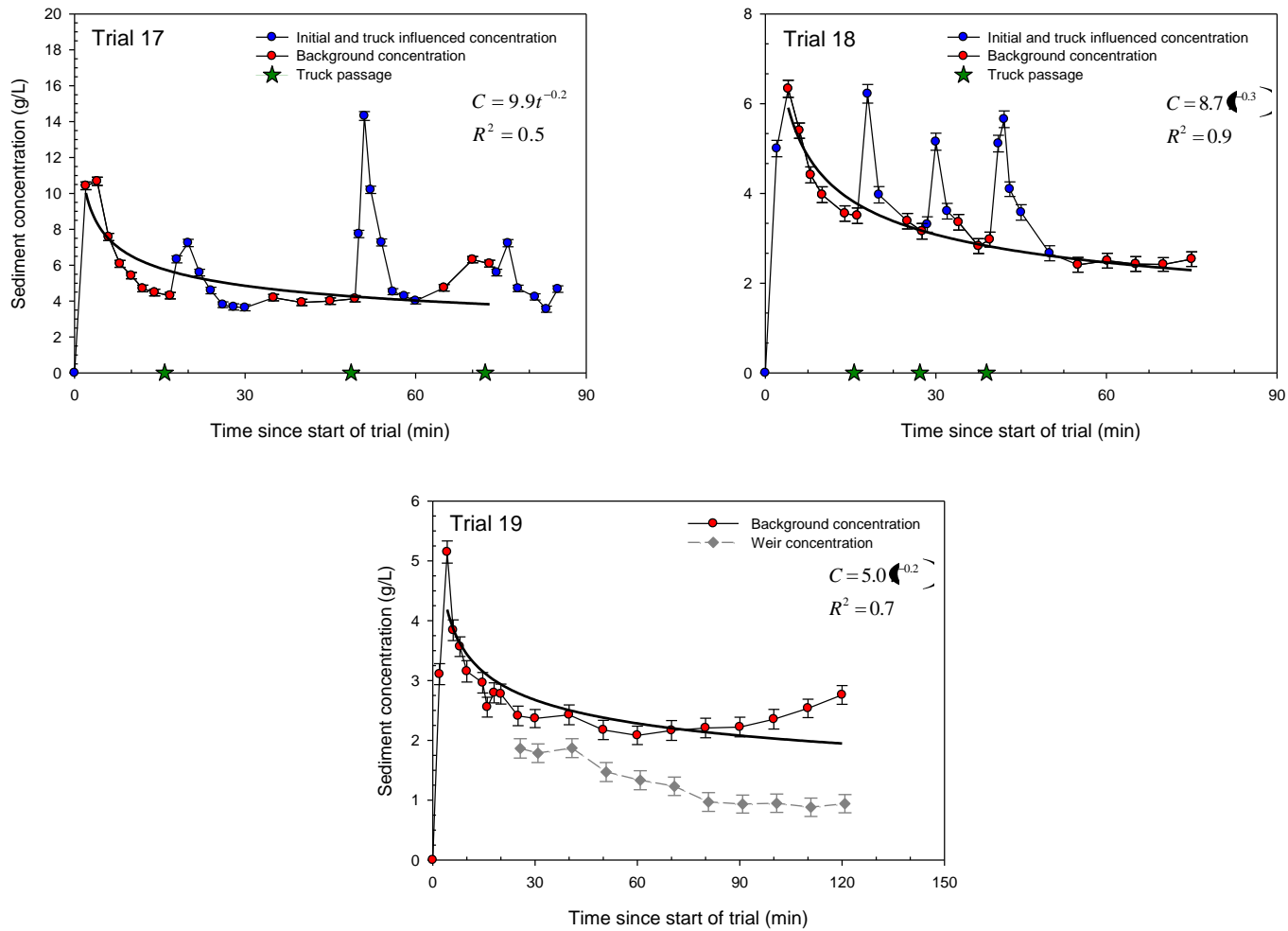
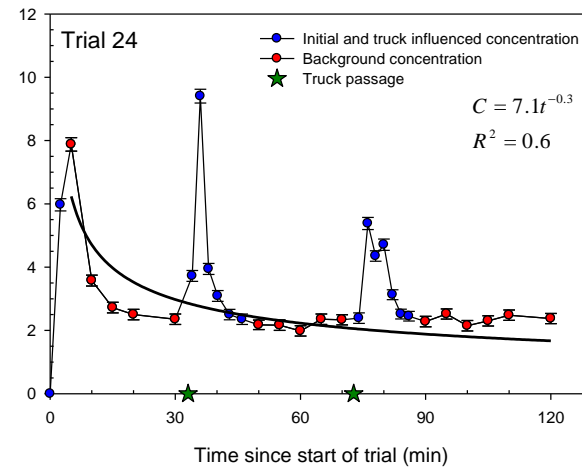
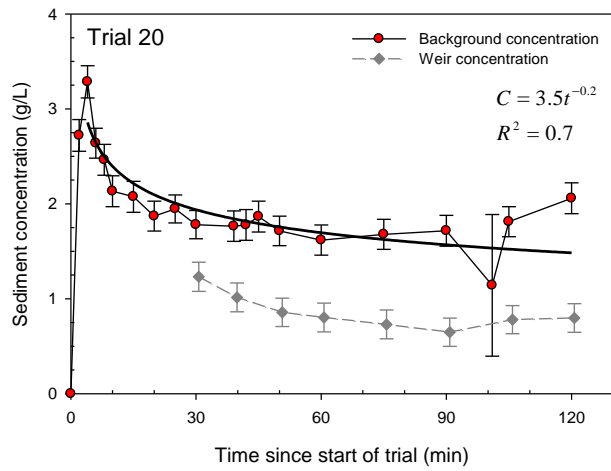
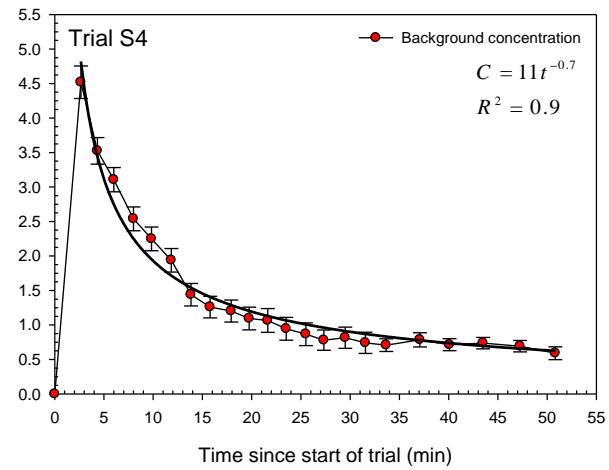
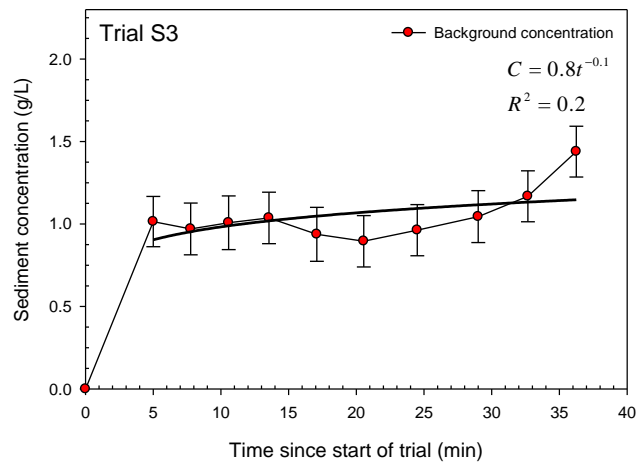
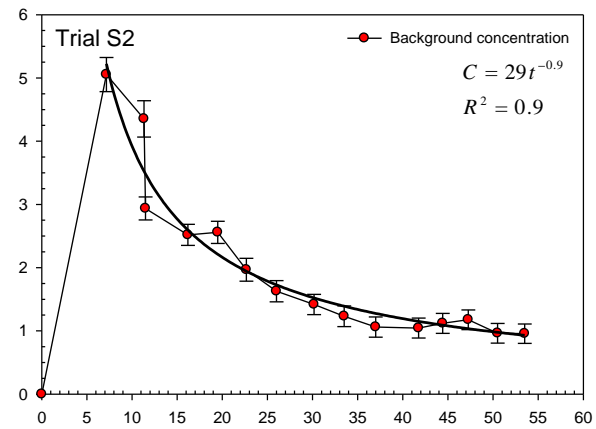
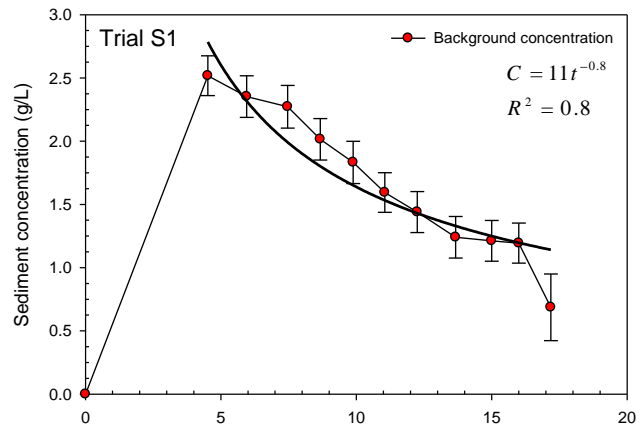


Figure 2.15 a. Sediment concentrations in the gutter and weir outflow during high intensity trials. The times that a loaded logging truck passed the site are indicated by a star. The equation represents the best fit line for the background concentrations



**Figure 2.15 b. Sediment concentrations in the gutter and weir outflow during high intensity trials continued. The times that a loaded logging truck passed the site are indicated by a star. The equation represents the best fit line for the background concentrations**



**Figure 2.16 a. Sediment concentrations during small scale trials. The equation represents the best fit line for the background concentrations**

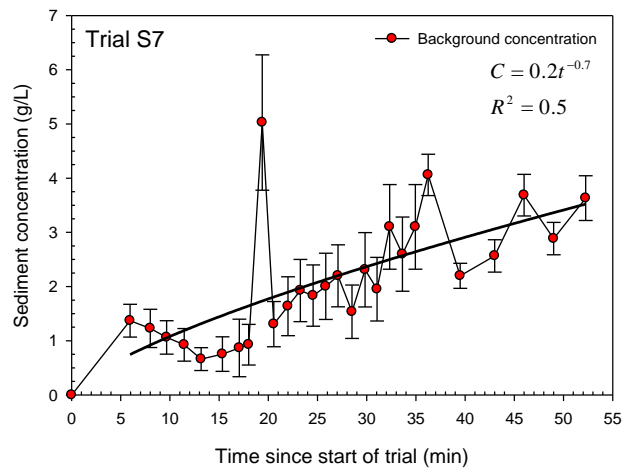
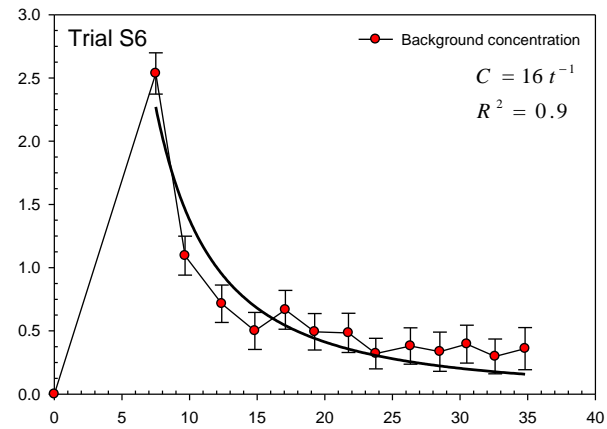
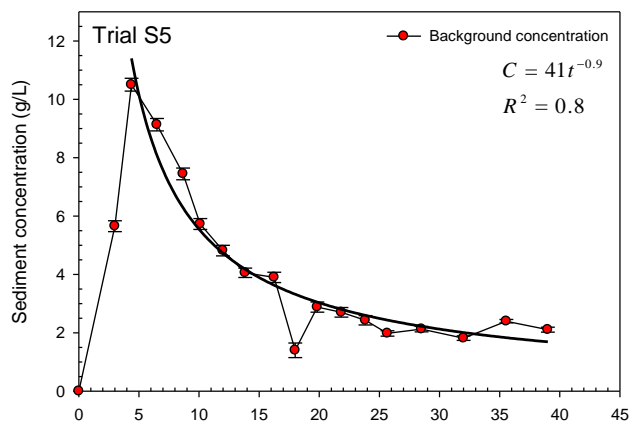


**Figure 2.16 b. Sediment concentrations during small scale trials continued. The equation represents the best fit line for the background concentrations**

trials using nozzle 11, samples between 3 and 20 minutes after the passage of a loaded logging truck were removed and the trend line was fitted to the remaining data points occurring at least 10 minutes into the experiment. For trials using nozzle 22, samples between 1 and 15 minutes after the passage of a loaded logging truck were removed and the trend line was fitted to data points at least 2 minutes into the experiment.

The initial increase in sediment concentration during the large scale experiments was not observed for any of the small scale trials, except S5. Trials S3 and S7 did not show the typical decline to a steady state concentration, likely due to icy conditions at these sites allowing gradual melting and release of sediment with time. A power trend line was fit to the remaining small scale experiments to represent the decline to steady state concentrations (Figure 2.16).

### **2.3.5.2 Determination of mass eroded**

To convert the sediment concentrations into a mass of sediment delivered from the road surface to the gutter, point measurements of sediment concentration were multiplied by the outflow calculated for that time and the time period half way between the previous and following measurement points. The cumulative mass of sediment leaving the road was also determined for each trial. The total mass of sediment eroded by each loaded truck passage was determined similarly. For loaded trucks that passed in succession, meaning a second loaded truck passed before the influence of the previous loaded truck was finished, the total amount of sediment generated by traffic was summed and then divided by the total number of trucks that had passed (Table 2.5).

### 2.3.5.3 Antecedent precipitation index

The antecedent precipitation index was calculated for the large scale simulations based on natural precipitation data collected 2 km north of the large scale rainfall simulation site at Grapple 10 (Figure 2.1) and previous rainfall simulation rainfall. The small scale simulation antecedent precipitation index values only considered natural precipitation. Three, five and ten day antecedent precipitation index values were calculated for the beginning of each trial:

$$API_n = \sum_{i=1}^n \left( \frac{P_i}{i} \right)$$

where  $API_n$  is the antecedent precipitation index,  $P_i$  is the precipitation measured on the  $i^{\text{th}}$  day prior to the trial, and  $n$  is 3, 5 or 10.

### 2.3.5.4 Antecedent traffic

The traffic recorder deployed at the large scale simulation location (km 8) was set to measure the size and duration of disturbances in the earth's magnetic field as vehicles passed, giving a date, time and signal proportional to the size of each vehicle. If a vehicle passed the counter slowly it was counted multiple times. To remove multiple counts created by a single vehicle, signals recorded within 15 seconds of each other were grouped together and attributed to the same vehicle and the maximum value within the group was used.

Comparing values recorded by the traffic recorder with known loaded logging truck, empty logging truck, work truck and personal vehicle or pickup truck passages revealed that loaded and empty logging trucks and work trucks resulted in similar signals with disturbance values above 20 units, while small vehicles and pickup trucks resulted in



**Table 2.5 Overview of the calculated background mass and mass from traffic for the large scale trials**

Trial	Total mass		Total background mass		Total mass due to traffic		% of total mass caused by traffic (%)	# of trucks	Average mass per truck	
	(g)	(±g)	(g)	(±g)	(g)	(±g)			(g)	(±g)
<b>Nozzle 6</b>										
1	4.8x10 <sup>3</sup>	4.6x10 <sup>3</sup>	4.8 x10 <sup>3</sup>	4.6 x10 <sup>3</sup>	-	-	-	-	-	-
2	2.3x10 <sup>3</sup>	1.3 x10 <sup>3</sup>	2.0 x10 <sup>3</sup>	8.2 x10 <sup>2</sup>	2.5 x10 <sup>2</sup>	5.0 x10 <sup>2</sup>	11	4	63	44.8
3	4.4x10 <sup>3</sup>	2.7 x10 <sup>3</sup>	3.3 x10 <sup>3</sup>	1.5 x10 <sup>3</sup>	1.1 x10 <sup>3</sup>	1.3 x10 <sup>3</sup>	25	9	121	51.8
4	2.8x10 <sup>3</sup>	1.7 x10 <sup>3</sup>	2.0 x10 <sup>3</sup>	8.2 x10 <sup>2</sup>	7.0 x10 <sup>2</sup>	8.3 x10 <sup>2</sup>	26	4	176	32.5
5	2.5x10 <sup>3</sup>	4.4 x10 <sup>2</sup>	2.5 x10 <sup>3</sup>	4.4 x10 <sup>2</sup>	-	-	-	-	-	-
6	1.4x10 <sup>3</sup>	6.1 x10 <sup>2</sup>	1.4 x10 <sup>3</sup>	6.2 x10 <sup>2</sup>	-	-	-	-	-	-
7	5.8x10 <sup>2</sup>	2.8 x10 <sup>2</sup>	5.8 x10 <sup>2</sup>	2.8 x10 <sup>2</sup>	-	-	-	-	-	-
8	2.3x10 <sup>3</sup>	7.6 x10 <sup>2</sup>	1.8 x10 <sup>3</sup>	4.8 x10 <sup>2</sup>	5.5 x10 <sup>2</sup>	2.8 x10 <sup>2</sup>	24	2	276	11.8
9	7.3x10 <sup>3</sup>	2.1 x10 <sup>3</sup>	6.0 x10 <sup>3</sup>	1.3 x10 <sup>3</sup>	1.3 x10 <sup>3</sup>	8.2 x10 <sup>2</sup>	17	8	160	46.8
22	5.8x10 <sup>2</sup>	5.1 x10 <sup>2</sup>	5.8 x10 <sup>2</sup>	5.1 x10 <sup>2</sup>	-	-	-	-	-	-
23	3.4x10 <sup>3</sup>	1.0 x10 <sup>3</sup>	1.2 x10 <sup>3</sup>	4.0 x10 <sup>2</sup>	2.2 x10 <sup>3</sup>	6.1 x10 <sup>2</sup>	64	6	358	9.5
<b>Nozzle 11</b>										
10	1.8x10 <sup>4</sup>	2.4 x10 <sup>3</sup>	1.5 x10 <sup>4</sup>	1.7 x10 <sup>3</sup>	2.9 x10 <sup>3</sup>	7.7 x10 <sup>2</sup>	16	4	724	47.0
11	1.1x10 <sup>4</sup>	1.9 x10 <sup>3</sup>	1.1 x10 <sup>4</sup>	1.9 x10 <sup>3</sup>	-	-	-	-	-	-
12	1.8x10 <sup>4</sup>	3.8 x10 <sup>3</sup>	1.4 x10 <sup>4</sup>	2.3 x10 <sup>3</sup>	4.7 x10 <sup>3</sup>	1.6 x10 <sup>3</sup>	26	6	789	61.4
13	1.3x10 <sup>4</sup>	2.6 x10 <sup>3</sup>	9.5 x10 <sup>3</sup>	1.7 x10 <sup>3</sup>	3.6 x10 <sup>3</sup>	8.8 x10 <sup>2</sup>	27	3	1183	32.3
14	6.5x10 <sup>3</sup>	1.0 x10 <sup>3</sup>	6.5 x10 <sup>3</sup>	1.0 x10 <sup>3</sup>	-	-	-	-	-	-
15	2.0x10 <sup>4</sup>	3.0 x10 <sup>3</sup>	1.2 x10 <sup>4</sup>	1.6 x10 <sup>3</sup>	8.0 x10 <sup>3</sup>	1.5 x10 <sup>3</sup>	40	5	1604	36.9
16	1.8x10 <sup>4</sup>	2.5 x10 <sup>3</sup>	1.5 x10 <sup>4</sup>	1.8 x10 <sup>3</sup>	2.2 x10 <sup>3</sup>	7.3 x10 <sup>2</sup>	13	3	735	57.8
21	3.1x10 <sup>3</sup>	1.1 x10 <sup>3</sup>	3.1 x10 <sup>3</sup>	1.2 x10 <sup>3</sup>	-	-	-	-	-	-
<b>Nozzle 22</b>										
17	5.2x10 <sup>4</sup>	7.5 x10 <sup>3</sup>	4.6 x10 <sup>4</sup>	5.7 x10 <sup>3</sup>	6.6 x10 <sup>3</sup>	1.8 x10 <sup>3</sup>	13	3	2193	144.9
18	2.5x10 <sup>4</sup>	3.3 x10 <sup>3</sup>	2.3 x10 <sup>4</sup>	3.0 x10 <sup>3</sup>	1.1 x10 <sup>3</sup>	3.3 x10 <sup>2</sup>	4	1	1067	75.6
19	2.9x10 <sup>4</sup>	2.1 x10 <sup>3</sup>	2.9 x10 <sup>4</sup>	2.1 x10 <sup>3</sup>	-	-	-	-	-	-
20	2.2x10 <sup>4</sup>	4.3 x10 <sup>3</sup>	2.2 x10 <sup>4</sup>	4.3 x10 <sup>3</sup>	-	-	-	-	-	-
24	3.4x10 <sup>4</sup>	8.1 x10 <sup>3</sup>	3.1 x10 <sup>4</sup>	6.9 x10 <sup>3</sup>	2.7 x10 <sup>3</sup>	1.2 x10 <sup>3</sup>	34	2	1360	34.6

disturbance values less than 20 units. The total number of logging and work trucks, the total number of pickup trucks or personal vehicles, and the total number of vehicles passing the site each hour were computed based on this threshold. The number of logging and work trucks and the number of pickup trucks or personal vehicles and the total number of vehicles passing in the one, two, three and six hour period prior to each large scale experiment were calculated. The TrafX recorder at km 3 of the Queen Charlotte Mainline Forest Road South was not set to distinguish between different sized vehicles. When km 8 traffic data were not available the km 3 data was used. Data from the TrafX recorder at km 3 was used for all small scale trial antecedent traffic values

#### **2.3.5.5 Multiple Linear regression**

The dependence of the total mass of sediment generated by the road during a large scale trial on precipitation intensity, duration of the trial, number of truck passages during the trial, the total number of vehicles passing in the previous 2 hours and the three day antecedent precipitation index was determined using multiple linear regression computed in Microsoft Excel 2007. The dependence of the mass of sediment produced by a loaded logging truck on precipitation intensity, truck speed, and time since the beginning of the trial was also assessed this way.

## **2.4 Results and discussion**

### **2.4.1 Non-truck related sediment mass**

There was no relation between trial duration and the total mass of non-truck related sediment generated by the road for the large scale trials (Figure 2.17). This suggests that for the durations in this study (< 5 hours), the size of the initial sediment pulse dominates the total mass of non-truck related sediment generated by the road, not

the steady state sediment removal rate reached later during the trials. This follows the findings of Hairsine and Rose (1992) who showed that erosion rates are greatest near the beginning of storms and Arnáez et al. (2004) who reported greatly reduced sediment concentrations in runoff after the first few minutes of precipitation.

Clockwise hysteresis was evident in the relation between non-truck related sediment concentrations and flow rate for the large scale experiments (Figure 2.18). This suggests sediment transport from the road is a supply, rather than a transport, limited system where the amount of sediment available for transport is less than the transport capacity of the road surface runoff, similar to the findings of Bilby et al. (1989).

There was a positive linear relation between precipitation intensity and the mass of non-truck related sediment generated during the first hour of each trial and the total mass of non-truck related sediment generated throughout the entire trial (Figure 2.19). There was also a positive linear relation between the depth of precipitation and the mass of non-truck related sediment generated during the first hour of each trial and between the total depth of precipitation and the total mass of non-truck related sediment generated throughout the entire trial (Figure 2.20). The relations with precipitation intensity were stronger than those with depth of precipitation, with  $R^2$  values of 0.88 and 0.84 vs. 0.64 and 0.81 for the entire experiment and the first hour respectively. These results suggest that rainfall intensity is the dominant control on sediment generation from forest roads in the absence of traffic. These results are in agreement with those of Amman (2004), who found that variations in suspended sediment concentrations in forest road runoff during rain events for a site in Oregon, were best described by precipitation intensity when it was time lagged to account for sediment transport. These results are, however,

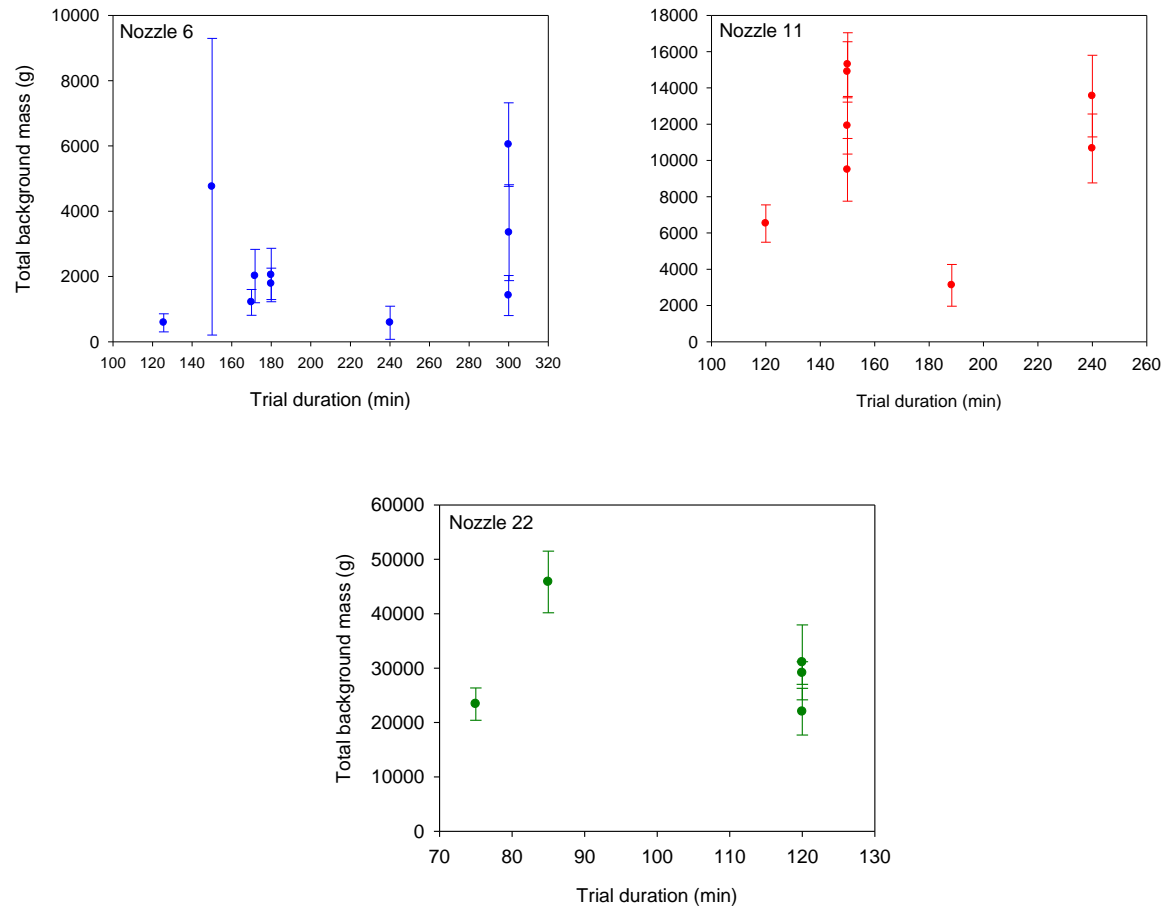


**Figure 2.17** The relations between total background mass and trial duration for the large scale trials. None of the relations are significant at the 95% confidence interval. Error bars represent the maximum possible error

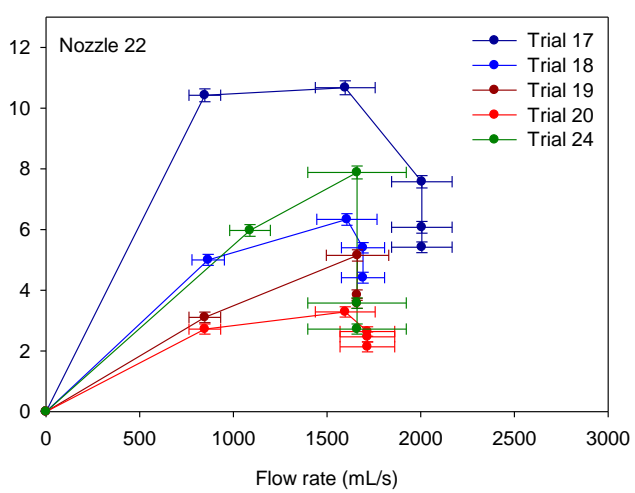
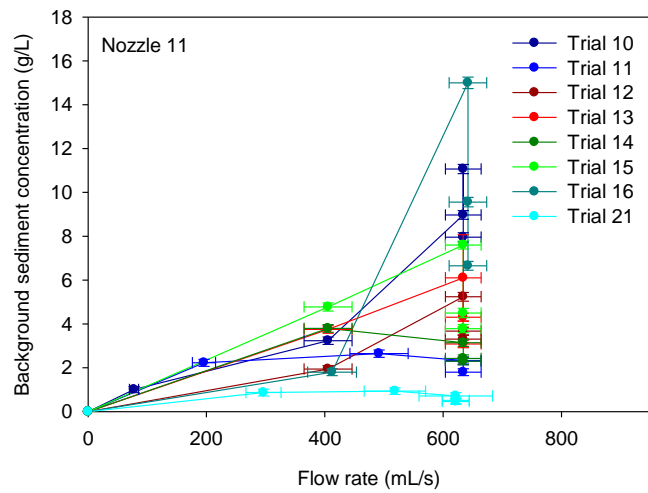
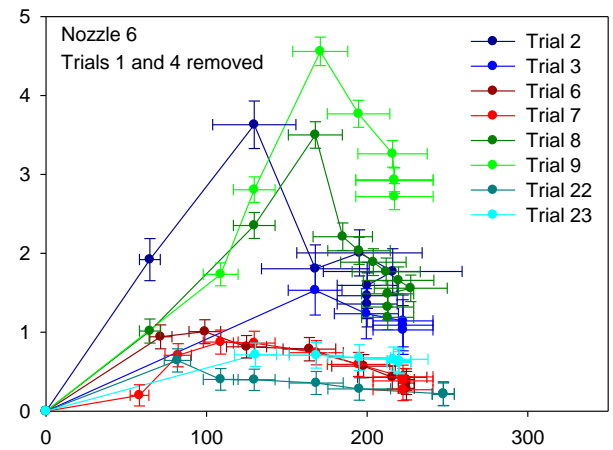
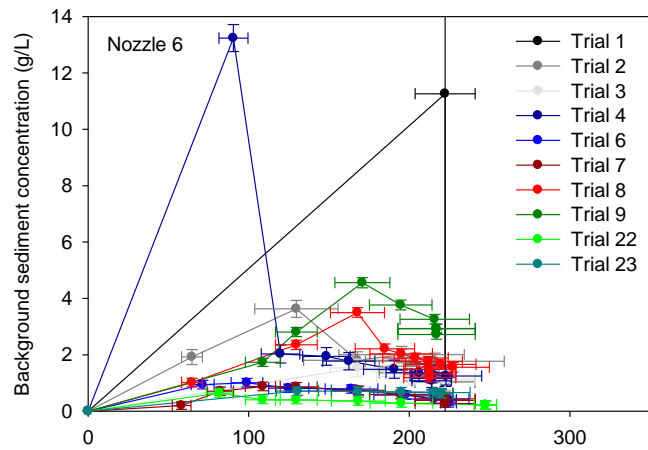


**Figure 2.18 Clockwise hysteric relation between flow rate and background sediment concentration**

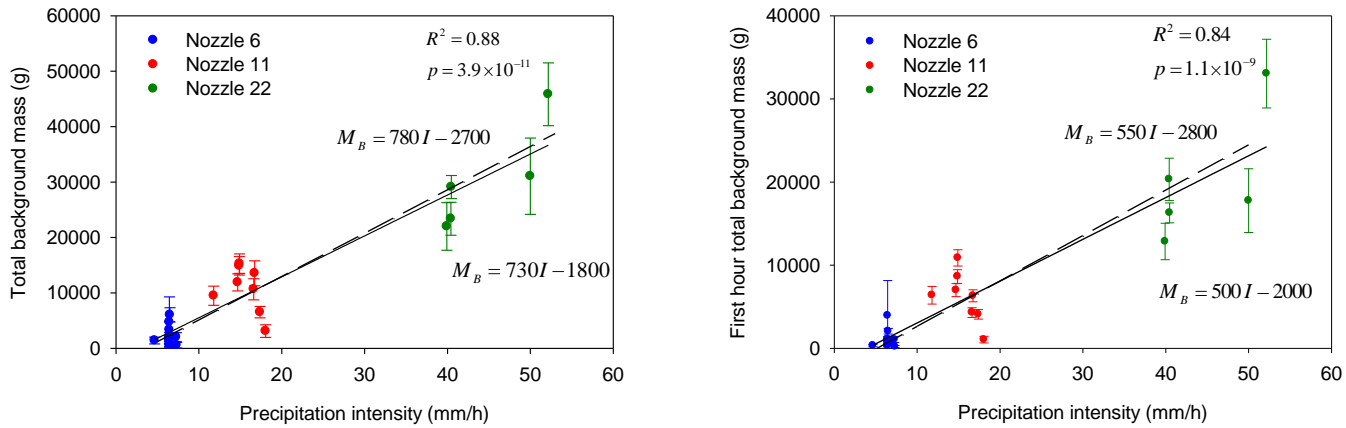


**Figure 2.19** The relation between background mass ( $M_B$ ) and precipitation intensity ( $I$ ) for the large scale trials. Functional analysis relations are shown by the dashed lines while linear regression relations are shown by the solid lines

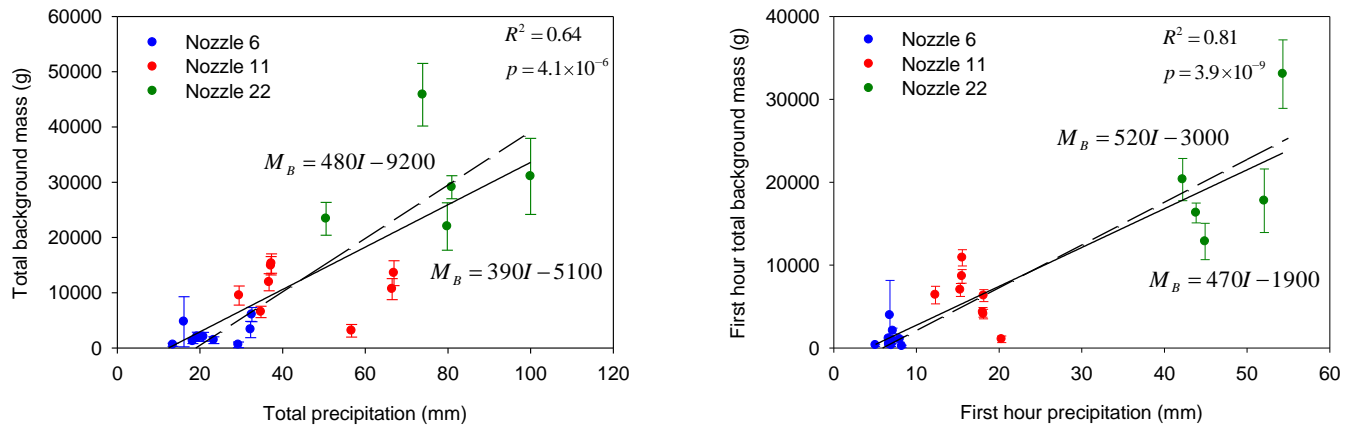


**Figure 2.20** The relation between background mass and ( $M_B$ ) precipitation ( $P$ ) for the large scale trials. Functional analysis relations are shown by the dashed lines while linear regression relations are shown by the solid lines

contradictory to the findings of Reid and Dunne (1984), who found only a poor relation between sediment concentration and precipitation intensity or precipitation amount for a site in Washington. This also disagrees with the findings of Croke et al. (2006) who found no significant relation between sediment concentrations in road surface runoff samples and rainfall intensity for a site in southeastern New South Wales, Australia.

The intercepts of the relations between precipitation and background mass suggest that threshold precipitation intensities and depths may be required to initiate sediment transport off the road. Regression intercepts were, however, not significant at the 95% confidence interval, possibly due to the low number of trials. Additional trials would thus be required to confirm this.

There was a positive linear relation between the steady state gutter outflow rate reached by the end of each large scale trial and the total non-truck related mass of sediment produced during a trial (Figure 2.21). There was also a positive linear relation between the steady gutter outflow rate and the steady state non-truck related sediment concentration (Figure 2.22). This supports the conclusion that rainfall intensity is the primary control on sediment generation from the road surface.

The relation between the 3, 5 and 10 day Antecedent Precipitation Index (API) and the total amount of non-truck related sediment generated from the road during each trial (Figure 2.23), as well as the relation between the 3, 5 and 10 day API and the amount of non-truck related sediment generated during the first hour of each trial (Figure 2.24) were not significant at the 95% confidence interval. These results suggest that antecedent moisture conditions only have a minor effect on sediment generation from this forest road, though the low number of trials also reduces the strength of these relations.

While there appears to be a non-linear decline in total and first hour non-truck related sediment with increased API, it may be the result of more trials being completed during lower API conditions. Additional trials, with a greater range of API values would be required to confirm the relation. Antecedent moisture conditions were also not significantly related to the runoff ratio, suggesting runoff from the road occurs regardless of antecedent conditions. The runoff ratio was also not significantly related to rainfall amount or rainfall intensity.

The relation between non-truck related sediment generated by the road in the first hour of a large scale trial and both the number of large trucks and the total number of vehicles passing through the site in the previous one, two, three and six hour periods was not significant at the 95% confidence interval except for medium intensity trials (Figure 2.25). Although a linear relation can be visually determined for low and high intensity trials, the low number of trials reduces the statistical significance of these relations. The (non-significant relations) suggest a higher sensitivity to antecedent traffic exists at higher rainfall intensities. However, additional trials are needed to confirm this relation. The visual relations are in agreement with findings presented by Bilby et al. (1989) who showed the total number of axles since the last storm influenced sediment concentrations in ditch flow for normal traffic conditions.

#### **2.4.2 Mass due to traffic**

Elevated sediment levels lasted for 30 minutes following the passage of a loaded logging truck during low intensity trials and for shorter times at higher rainfall intensities. This supports the findings of Luce and Black (2001) who found traffic related sediment pulses during precipitation events persisted on a time scale of tens of minutes.



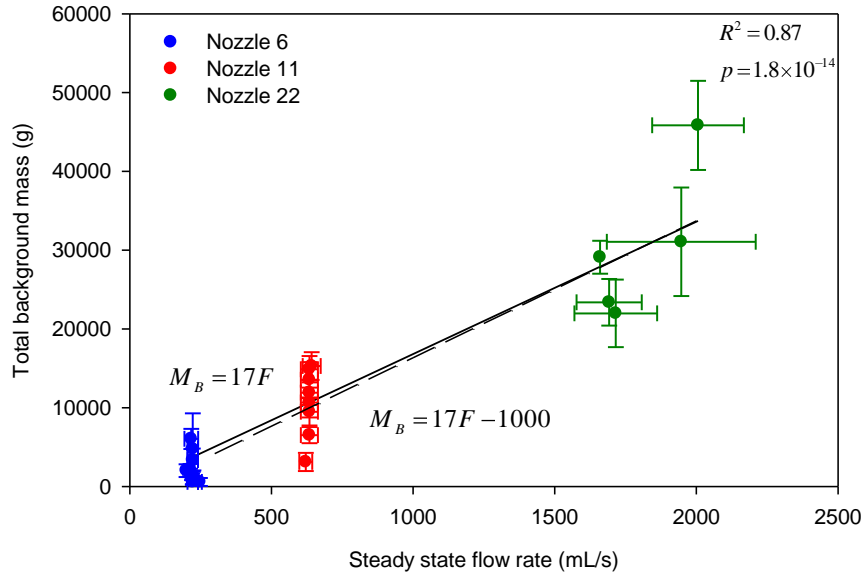


**Figure 2.21** The relation between steady state gutter outflow ( $F$ ) and total non-truck related mass ( $M_B$ ) generated during a large scale trial. The functional analysis relation is shown by a dashed line while the linear regression relation is shown by a solid line

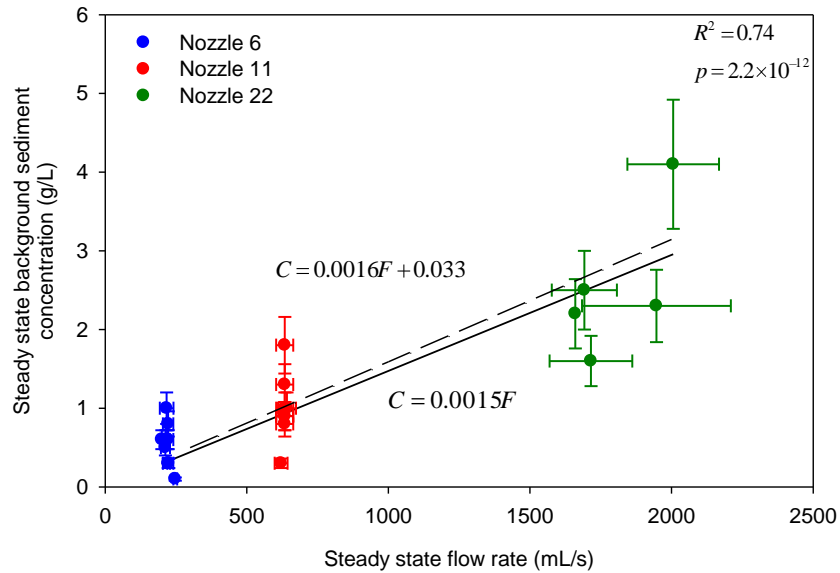


**Figure 2.22** The relation between steady state gutter outflow ( $F$ ) and steady state sediment concentration ( $C$ ) during large scale trials. The functional analysis relation is shown by a dashed line while the linear regression relation is shown by a solid line

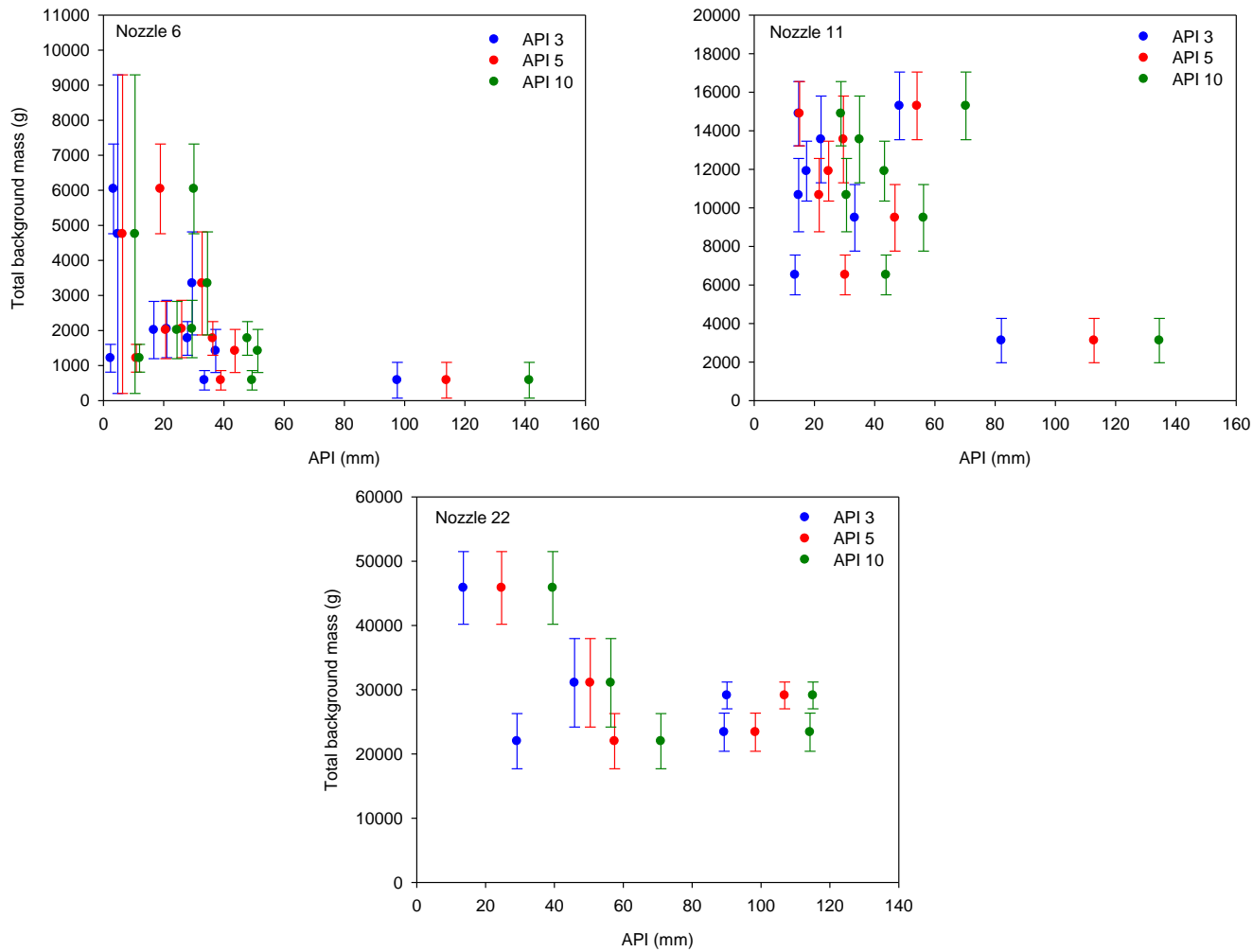


**Figure 2.23 Total background mass during large scale trials as a function of the antecedent precipitation index (API). None of the relations are significant at the 95% confidence interval**

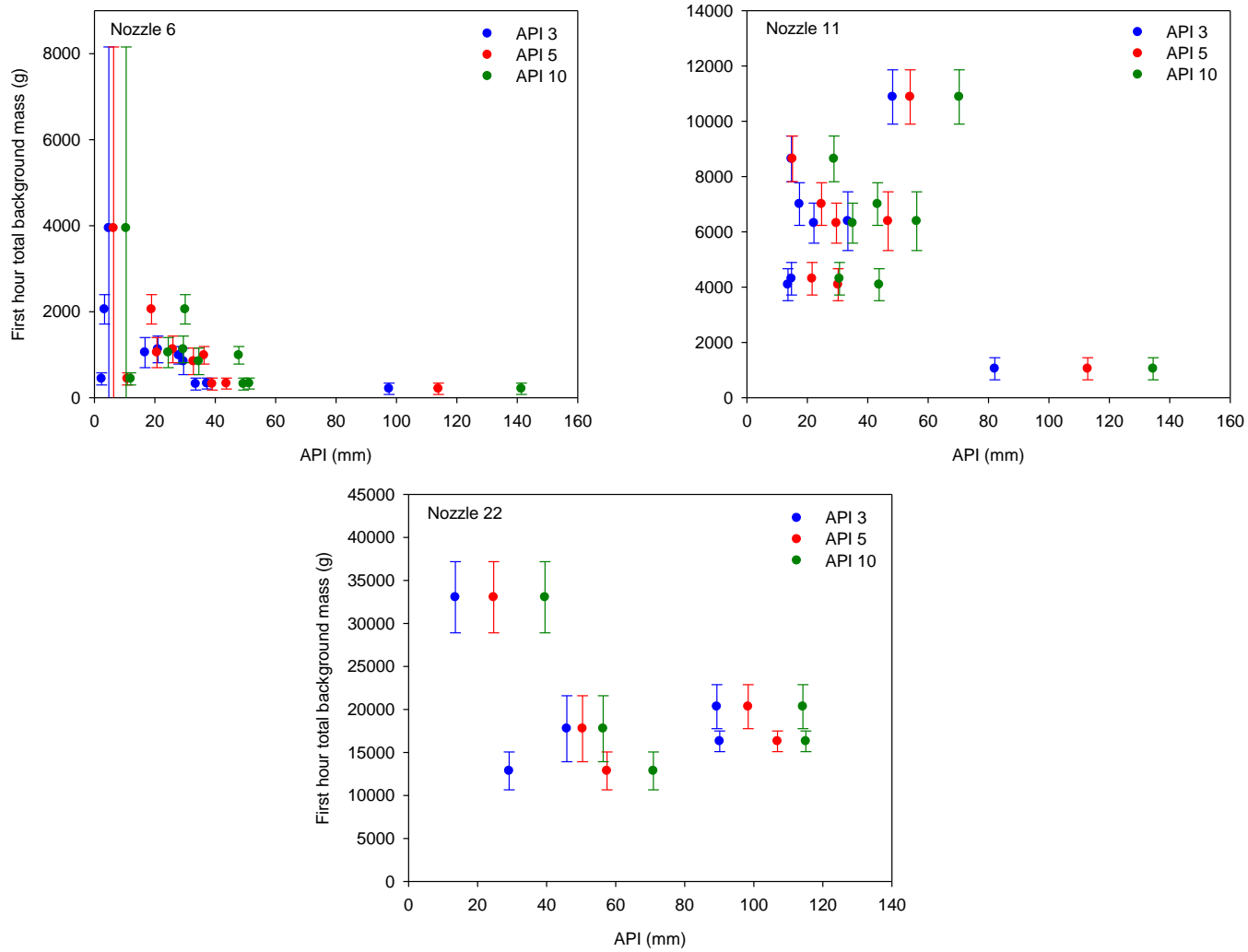


**Figure 2.24 First hour background mass during large scale trials as a function of the antecedent precipitation index (API). None of the relations are significant at the 95% confidence interval**

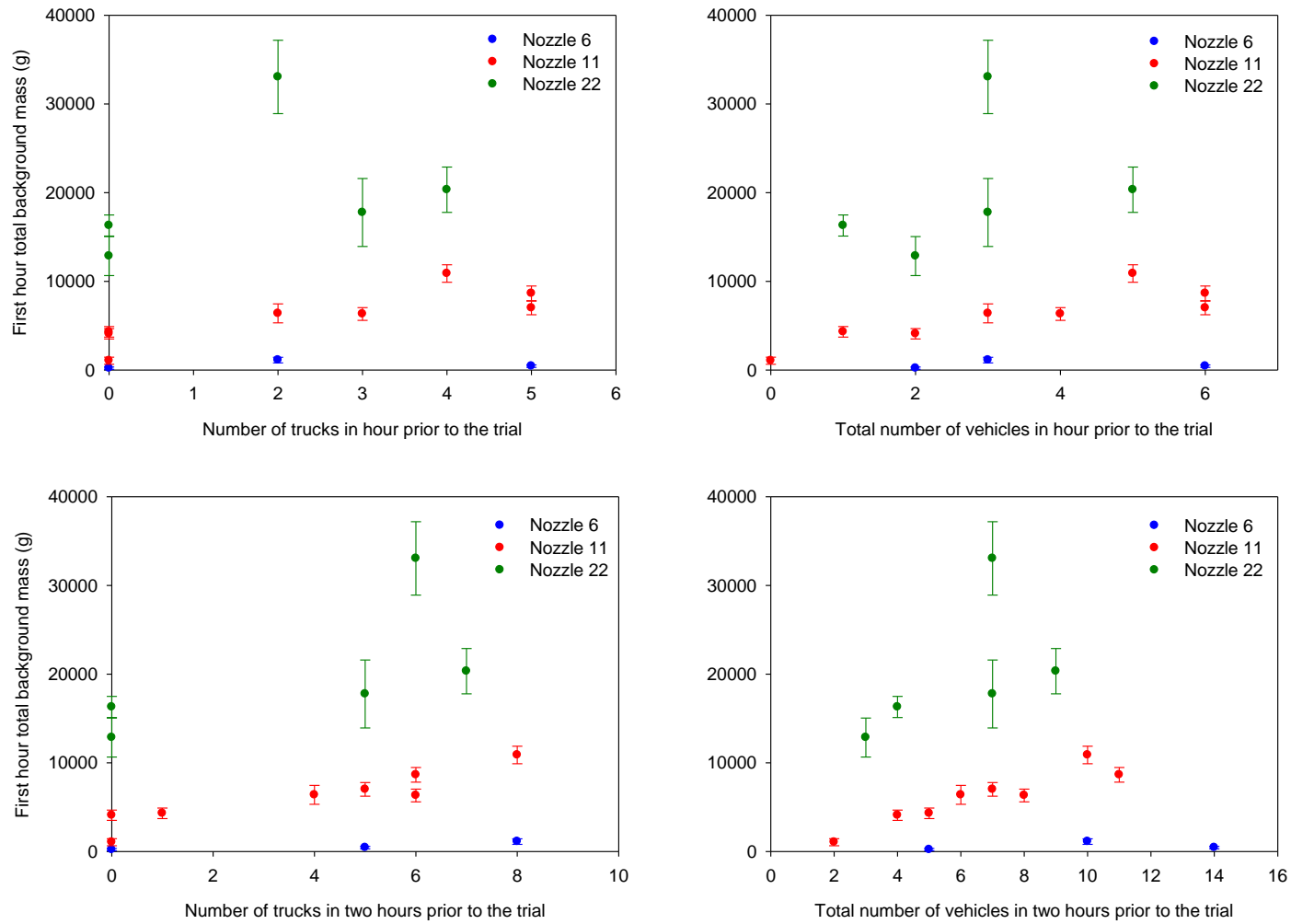


**Figure 2.25 a. The relation between antecedent traffic intensity and the mass of background sediment generated in the first hour of a large scale trial. Only nozzle 11 trials are significant at the 95% confidence interval**

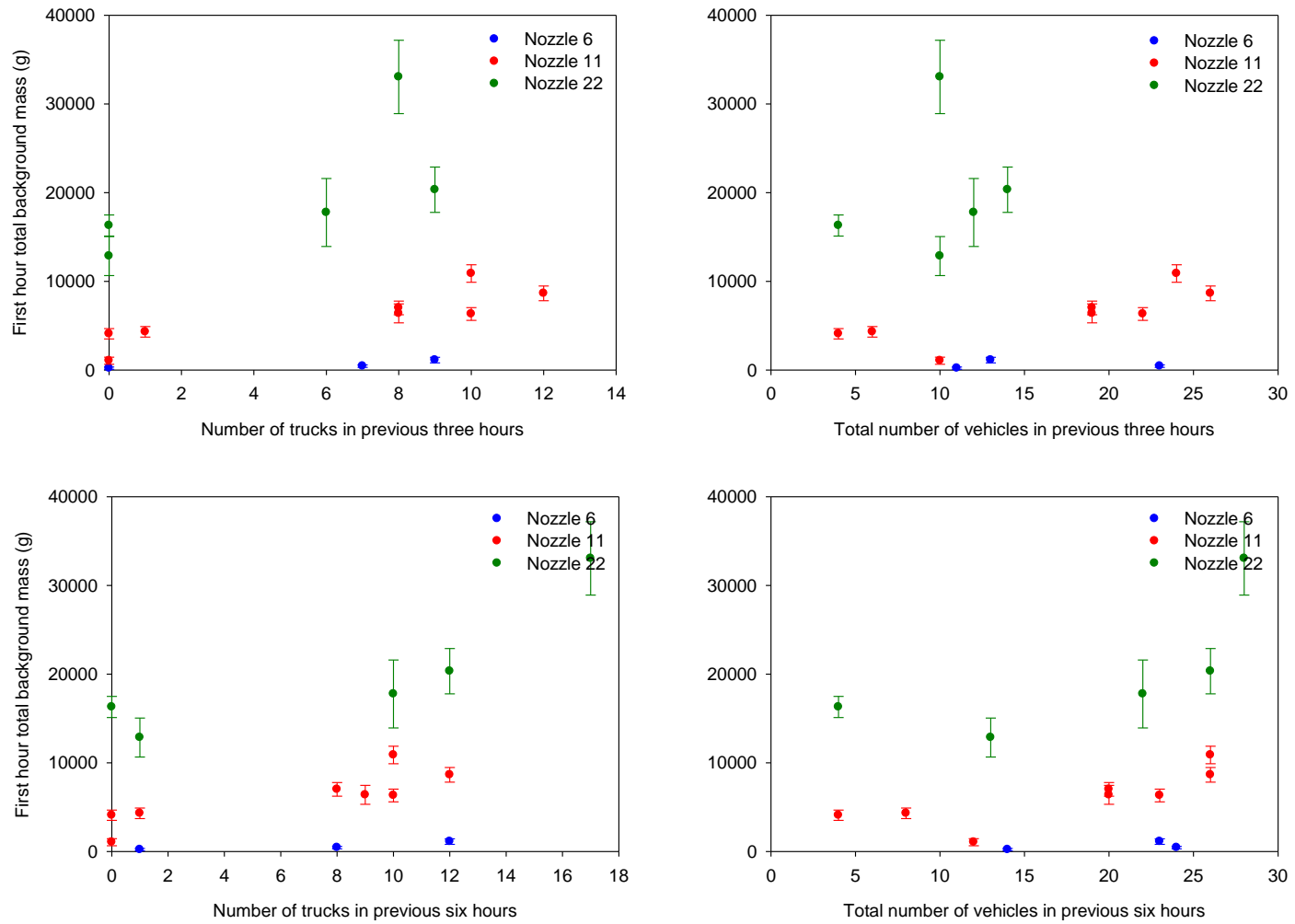


**Figure 2.25 b. The relation between antecedent traffic and the mass of background sediment generated in the first hour of a large scale trial continued. Only nozzle 11 trials are significant at the 95% confidence interval**

pulses during precipitation events persisted on a time scale of tens of minutes (See Section 2.3.5.1).

The relation between the number of loaded logging trucks passing during a trial and the total volume of sediment generated by trucks during the trial was not significant at the 95% confidence interval for low, medium or high intensity trials (Figure 2.26). This is probably due to the small number of trucks passing during each trial as (non-significant) positive linear relations can be noted visually for low, medium and high intensity trials. A relation between the number of loaded logging trucks passing during a trial and the total volume of sediment generated by trucks is expected based on the results of Bilby et al. (1989) who found the number of axles during a precipitation event was a main factor in explaining the sediment concentrations in ditch flow. Additional trials are necessary to determine if a similar relation exists for the Queen Charlotte Mainline Forest Road South. The non-significant relations suggest that the total volume of sediment generated by trucks is more sensitive to truck passage during high intensity rainfall than during low intensity rainfall.

The volume of sediment generated by the passage of a loaded logging truck increased with precipitation intensity in a logarithmic fashion (Figure 2.27). A logarithmic relation was chosen over a linear relation as it explained more of the variation in the volume of sediment generated. This non-linear relation suggests the volume of sediment generated by a truck will reach a maximum value at a certain precipitation intensity, or that there is more variability in the volume of sediment generated by a truck at higher precipitation intensities.

Although the relation between the time into the trial when a truck passed and the volume of sediment the truck produced was significant at the 95% confidence interval for low intensity trials, the nature of the relation was not obvious (Figure 2.28). Bilby et al. (1989) suggest that accumulation of fine sediments during heavy traffic buffers the road surface from further abrasion and sediment production, resulting in decreased sediment from truck passage later during a rainfall event. This was not seen on the Queen Charlotte Mainline Forest Road South. The smaller number of trucks observed later during the trials, however, may have influenced this result.

The relation between truck speed and the amount of sediment it generated was not significant at the 95% confidence interval (Figure 2.29), although this could in part be due to the high uncertainty in the truck speed measurements. There was also no significant relation at the 95% confidence interval between the volume of sediment generated by traffic during each trial and the antecedent precipitation conditions, even when only the first truck in an experiment was considered (Figure 2.30), suggesting trucks generate sediment pulses regardless of antecedent precipitation conditions.

### **2.4.3 Total mass**

There was a positive linear relation between total mass of sediment generated during a trial and precipitation intensity as well as between the total mass of sediment generated during a trial and precipitation depth (Figure 2.31). This follows from the relations between non-truck related sediment mass as well as truck related sediment mass and precipitation intensity and precipitation depth. Similar to the relations for non-truck related mass and truck related mass, total sediment mass was more dependent on

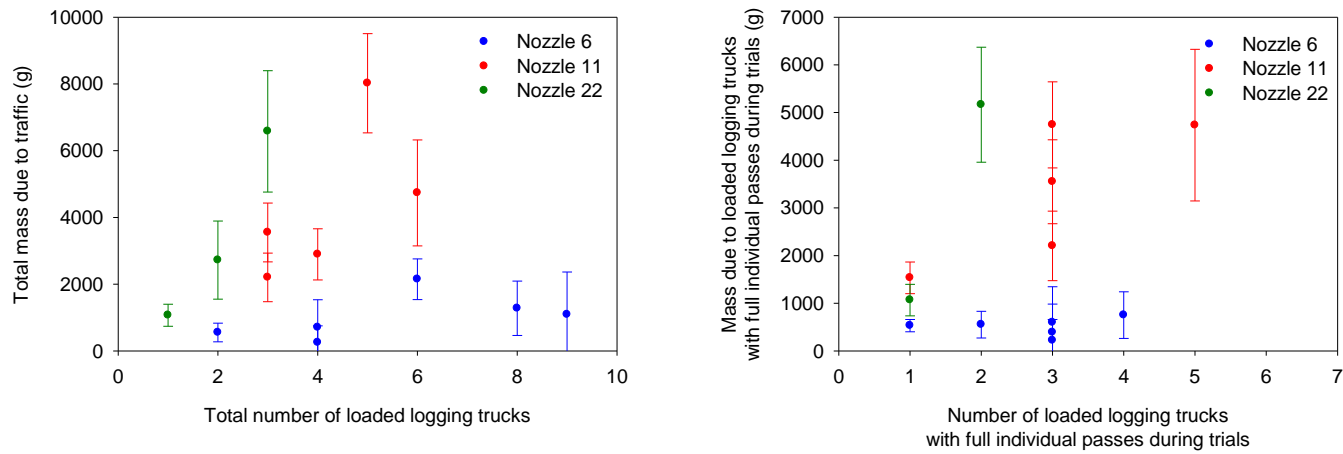


**Figure 2.26** The relation between mass due to traffic and number of truck passages during a trial. None of the relations are significant at the 95% confidence interval

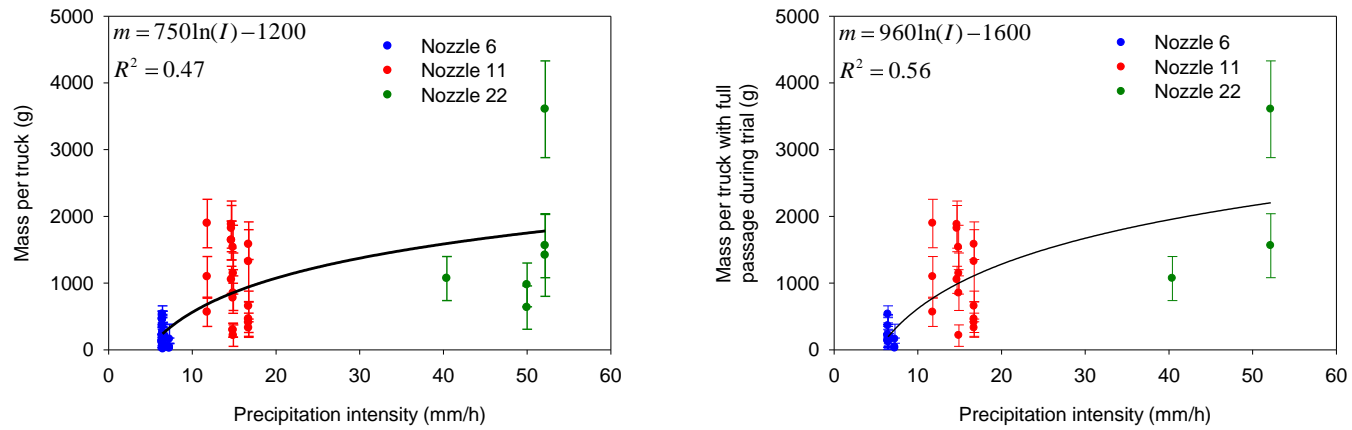


**Figure 2.27** The relation between mass per truck ( $m$ ) and precipitation intensity ( $I$ )



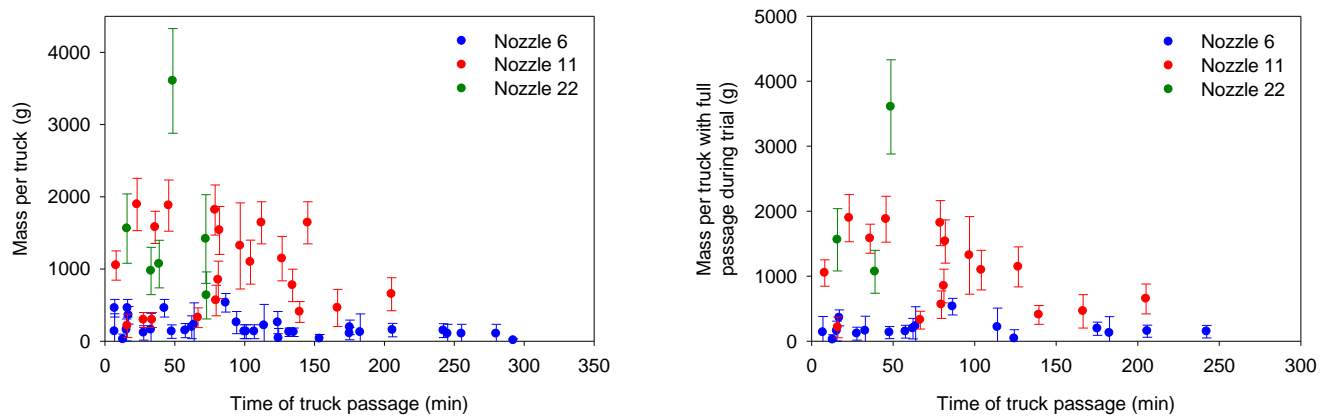


**Figure 2.28** The relation between sediment mass due to a truck passage and time in the trial. The relations are significant at the 95% confidence interval for nozzle 6 trials only

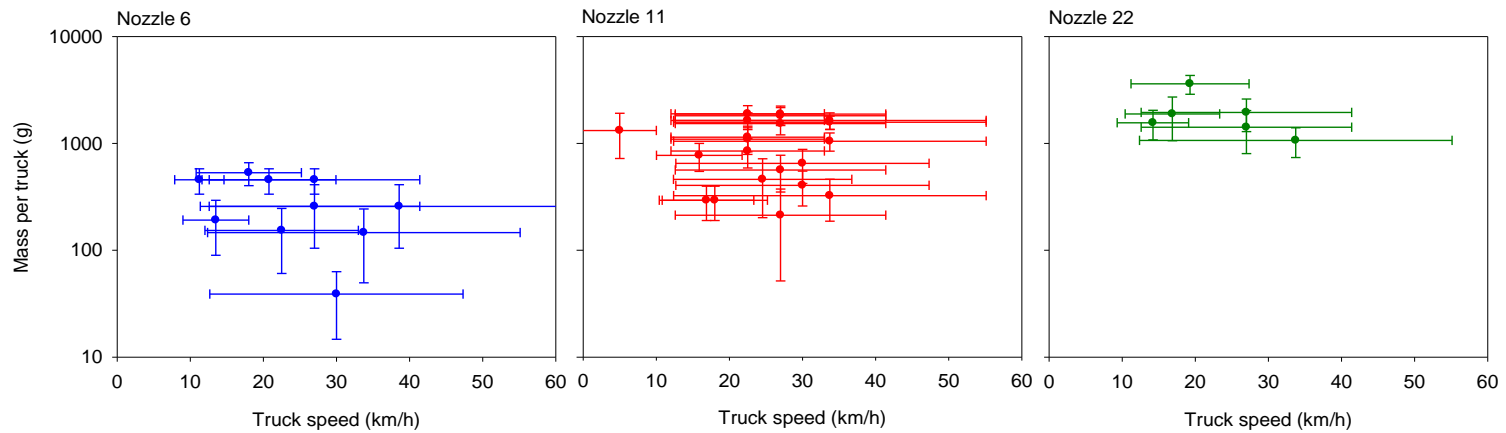


**Figure 2.29** The relation between mass per truck passage and truck speed. None of the relations are significant at the 95% confidence interval

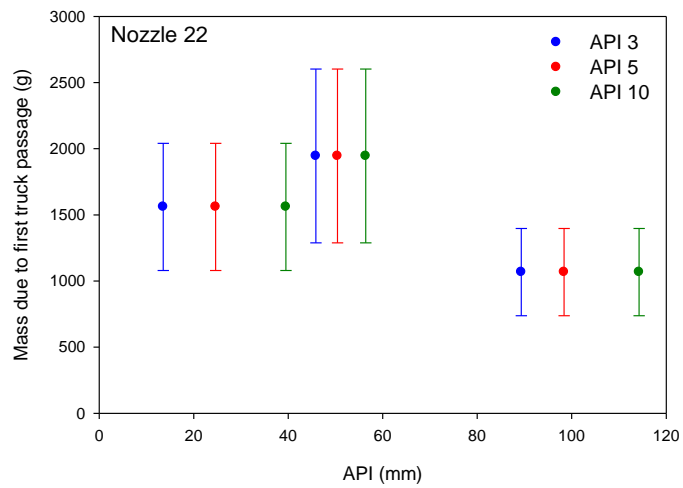
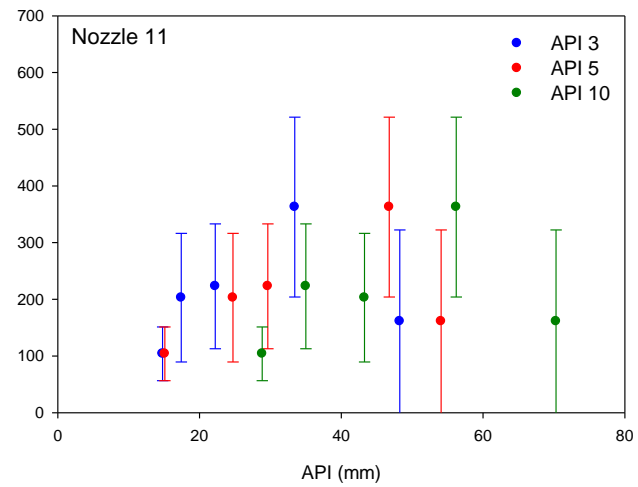
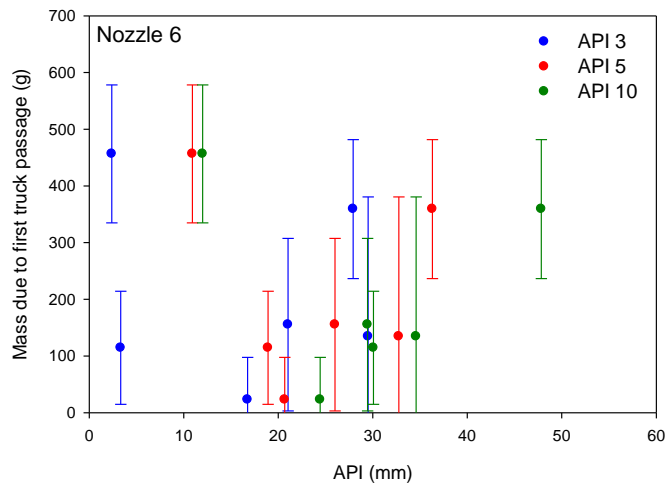


**Figure 2.30 Mass of sediment generated by the first truck passage during a trial compared to 3, 5 and 10 day antecedent precipitation indexes. None of the relations are significant at the 95% confidence interval**

precipitation intensity than precipitation depth as there was no clear relation between trial duration and total sediment generated during the trial.

Similar to the relations between the number of loaded logging trucks passing during a trial and the volume of sediment generated by trucks (Figure 2.26), the relation between the total mass of sediment produced during a trial and the number of loaded logging trucks passing during a trial was only significant at the 95% confidence interval for medium intensity trials (Figure 2.32). The relations for low and high intensity trials may become significant when a greater number of trials are tested. Reid and Dunne (1984) and Croke et al. (2005) showed a large proportion (68% and 95% respectively) of their observed variation in sediment concentration was accounted for by road use.

Similar to the relation between non-truck related sediment generated by the road and both the number of large trucks and the total number of vehicles passing through the site in the previous one, two, three and six hour periods, the relation between total mass of sediment generated during a large scale trial and the antecedent traffic was not significant at the 95% confidence interval except for medium intensity trials (Figure 2.33). Again a linear relation can be visually determined for low and high intensity trials, but the low number of trials reduces their significance.

Multiple linear regression showed the total mass of sediment generated during a trial was most strongly dependent on precipitation intensity and the number of trucks passing during a rainfall event. The influence of trial duration, antecedent traffic, and antecedent precipitation was not significant. The mass of sediment generated can be estimated by the equation:

$$M = 723I + 512n$$

where  $M$  is the total sediment mass generated by the event in g,  $t$  is the duration of the event in minutes,  $I$  is the precipitation intensity in mm/h,  $n$  is the number of loaded logging trucks passing during the event. A large amount of the variation in sediment production from the site is represented by this equation (adjusted  $R^2 = 0.85$ ).

#### **2.4.4 Ditchflow measurements**

The elevated sediment concentrations following the passage of trucks that were observed in the gutter were not mirrored in the east ditch (Figure 2.4). The initial peak in sediment concentration observed in gutter outflow at the beginning of each trial was also not evident in weir sediment concentrations. Flow at the weir, when it occurred, was also delayed compared to gutter outflow. This suggests significant mixing occurred in the ditch. Sediment concentrations in ditch water were generally lower than background (non-truck-influenced) sediment concentrations observed in the gutter during the first 90 minutes of medium intensity trials. At later times during low and medium intensity trials sediment concentrations measured at the weir were similar to the background sediment concentrations observed in the gutter (Figure 2.13 and Figure 2.14). For high intensity trials sediment concentrations measured at the weir were generally lower than the background sediment concentrations measured in the gutter (Figure 2.15).

The similarity between weir and gutter steady state sediment concentrations during low and medium intensity trials suggests road surface runoff dominated ditch flow. The lower weir steady state sediment concentrations observed during high intensity trials suggests some settling of road surface sediment occurred. In July 2010 it was observed that significant sedimentation (approximately 11 cm) had occurred behind the weir plate since August 2009.

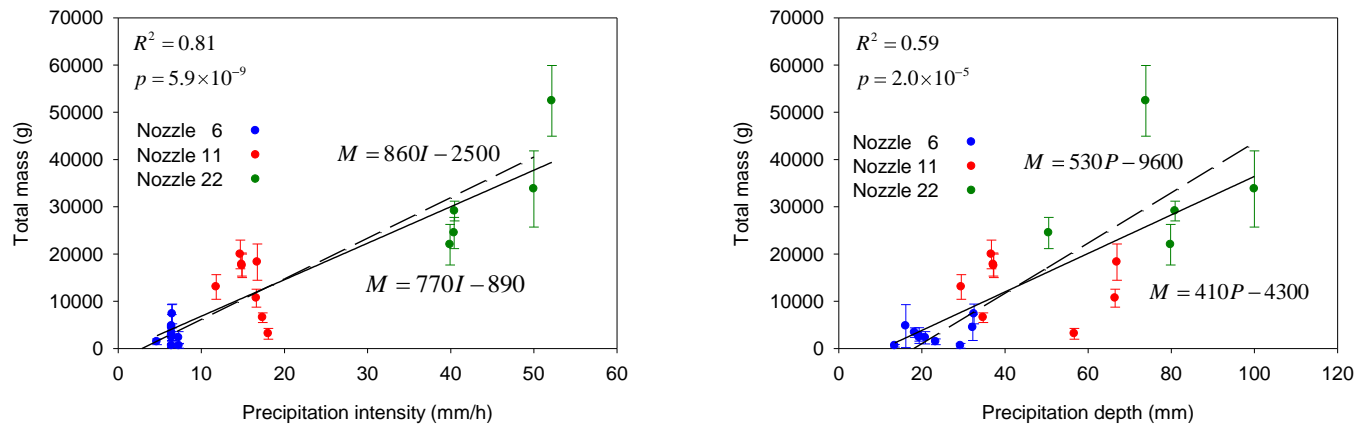


**Figure 2.31** The relation between total sediment mass (*M*) generated during a trial and precipitation intensity (*I*) and depth (*P*). Functional analysis relations are shown by the dashed lines while linear regression relations are shown by the solid lines

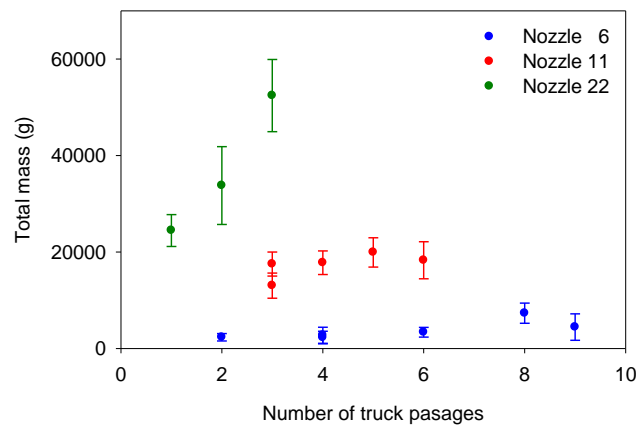


**Figure 2.32** The relation between total sediment mass generated during a trial and number of truck passages. None of the relations are significant at the 95% confidence interval

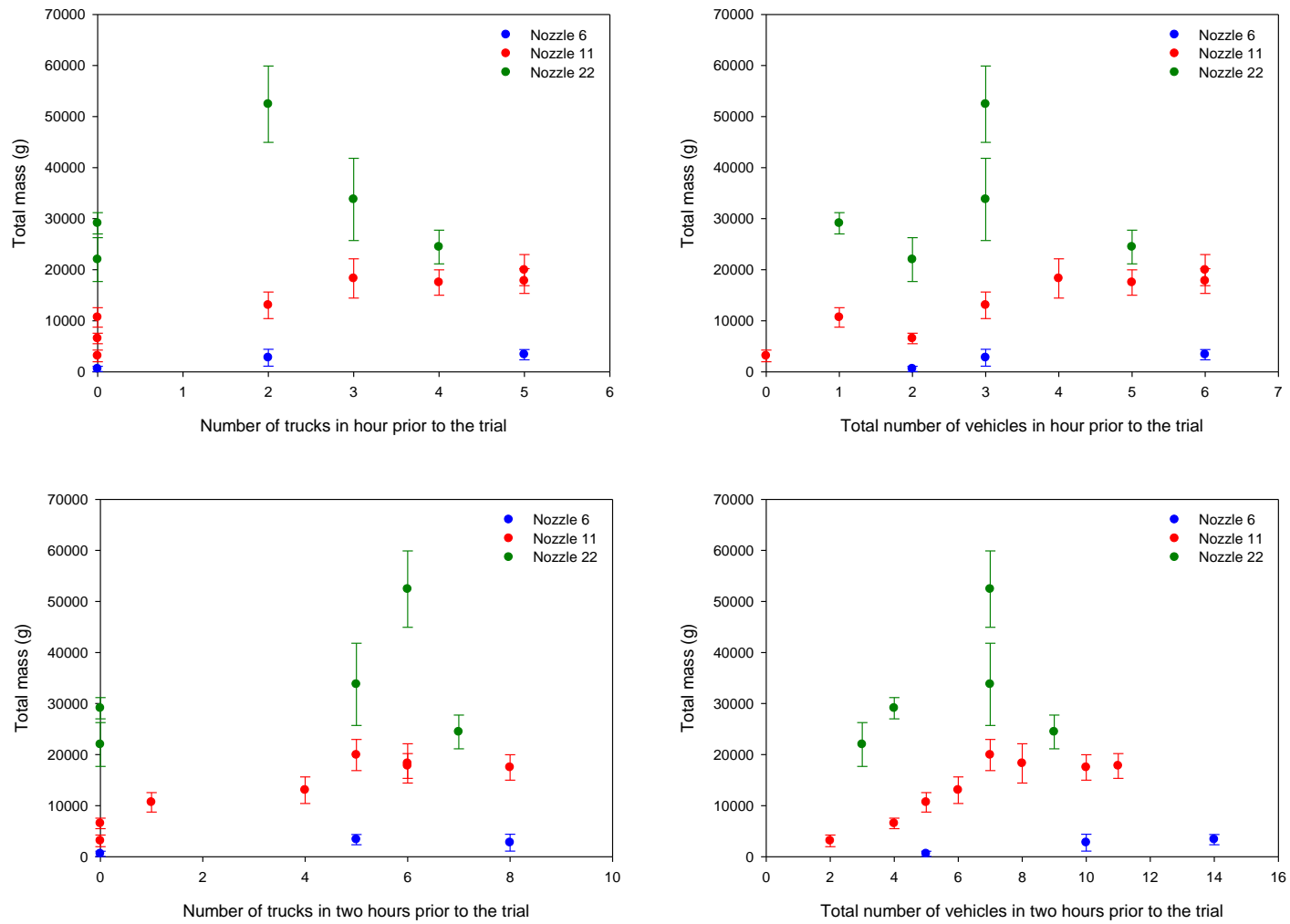


**Figure 2.33 a. The relation between antecedent traffic and the total sediment mass generated during a large scale trial. Only nozzle 11 trials are significant at the 95% confidence interval**

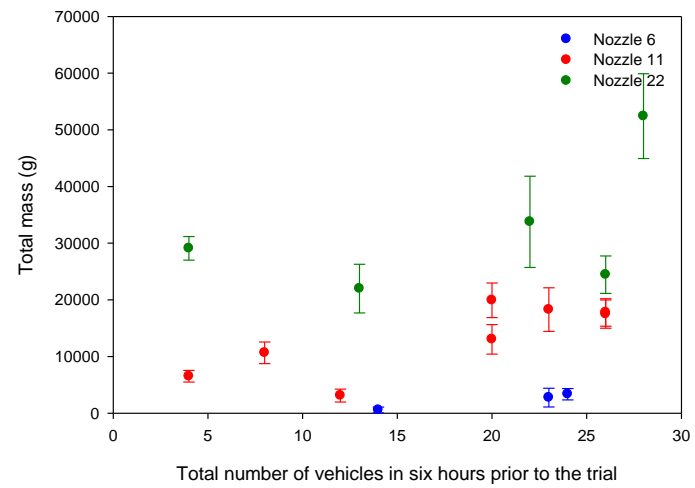
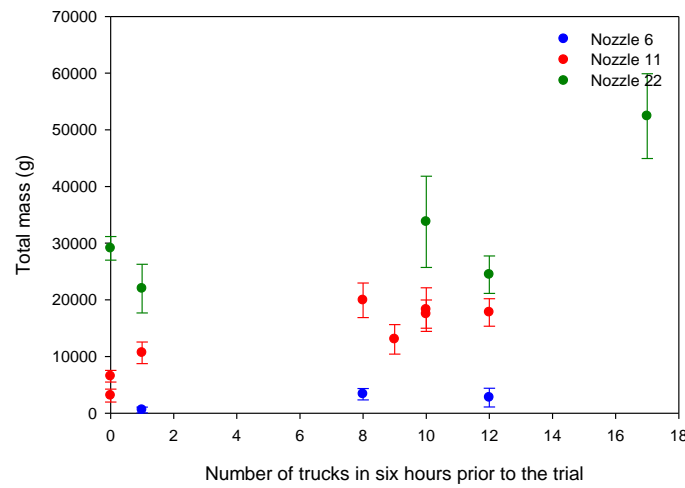
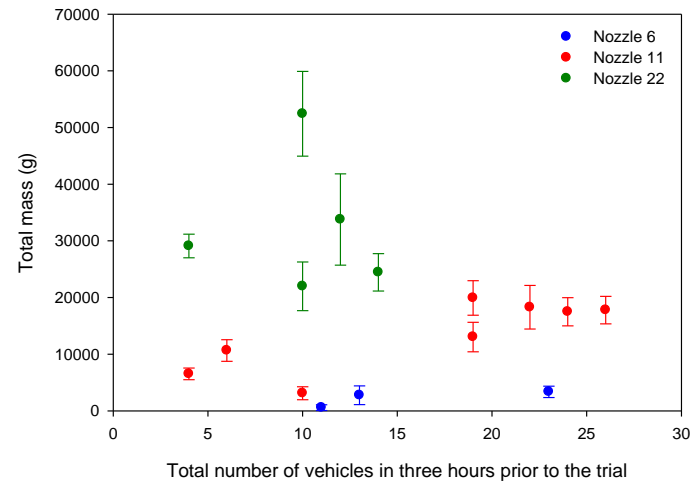
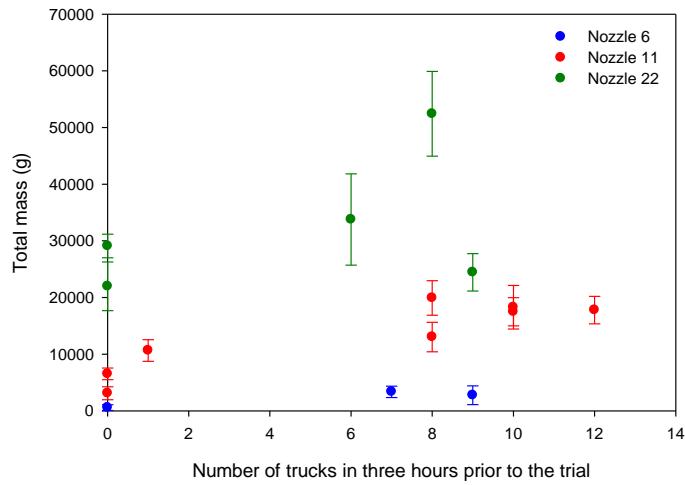


**Figure 2.33 b. The relation between antecedent traffic and the total mass of sediment generated during a large scale trial. Only nozzle 11 trials are significant at the 95% confidence interval**

### 2.4.5 Small scale results

There was a large variation in the peak sediment concentrations and total mass of sediment generated during small scale trials (Figure 2.16). This reveals a large spatial variability in sediment generation from the road surface. Steady state sediment concentrations reached at the end of each small scale trial, however, were similar for all small scale and large scale rainfall simulations.

There was no significant relation between the total mass of sediment generated during a small scale trial and either precipitation intensity or depth of precipitation (Figure 2.34 and Figure 2.35). There was also no significant relation between the total mass of sediment generated and trial duration or antecedent precipitation conditions for the small scale trials.

There was a no significant relation between slope of the road and total mass of sediment generated during small scale trials (Figure 2.36), however further trials on a wider range of slopes would be required to confirm these results.

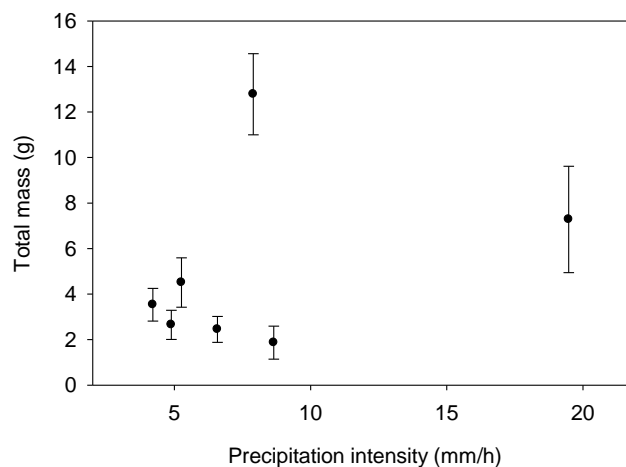


**Figure 2.34 The relation between the total mass of sediment and precipitation intensity for the small scale trials. The relation is not significant at the 95% confidence interval**



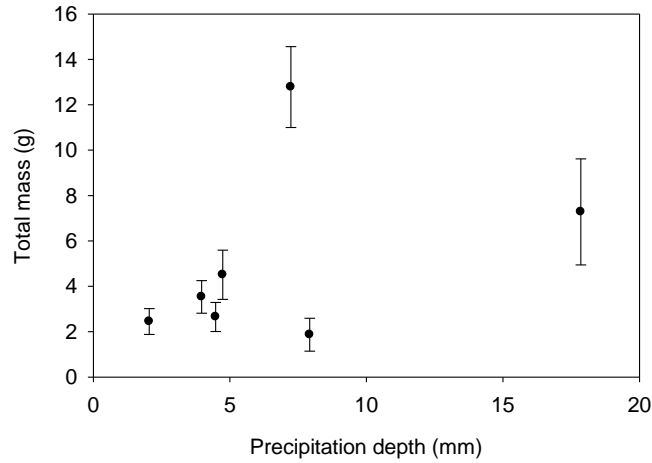


**Figure 2.35 The relation between the total mass of sediment and precipitation depth for the small scale trials. The relation is not significant at the 95% confidence interval**

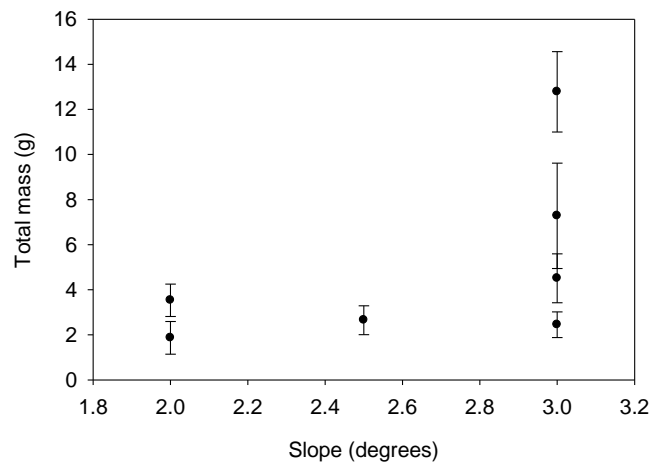


**Figure 2.36 The relation between the total mass of sediment and road surface slope for the small scale trials. The relation is not significant at the 95% confidence interval**

## 2.5 Conclusions

The rainfall simulation results show that precipitation intensity is the dominant control on the amount of sediment generated from a forest road and that antecedent precipitation conditions are not important. If precipitation intensity and traffic volumes are known then the volume of sediment generated by a precipitation event may be

estimated using the multiple linear regression equation. The large spatial variability in initial response demonstrated by the small scale trials, however, indicate that application of this equation must be done very cautiously. Additional rainfall simulation trials at other locations along the Queen Charlotte Mainline Forest Road South may improve the accuracy of this prediction. Additional rainfall simulation trials may also increase the significance of many of the relations discussed above.

The lack of relation between the duration of an event and the total mass of non-truck related sediment generated by the road suggests that for rainfall events shorter than five hours, in the absence of traffic, it is the initial sediment peak that controls the total mass of sediment generated from the road, not the steady state sediment removal rate reached later in the event. The hysteretic relation between the increase in sediment generated from the road and the increase in flow rate at the beginning of the large scale trials shows that the increase in discharge is preceded by the increase in concentration, suggesting a supply limited erosion scenario.

The relation between the number of loaded logging trucks during a trial and the total mass of sediment generated by trucks suggests that each truck passage results in a new sediment pulse either due to aggregate breakdown, the upward forcing of fine grained material or the breakdown of the armor layer. Because the surface material can in some places be crushed by hand, it is likely that aggregate breakdown is an important factor.

The lack of a relation between truck speed and sediment generated by a truck suggests speed restrictions during storm events are unlikely to be an effective way to manage sediment generation due to traffic. The low percent of total mass due to traffic

for some trials indicates a significant amount of sediment would be generated during rainfall events even if no trucks were present. This suggests road closures during rainfall events will not prevent sediment generation from the road, but will reduce it by 10-60%.

## **3 TURBIDITY MONITORING**

### ***3.1 Introduction***

This study monitored turbidity, as a measure of suspended sediment concentration, throughout the Honna Watershed between August 2009 and July 2010 in order to quantify the amount of suspended sediment transported by the Honna River and its tributaries, obtain information on suspended sediment concentrations during natural precipitation events and develop turbidity frequency graphs to indicate the prevalence of high turbidity events. River monitoring data also allowed the validation of information derived from the rainfall simulation experiments (Chapter 2), which is described in Chapter 4.

Because the quantity and type of suspended sediment a stream can carry depends on the kinetic energy of the moving water and characteristics of the sediment in a catchment, it should be possible to develop a relation between stream stage and suspended sediment concentration for a watershed. Previous studies, however, have shown the relation is not simple (Marquis, 2008). Generally suspended sediment concentrations within a watershed vary to a greater degree during high flow events compared to low flow conditions and rising hydrograph limbs tend to be associated with higher sediment concentrations compared to falling limbs due to sediment supply differences (Marquis, 2008). Some studies have shown suspended sediment concentrations also vary seasonally, with higher concentrations before the annual peak flow event (Beschta, 1978). Turbidity was therefore monitored continuously for almost a year in the Honna Watershed (Table 3.1).

<b>Table 3.1 Overview of turbidity monitoring data</b>							
<b>Site</b>	<b>Location</b>	<b>Logger type</b>	<b>UTM Zone 08U</b>	<b>Deployment period</b>	<b>Missing turbidity data period</b>	<b>Waterlevel measurements</b>	<b>D<sub>84</sub> (cm)</b>
Honna Intake	In the Honna River beside the Drinking Water Intake	Starlogger	0690510E 5904998N	Aug 9, 2009 - Jun 30, 2010	Oct 23, 2009 - Oct 24, 2009 Feb 21, 2010 - Mar 10, 2010	Sep 10, 2009 - May 27, 2010	-
Honna km 5	In the Honna River beside km 5 of the QC Mainline South	Starlogger	0690033E 5907453N	Aug 12, 2009 - Sep 10, 2009	-	-	-
Honna km 6	In the Honna River beside km 6 of the QC Mainline South	Starlogger	0689924E 5908299N	Aug 9, 2009 - Jun 30, 2010	-	Sep 10, 2009 - May 27, 2010	17.9
Honna km 7	In the Honna River beside km 7 of the QC Mainline South	Starlogger	0690092E 5909117N	Aug 12, 2009 - Aug 21, 2009	-	-	-
Honna North West	In the tributary just upstream from km 7 of the QC Mainline South	Starlogger	0689905E 5909566N	Aug 26, 2009 - Jun 30, 2010	Oct 6, 2009 - Oct 28, 2009	Sep 10, 2009 - May 27, 2010	15.1
Stanley Lake Tributary	In the Stanley Lake tributary	Starlogger	0690004E 5909250N	Aug 18, 2009 - Oct 31, 2009	Aug 22, 2009 - Aug 30, 2009 Sep 1, 2009 - Oct 4, 2009 Oct 17, 2009 - Oct 21, 2009	Sep 10, 2009 - Oct 31, 2009	16.9
Tributary 1 Upstream	Upstream from the road crossing near km 5 of the QC Mainline South	Hobo	0690042E 5907588N	Aug 11, 2009 - Mar 9, 2010	Oct 1, 2009 - Dec 3, 2009	-	-
Tributary 1 Downstream	Downstream from the road crossing near km 5 of the QC Mainline South	Hobo	0690078E 5907505N	Aug 11, 2009 - May 8, 2010	Sep 12, 2009 - Sep 14, 2009 Oct 24, 2009	Sep 10, 2009 - May 8, 2010	2.7
Tributary 2 Upstream	Upstream from the road crossing near km 7 of the QC Mainline South	Hobo	0690045E 5908809N	Aug 26, 2009 - Mar 10, 2010	Sep 13, 2009 - Nov 29, 2009	Sep 10, 2009 - Mar 10, 2010	-
Tributary 2 Downstream	Downstream from the road crossing near km7 of the QC Mainline South	Hobo	0689997E 5908826N	Aug 26, 2009 - Jun 10, 2010	Sep 7, 2009 - Feb 19, 2010	-	-

## **3.2 Study Site**

Nine turbidity probes were deployed throughout the Honna Watershed to assess suspended sediment concentrations at key locations (Table 3.1). Three probes were placed along the Honna River and two probes were deployed in important tributaries. Two small tributaries with road crossings near their confluence with the Honna River were fit with two probes each: one above and one below the crossing (Figure 3.1). The specific turbidity probe locations were chosen based on installation requirements (see section 3.3.1 below).

Capacitance water level loggers (Odyssey, Christchurch, New-Zealand) were installed in conjunction with most turbidity probes and an additional water level recorder was installed near the Environment Canada gauging station (station 08OA004 Honna near the mouth), located in the lower reach of the Honna River (Figure 1.2). Two rain gauges (Onset, Bourne MA, USA) were also installed within the watershed, one at a low elevation (145 m) and one at a high elevation (250 m) (Figure 1.2).

## **3.3 Methods**

### **3.3.1 Turbidity measurements**

Analite NEP9500 series turbidity probes (McVan Instruments, Mulgrave, VIC, Australia) with detection ranges of 0-400 and 0-1000 NTU were used to monitor turbidity continuously. All probes had similar optical window and wiper configurations and used 90° scatter detection to measure turbidity. They emitted an infrared light beam and used a modulation technique to reject nearly all ambient light induced noise. Probes were deployed in conduits (metal in high flow locations and PVC in lower flow tributaries) attached to trees or rocks on banks beside pools in the river (Figure 3.2).

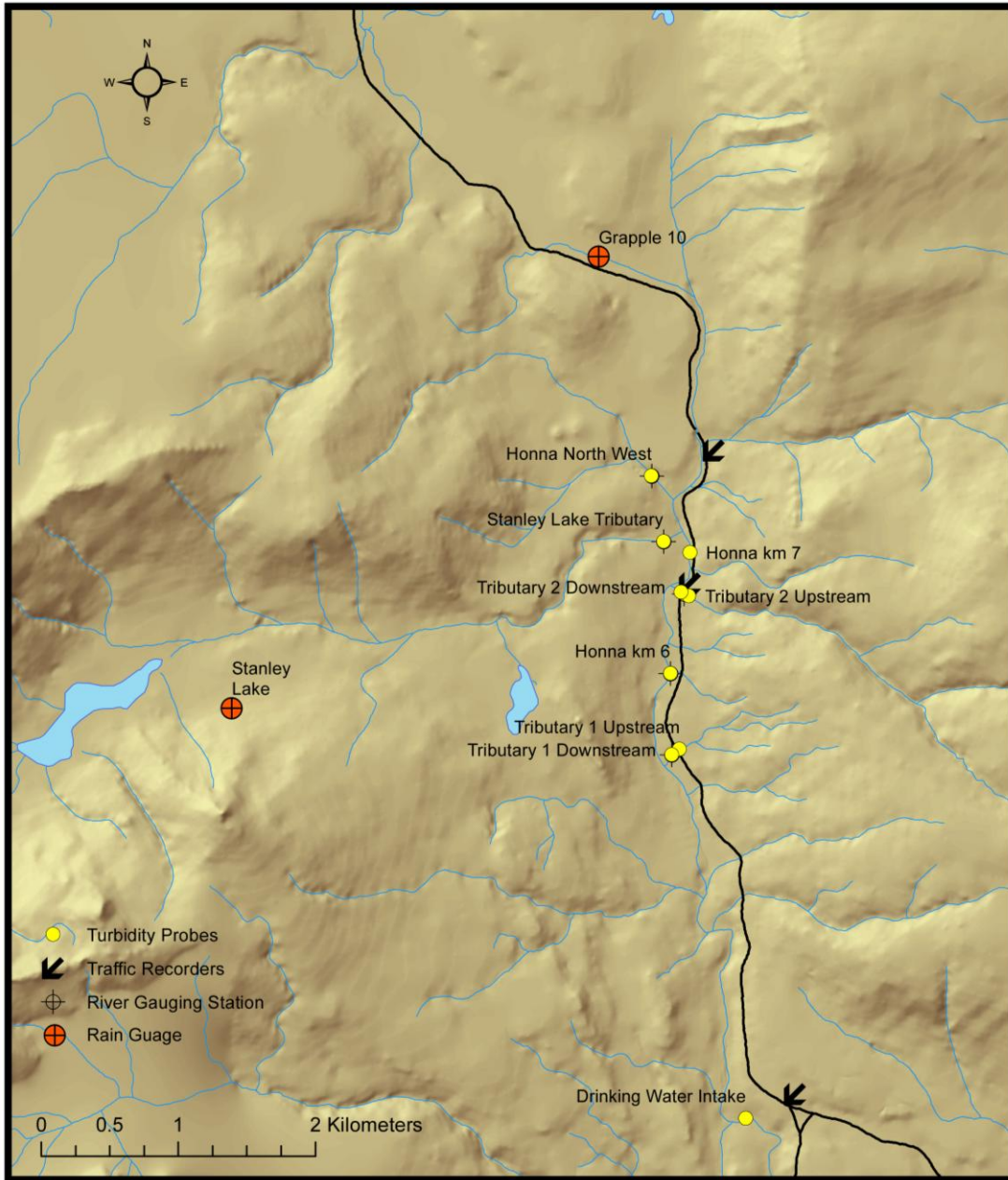


**Figure 3.1 Location of turbidity monitoring equipment**

The turbidity probes were connected to either StarLogger data loggers (Unidata, O'Connor WA, Australia), which had the ability to record the maximum, minimum and average turbidity values for a set time interval, or Hobo U12-006 data loggers (Onset, Bourne MA, USA), which recorded the turbidity reading at a given time interval.

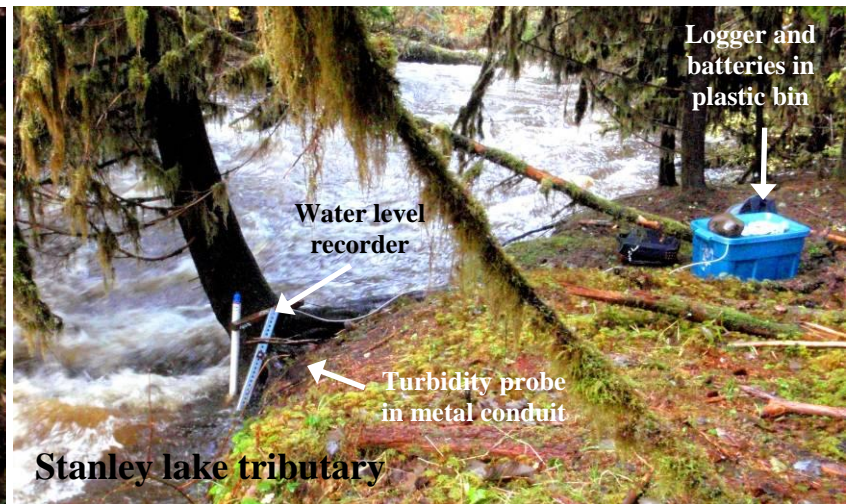
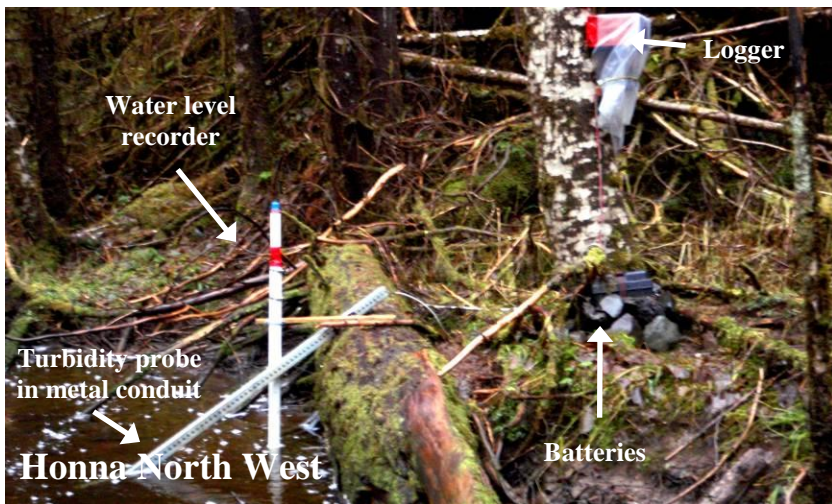
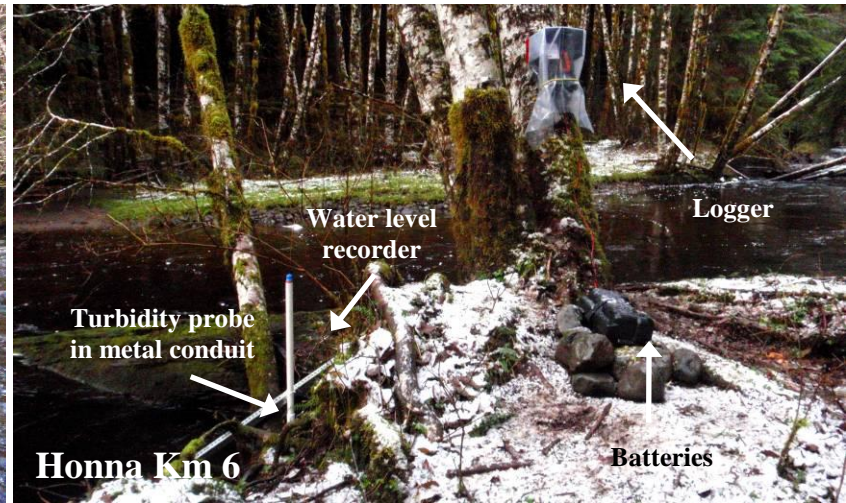


Figure 3.2 a. Turbidity monitoring sites showing the location of the equipment



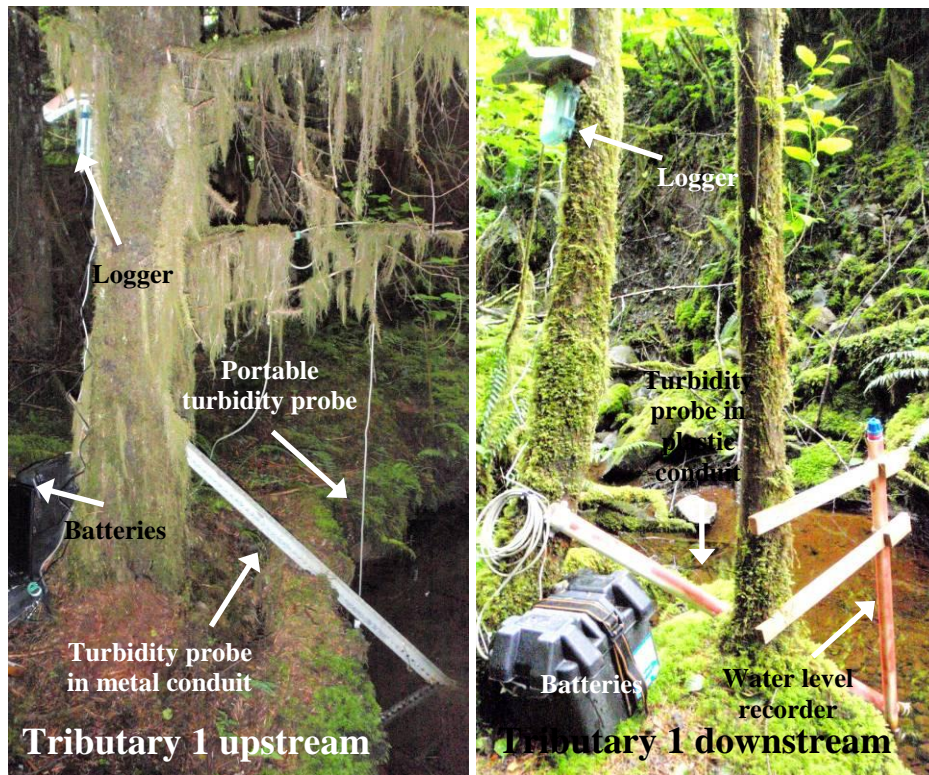


Figure 3.2 b. Turbidity monitoring sites showing the location of the equipment

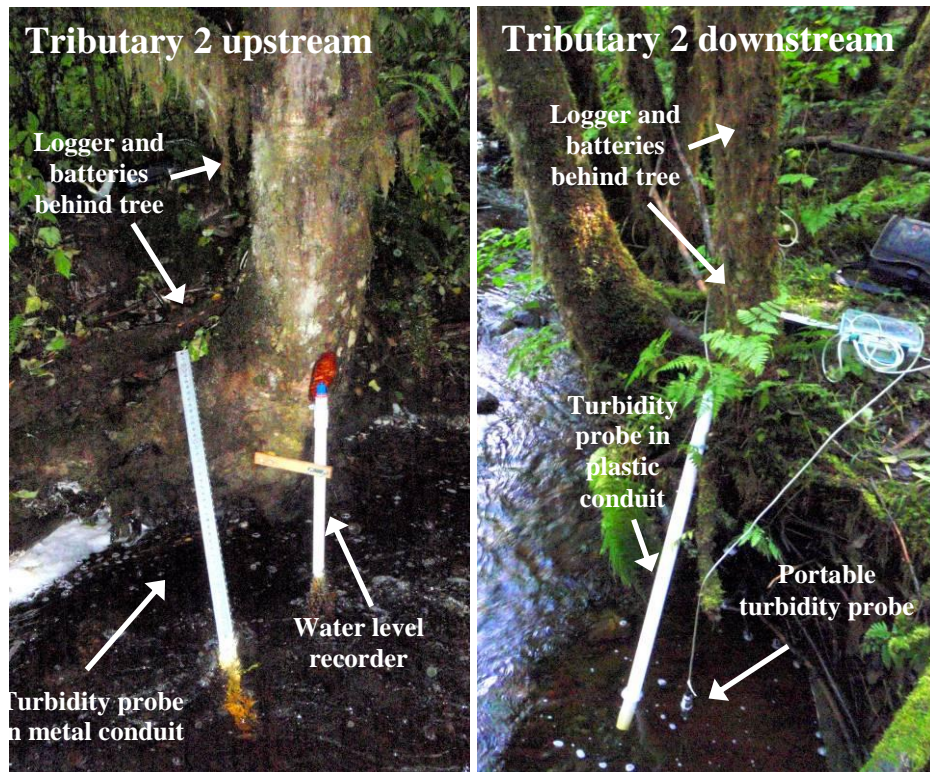


Figure 3.2 c. Turbidity monitoring sites showing the location of the equipment

Depending on the expected time between site visits, loggers were set to record at 5, 10 or 15 minute intervals, with Hobo loggers generally set to record more frequently than Unidata loggers. Probes were powered by 12 Volt batteries which required replacement approximately every one to two months.

### 3.3.1.1 Turbidity probe deployment

Because of the optical nature of turbidity probes, they do not operate well in very turbulent water as bubbles and debris can scatter the probe's beam and give false (high-turbidity) readings. Turbidity probes also do not operate well in warm stagnant water because of bio-fouling of the optical face. Additionally, Analite 9500 series probes must be deployed with a minimum of 5 cm clearance around their optical faces because otherwise they will give false (high-turbidity) readings.

All monitoring equipment was deployed in relatively calm deep flow areas that were still well connected to the main channel. Turbidity probes were deployed pointing downstream to decrease the chance of bubbles and debris building up on their optical faces, with wipers operating every 2 hours to prevent algae, bubble and debris buildup. The turbidity probe in the Stanley Lake tributary and in Tributary 1 upstream did not have working wipers for the entire deployment period. Probes were placed with their optical faces no less than 5 cm from the river bed and surrounding banks.

The number of appropriate locations for turbidity probe deployment along the Honna River and its tributaries was limited and some probes were necessarily deployed adjacent to undercut banks (Figure 3.2). Although not ideal, these locations were considered the best available and banks were inspected visually throughout the deployment period to ensure undercutting was not rapid and did not create locally high turbidity readings. Despite careful turbidity probe deployment certain probes did not always operate optimally, resulting in sections of unreliable or missing data (Table 3.1).

### **3.3.1.2 Turbidity probe calibration**

Deionized water, 100 NTU and 1000 NTU standard formazine solutions were used to compare all turbidity probes prior to deployment, allowing NTU readings to be equated to each other. Because many of the probes remain deployed, a post-research calibration was not possible. In order to detect any sensor drift during deployment, a portable turbidity probe, compared to the standard formazine solutions throughout the deployment period, was used to make periodic readings at all turbidity monitoring locations. No drift was detected in either the portable probe or deployed probes throughout the study period. Linear regression relations were determined between the

readings of the deployed and the portable probe for each site in order to standardize values of each probe to those given by the portable probe (Table 3.2).

<b>Table 3.2 Linear regression relations between portable and deployed turbidity probe measurements</b>				
<b>Site</b>	<b>Relation</b>	<b>R<sup>2</sup></b>	<b>n</b>	<b>p</b>
Drinking Water Intake	$T = 0.9453(RC) + 1.8492$	0.995	4	$2 \times 10^{-3}$
km 5	$T = 1.1770(RC) + 2.0698$	N/A/	2	N/A
km 6	$T = 1.5625(RC) + 0.5600$	0.941	7	$3 \times 10^{-4}$
km 7	$T = 0.9263(RC) + 4.3011$	0.831	3	$3 \times 10^{-1}$
Honna North West	$T = 1.2181(RC) + 2.0974$	0.816	6	$1 \times 10^{-2}$
Stanley Lake tributary	$T = 1.4949(RC) + 3.2108$	0.999	3	$2 \times 10^{-2}$
Tributary 1 Upstream	$T = 1.2614(RC) + 1.9036$	0.965	4	$2 \times 10^{-2}$
Tributary 1 Downstream	$T = 1.1252(RC) + 1.1808$	0.927	3	$2 \times 10^{-1}$
Tributary 2 Upstream	$T = 1.2511(RC) + 2.4140$	0.947	6	$1 \times 10^{-3}$
Tributary 2 Downstream	$T = 1.0418(RC) - 4.8854$	0.867	3	$2 \times 10^{-1}$

T = Turbidity measured by portable probe

RC = Recorded turbidity measured by deployed probe

To develop a relation between stream turbidity and suspended sediment concentrations, sediment was taken from roadside ditches of the Queen Charlotte Mainline Forest Road South and used to make sediment concentration standards. Sediment in these standards was kept in suspension using a submersible pump and mechanical stirring. The turbidity of these standards was measured using the portable turbidity probe, as its values could be related to all deployed probes (Figure 3.3). Sediment taken from the watershed was used in the standards in order to approximate the shape and size of suspended sediment in the Honna River because turbidity measurements are particle shape and size dependent (Gippel, 1995). Grab samples of river water were collected at the turbidity monitoring sites throughout the deployment period and analyzed for sediment concentrations. However concentrations were always

below the detection limit (0.01 g) even when large samples (3 L) were collected from relatively turbid flows.

The relation developed to predict sediment concentration from turbidity in the Honna River is similar to those found by Marquis (2005) and Hudson (2001) for turbidity caused predominantly by very fine to fine sand sized mineral based particles. If the Honna River predominantly transports finer sediment with a greater amount of organic material then this relation may overestimate sediment concentrations. Marquis (2005) developed a sediment concentration – turbidity relation for a different watershed on Haida Gwaii which also suggests the relation used in this study may overestimate sediment concentrations in the Honna River.

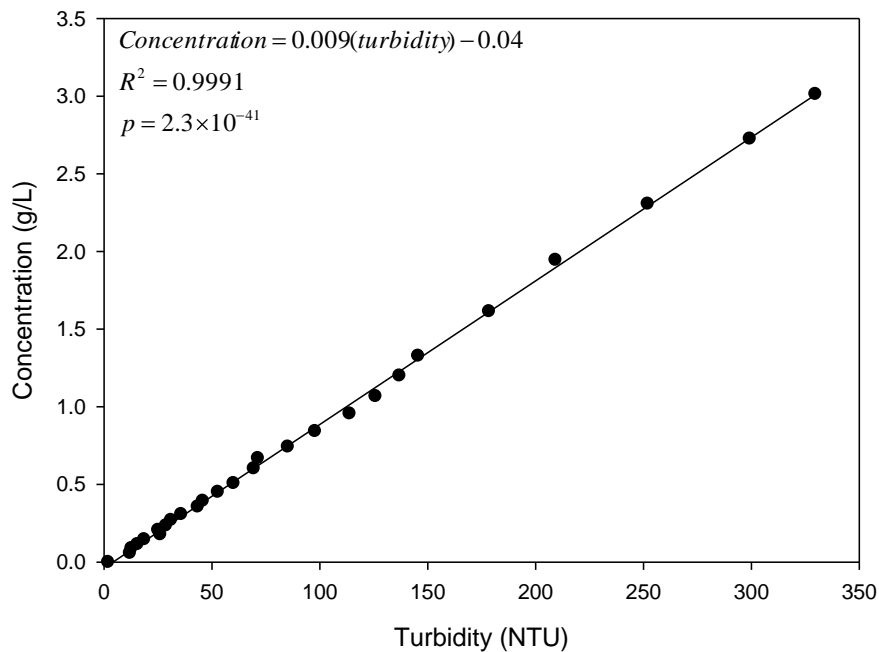


**Figure 3.3 Turbidity-suspended sediment concentration relation for the portable turbidity probe**

Due to the dependence of turbidity probe readings on sediment colour and size, the turbidity-suspended sediment relation in natural rivers has been shown to display

rising limb-falling limb and seasonal hysteresis (Marquis, 2008). These variations are expected to be within the error of the turbidity-suspended sediment relation developed above for the Honna River.

### **3.3.2 Discharge measurements**

A rating curve was developed for the water level recorder installed near the Environment Canada gauging station in the lower reach of the Honna River, as well as for the water level recorder installed at the Honna North West turbidity monitoring station. Discharge measurements were made using a Swoffer 2100 Current Velocity Meter (Swoffer Instruments, Seattle WA, USA) during low, medium and moderately high flow periods between September and December 2009. Very high flows were not measured due to safety concerns. The lower Honna River rating curve was compared to the rating curve for the nearby (approximately 100 m upstream) Environment Canada station. Both curves had a similar shape, although they were slightly offset due to differences in the placement of the water level recorders. Therefore, the newly measured curve was considered accurate even for high flows (Figure 3.4). The rating curves were used to determine discharge at their respective sites throughout the period for which stage data was available.

Instantaneous discharge was measured at the Tributary 1 Downstream, Tributary 2 Upstream, Honna North West and Stanley Lake tributary turbidity monitoring sites on July 3<sup>rd</sup> and 4<sup>th</sup>, 2010, using the slug injection method and a Cyclops-7 Rhodamine probe (Turner Designs, Sunnyvale CA, USA). These discharge values were compared to the discharge in the lower reach of the Honna River determined from the rating curve. A reasonably good contributing area-discharge relation was found for these sites

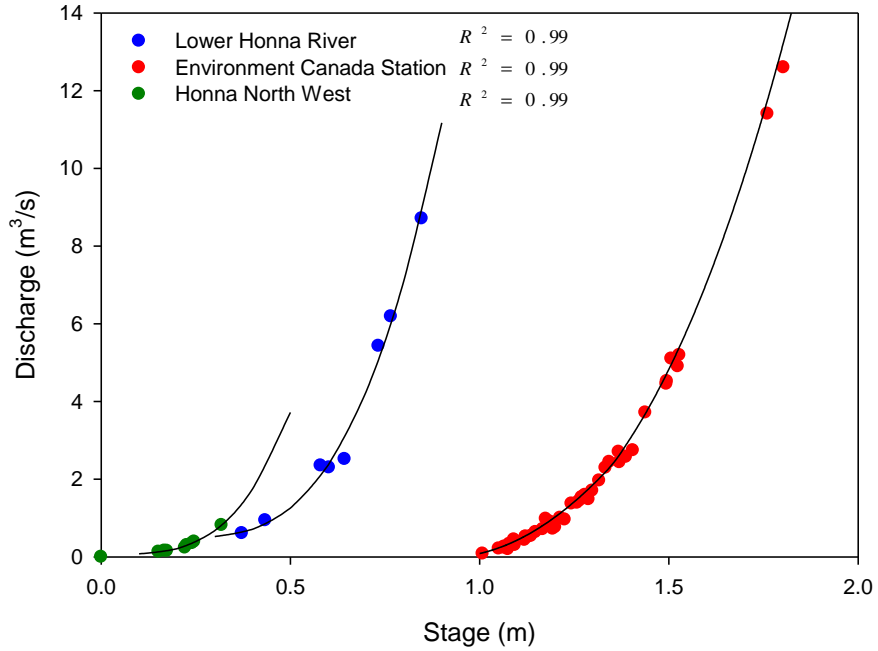


**Figure 3.4 Rating curves for the water level recorders installed in the lower reach of the Honna River and the Honna North West and the Environment Canada gauging station rating curve**

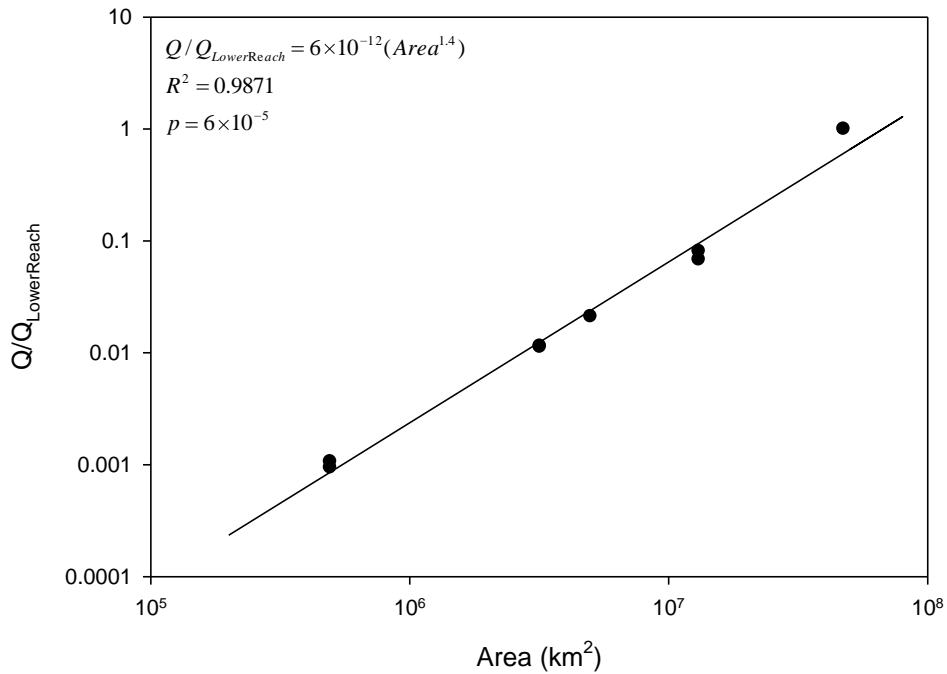


**Figure 3.5 Contributing area-discharge relation for the Honna Watershed**

(Figure 3.5). Continuous discharge values for all turbidity monitoring sites were estimated based on this contributing area-discharge relation for periods when discharge data was available for the lower reach of the Honna River.

Wolman pebble counts were taken at each stage recorder location, except for in Tributary 2 upstream and in the lower reach of the Honna River. The 84<sup>th</sup> percentile pebble size was determined (Table 3.1) and the depth averaged mean velocity equation for steady uniform flow was applied to adjusted stage values for each site (van Rijn, 1994):

$$\bar{U} = \frac{u_*}{\kappa} \ln\left(\frac{h}{z_o}\right)$$

where  $\bar{U}$  is the average stream velocity in m/s,  $u_*$  is the shear velocity estimated as  $\sqrt{ghS}$  where  $g$  is gravitational acceleration,  $h$  is the water depth determined from the nearby stage measurements and  $S$  is the water surface slope, which was approximated by the slope of the stream bed at each surveyed stream sections,  $\kappa$  is the Von Kármán constant (0.41) and  $z_o$  is the height of the zero velocity plane estimated as  $e0.1D_{84}$  (Whiting and Dietrich, 1990) where  $D_{84}$  is the 84<sup>th</sup> percentile of the particle size distribution on the river bed. The average stream velocity was used with information from surveyed cross sections to determine discharge for every location with Wolman pebble count and stage data available.

Although discharge timing is more accurate when based on the depth-averaged-velocity, contributing area-discharge based estimates of stream flow were used because Wolman pebble counts were not taken at the Drinking Water Intake turbidity probe and



the river bed near the Tributary 2 water level recorder had been artificially modified. The river bed near km 6 and possibly the Honna North West may also have been modified, affecting pebble count results. The contributing area-discharge relation based discharge was therefore used for consistency. Depth-averaged-velocity measurements were used to illustrate the uncertainty associated with discharge measurements. Sediment volumes were not calculated for turbidity data with no corresponding discharge data (Table 3.1).

The depth-averaged-velocity based discharge values were generally larger (especially for the Honna North West) and non-linearly related to those based on the contributing area-discharge relation (Figure 3.6). The clockwise hysteresis between discharge derived from these two methods is due to the dependence of the depth-averaged-velocity based discharge on local stage. Stage responds more quickly to precipitation events in the upper reaches of the watershed. The contributing area-discharge values are based on stage in the lower reach of the Honna River, which responds more slowly to precipitation events. Cross correlation between river stage recorded in the lower reaches of the Honna and other locations in the watershed revealed a 50 minute lag at the lower reach gauging station compared to Tributary 1, 30 minutes compared to Tributary 2, 1 hour 45 minutes compared to the Honna North West, 25 minutes compared to Stanley Lake tributary and 10 minutes compared to km 6 of the Honna. The development of rating curves for each stage recorder would allow for improved discharge data and thus improved estimates of the sediment fluxes.

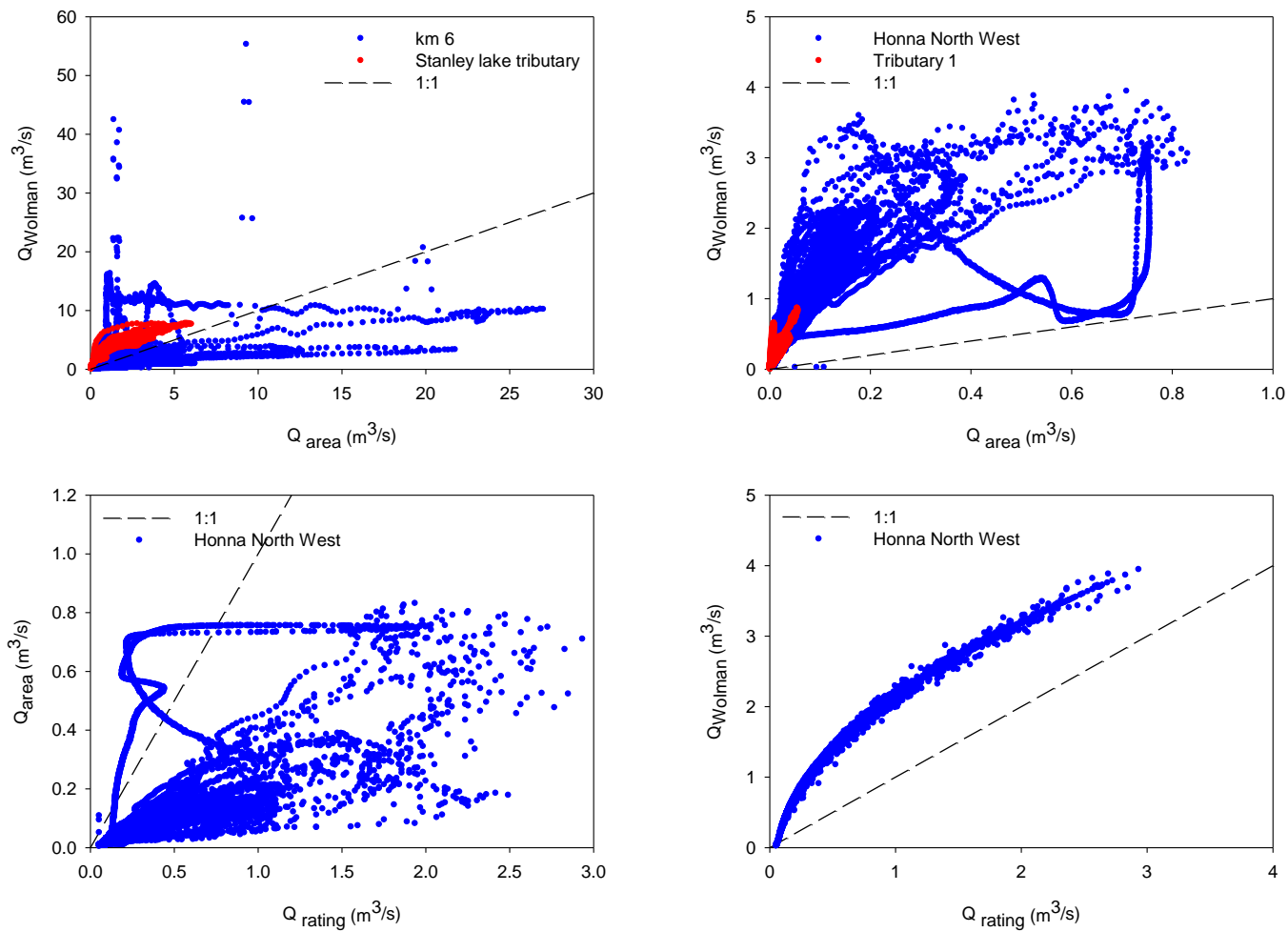


**Figure 3.6 Relation between instantaneous discharge derived from the depth-averaged-velocity equation ( $Q_{Wolman}$ ) and the contributing area-discharge relation ( $Q_{area}$ ) (top) and between the rating curve based discharge ( $Q_{rating}$ ) and the contributing area and depth-averaged-velocity based discharge (bottom)**

### **3.3.3 Turbidity data processing**

Sections of turbidity data recorded between November 2009 and March 2010 were adjusted to Greenwich Mean Time-7 to correspond with Pacific Time Zone daylight savings time as all probes were originally deployed during daylight savings time. Turbidity values from each deployed probe were adjusted to match portable turbidity probe values based on the linear regression relation between concurrent measurements of the deployed and portable probe (Table 3.2). All turbidity data was then run through a cleaning script in MatLab to remove outliers and noise. First, values above 500 and below 0 NTU were removed. Next, values more than 200 NTU greater than the previous reading were removed. Finally, turbidity readings more than 10% different from the average of the previous and subsequent 10 readings were replaced with the average of these values. This cleaning process was especially useful for data from probes attached to Hobo U12-006 loggers as they tended to be very noisy. Adjusted and cleaned turbidity readings were then converted into suspended sediment concentrations based on the turbidity-suspended sediment concentration relation developed for the portable turbidity probe (Figure 3.3).

Once turbidity data were converted into sediment concentrations the volume of sediment passing each probe was estimated based on stream discharge. For the turbidity probe located in the Honna North West, discharge was based on the local rating curve when local stage data was available (Sept 20, 2009 – May 27, 2010) and based on the contributing area-discharge relation and discharge at the gauging station in the lower reach of the Honna River when local stage data were not available. Discharge at the other sites was based on the contributing area-discharge relation and discharge at the gauging

station in the lower reach of the Honna River when stage data was available for this site and based on local stage data and the depth-averaged-velocity when lower reach stage data was not available (August 1 – September 10, 2009 and May 27 – July 31, 2010).

Suspended sediment concentrations vary with depth (Dingman, 2009) but because turbidity probes remained a set distance from the bed, they did not sample the same section of flow as stage rose and fell. Turbidity readings may therefore not have represented mean sediment concentrations for the entire depth of flow at any given time. Although there are equations which give the suspended sediment concentration profile if the concentration is known at a certain depth (e.g. the Rouse equation in Dingman, 2009), sediment carried in Honna River is predominantly wash load (composed of fine clay and silt particles) and is well mixed vertically. Similar to Sheridan and Noske (2007), turbidity and concentration values in this study were not corrected for flow depth.

### **3.3.4 Data analysis**

The time series of sediment concentration and sediment flux during the largest event of each month were analyzed for each station. The percent of time turbidity values were exceeded was determined for each month with data available. During months when turbidity recording switched from 5, 10 or 15 minute intervals, 10 minute intervals were considered twice and 15 minute intervals were considered three times. The percent of time with turbidity values greater than 10, 25 and 50 NTU was also determined.

The volume of sediment transported and peak sediment concentrations recorded at the Drinking Water Intake and in the Honna North West were determined for the largest event in each month. This was compared to the peak precipitation intensity, total precipitation during the event and the depth of precipitation in the 24 hours prior to the

event, peak discharge during the event, the season (represented by the cosine of the calendar day of the event) and for the Drinking Water Intake the number of vehicles driving along the forest road paralleling the river in the 24 hour period prior to the event (measured at km 3 of the Queen Charlotte Mainline Forest Road South using a TrafX vehicle counter, see section 2.3.1) using multiple linear regression in Microsoft Excel 2007.

### **3.4 Results and discussion**

#### **3.4.1 Turbidity exceedance graphs**

The turbidity exceedance graphs revealed that September had the highest turbidity values recorded for all the sites throughout the watershed. May, June and August were generally the months with the lowest peak turbidity values (Figure 3.7, Figure 3.8 and Figure 3.9). September was the month most likely to have turbidity values greater than 50 NTU, while March was the month most likely to have turbidity values greater than 10 NTU (Table 3.3, Figure 3.7, and Figure 3.8). All sites recorded turbidity values greater than 50 NTU for more than 1% of the time in September, with the exception of the turbidity probe installed upstream of the road crossing in Tributary 1. All sites recorded turbidity values greater than 10 NTU for more than 20% of the time in March, with the exception of the turbidity probes installed upstream of the road crossings in Tributaries 1 and 2. August, November, December, February, April and May had maximum turbidity values below 50 NTU at all locations except downstream of the road crossings in Tributaries 1 and 2 (Table 3.3).

Turbidity values equal to or larger than 10, 25 and 50 NTU were recorded for a much larger percent of time each month downstream from road crossings than upstream

of road crossings (Figure 3.9). Tributary 1 downstream of the road crossing was the site most likely to record high turbidity values (>50 NTU) for every month of the year, while Tributary 1 upstream of the road crossing was the site least likely to record high turbidity values for every month of the year (Table 3.3). Near km 6, turbidity values greater than 10, 25 and 50 NTU were recorded for a greater percent of time each month than at the Drinking Water Intake (Table 3.3). At the Drinking Water Intake turbidity values greater than 10 NTU were most common in March and least common in August, December, April and May. Turbidity values greater than 50 NTU were most common in September, January and March and least common throughout the remainder of the year (Figure 3.7). The percent of time turbidity in the Honna North West exceeded 25 and 50 NTU was similar to the percent of time it was exceeded near km 6 ( $\pm 1\%$ ) (Table 3.3).

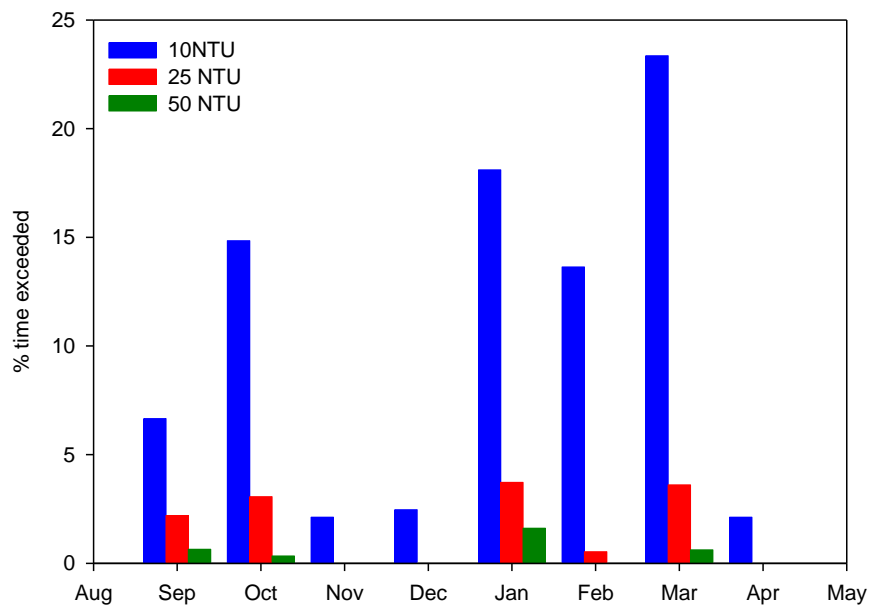


**Figure 3.7 Summary of the percent time a certain turbidity value was exceeded at the Drinking Water Intake**

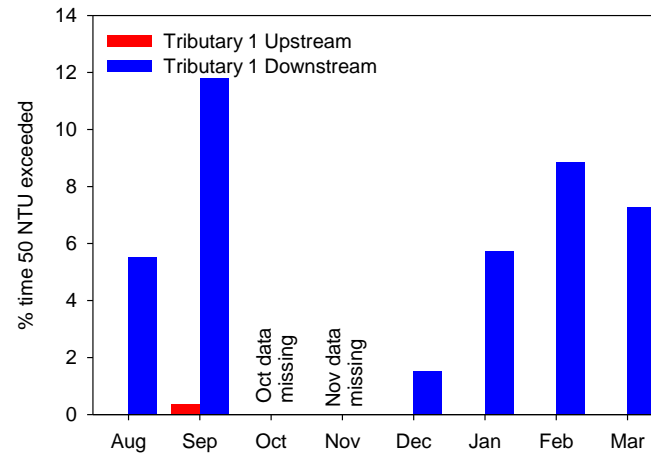
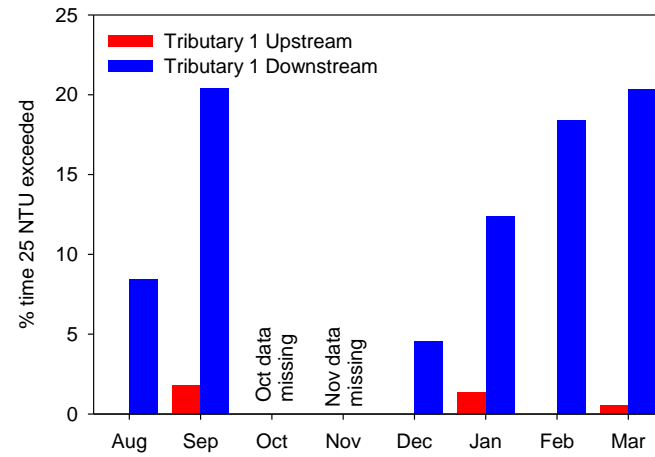
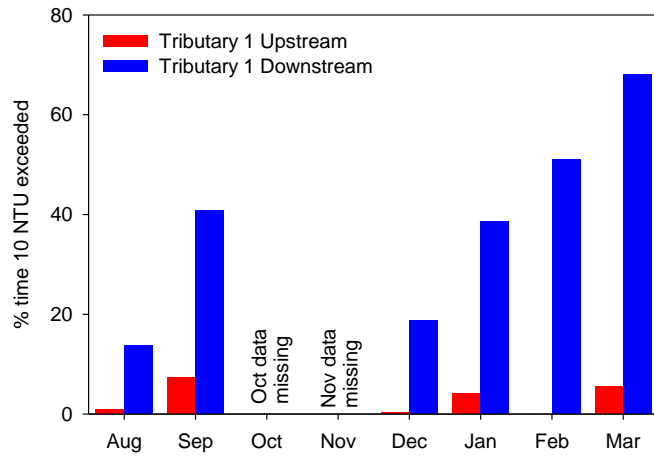


**Figure 3.8 Summary of the percent time a specific turbidity value was exceeded in Tributary 1 upstream and downstream of the road crossing**

<b>Table 3.3 Percent of time specific turbidity values were exceeded</b>							
	<b>% time exceeded</b>				<b>% time exceeded</b>		
	<b>10 NTU</b>	<b>25 NTU</b>	<b>50 NTU</b>		<b>10 NTU</b>	<b>25 NTU</b>	<b>50 NTU</b>
	<b>August</b>				<b>January</b>		
Drinking Water Intake	0	0	0	Drinking Water Intake	18	4	2
km 6	2	0	0	km 6	23	6	2
Honna NW	6	0	0	Honna NW	27	6	0
Tributary 1 Upstream	1	0	0	Tributary 1 Upstream	4	1	0
Tributary 1 Downstr.	14	8	6	Tributary 1 Downstr.	39	12	6
Tributary 2 Upstream	0	0	0	Tributary 2 Upstream	20	4	1
Tributary 2 Downstr.	15	9	5	Tributary 2 Downstr.	Missing Data		
	<b>September</b>				<b>February</b>		
Drinking Water Intake	7	2	1	Drinking Water Intake	14	1	0
km 6	12	3	1	km 6	16	2	0
Honna NW	19	3	1	Honna NW	12	1	0
Tributary 1 Upstream	7	2	0	Tributary 1 Upstream	0	0	0
Tributary 1 Downstr.	41	20	12	Tributary 1 Downstr.	51	18	9
Tributary 2 Upstream	7	4	2	Tributary 2 Upstream	49	0	0
Tributary 2 Downstr.	21	16	12	Tributary 2 Downstr.	3	0	0
	<b>October</b>				<b>March</b>		
Drinking Water Intake	15	3	0	Drinking Water Intake	23	4	1
km 6	26	6	1	km 6	34	6	2
Honna NW	34	5	0	Honna NW	33	6	2
Tributary 1 Upstream	Missing Data			Tributary 1 Upstream	6	1	0
Tributary 1 Downstr.	36	29	14	Tributary 1 Downstr.	68	20	7
Tributary 2 Upstream	Missing Data			Tributary 2 Upstream	48	0	0
Tributary 2 Downstr.	Missing Data			Tributary 2 Downstr.	8	2	1
	<b>November</b>				<b>April</b>		
Drinking Water Intake	11	1	0	Drinking Water Intake	2	0	0
km 6	22	3	0	km 6	6	0	0
Honna NW	33	2	0	Honna NW	6	0	0
Tributary 1 Upstream	Missing Data			Tributary 1 Upstream	Missing Data		
Tributary 1 Downstr.	35	10	3	Tributary 1 Downstr.	50	12	7
Tributary 2 Upstream	0	0	0	Tributary 2 Upstream	Missing Data		
Tributary 2 Downstr.	Missing Data			Tributary 2 Downstr.	10	5	3
	<b>December</b>				<b>May</b>		
Drinking Water Intake	2	0	0	Drinking Water Intake	0	0	0
km 6	5	0	0	km 6	2	0	0
Honna NW	5	1	0	Honna NW	2	0	0
Tributary 1 Upstream	0	0	0	Tributary 1 Upstream	Missing Data		
Tributary 1 Downstr.	19	5	2	Tributary 1 Downstr.	2	0	0
Tributary 2 Upstream	4	0	0	Tributary 2 Upstream	Missing Data		
Tributary 2 Downstr.	Missing Data			Tributary 2 Downstr.	8	5	2



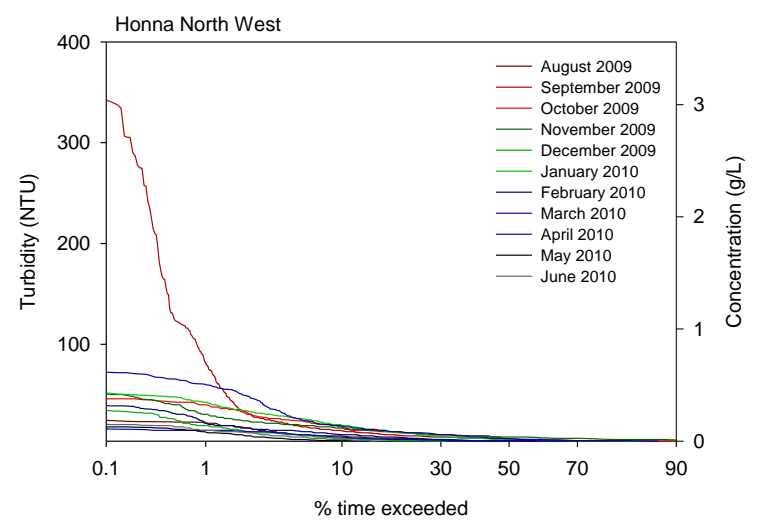
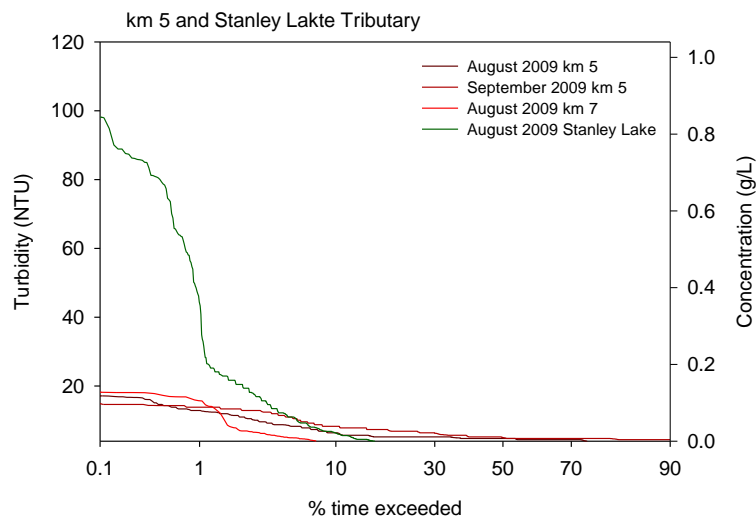
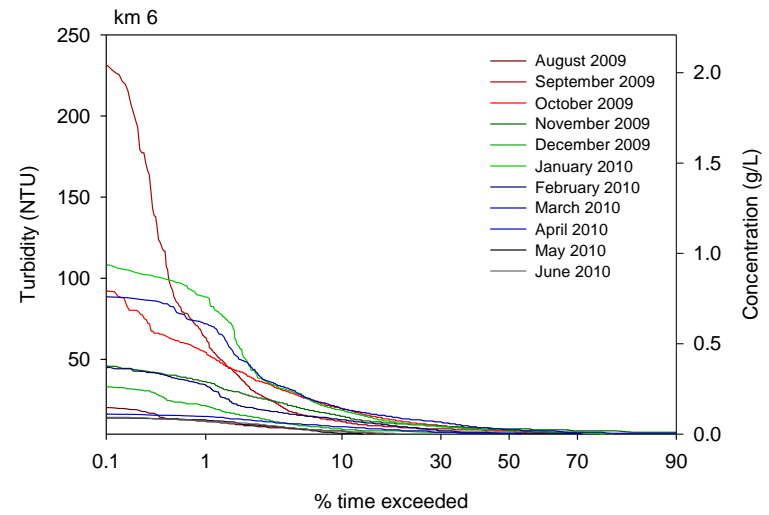
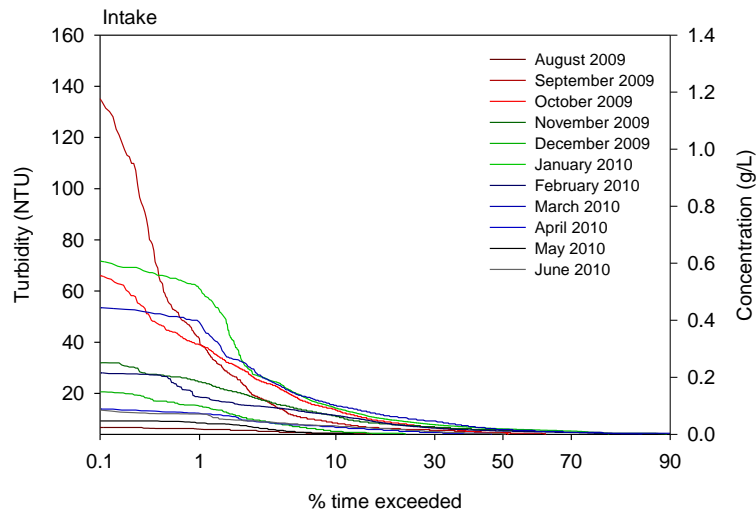
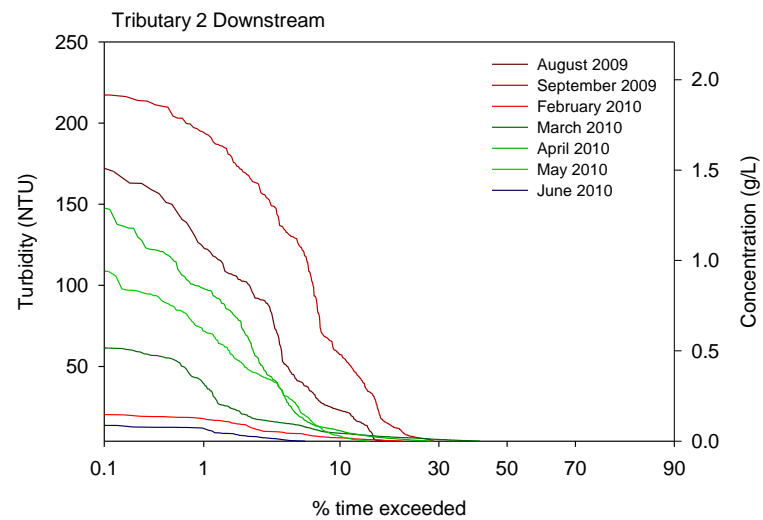
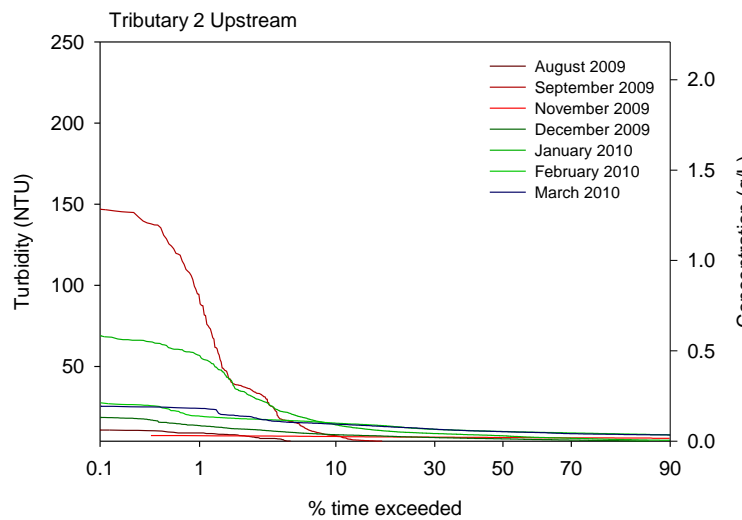
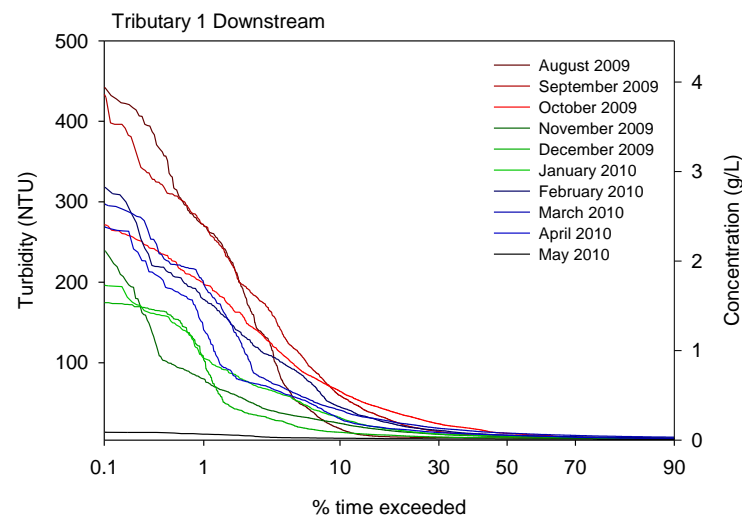
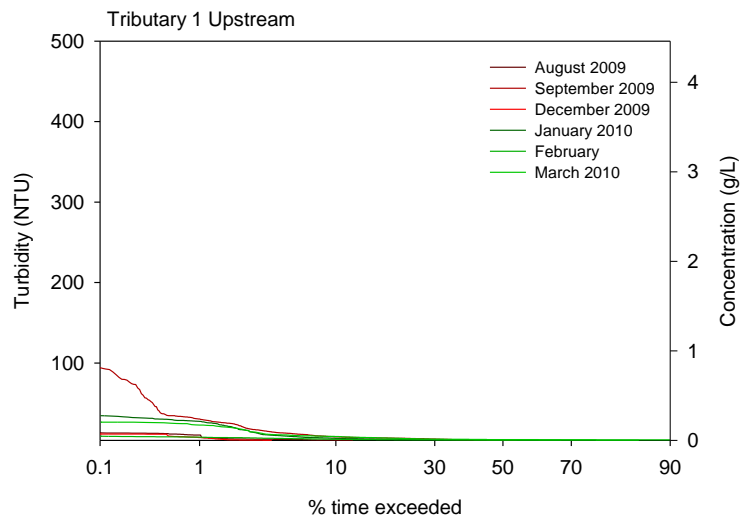


Figure 3.9 a. Turbidity exceedance graphs



**Figure 3.9 b. Turbidity exceedance graphs**

### **3.4.2 Individual turbidity events**

The turbidity probes deployed in the smaller tributaries displayed earlier and higher turbidity peaks during the largest event of each month than those in larger rivers. Peak turbidity values during the largest event of each month were higher and occurred earlier at the km 6 site than at the Drinking Water Intake site. Estimated sediment fluxes were similar at these two sites with fluxes at km 6 being slightly higher during the largest events of December, April and May and slightly lower during the largest February event (Figure 3.10). Higher turbidity values in the upper regions of the Honna River, combined with relatively constant (or decreasing) sediment mass fluxes along the river suggest the main sediment sources are located in the upper region of the watershed and sediment plumes are diluted (or even deposited) as they travel downstream.

The Stanley Lake tributary probe recorded lower and later peak turbidity values than the Honna North West probe during the largest October event and a large event in September. Unfortunately these are the only two events with data for both the Stanley Lake tributary and Honna North West tributary, so it is not known if these differences persist throughout the year. For the October event, the Honna North West probe recorded a more prolonged sediment crest which mirrored the precipitation intensity prior to and during the event, while the Stanley Lake tributary probe produced a sharper turbidity crest following the peak precipitation intensity. Although the Stanley Lake tributary drains an area four times larger than the Honna North West tributary and instantaneous discharge measured in July 2010 was 6 to 7 times greater for the Stanley Lake tributary than for the Honna North West, both tributaries had similar peak suspended sediment fluxes during the October event (Figure 3.10 c). Because the Honna North West is the

smaller of the two tributaries, the turbidity and sediment flux values of the October event imply that it carries a larger amount of sediment per unit discharge than the Stanley Lake tributary. The smaller discharge in this tributary allows minor turbidity events from low precipitation intensity events, which produce small amounts of sediment, to be observed. The more responsive nature of the Honna North West may be due to higher road use and road density in the sub-catchment compared to the Stanley Lake sub-catchment or because of the different geology of the two catchments. The Stanley Lake catchment is predominantly sandstone compared to a more mudstone and shale dominated lithology in the Honna North West catchment. Also the lake in the upper region of the Stanley Lake tributary (Figure 1.2) most likely collects sediment derived from areas higher in the catchment, dampening turbidity and sediment flux peaks. Information on the percent of area logged in each catchment and road use during and prior to the 2009-2010 season (which are currently unavailable) may reveal other causes for the observed differences between these two catchments.

Turbidity values were much higher at the sites downstream from the road crossings of Tributary 1 and 2 than at the upstream sites for all events with available data; suspended sediment fluxes were also much higher for the downstream sites (Figure 3.10). This confirms that road crossings are a source of sediment to the river. The downstream site at Tributary 1 recorded very high turbidity values compared to all other sites in the watershed, except during the January and March events, and turbidity responses tended to be earlier and sharper than for the other sites. Estimated sediment fluxes from Tributary 1 downstream, however, were relatively small compared to other sites. This demonstrates the importance of flow volume, not just sediment concentration, in determining stream

vulnerability to sediment influx. Low flows and small tributaries are most susceptible to high turbidity events as little sediment input is required to produce high turbidity values. The site downstream of the road crossing in Tributary 1 showed turbidity responses to very small precipitation events, which were not evident in turbidity measurements in the larger streams. This site also produced several turbidity responses when no precipitation was recorded by the Grapple 10 rain gauge. This suggests either very small amounts of precipitation are required to produce a turbidity response downstream of the road crossing in Tributary 1 or something else (e.g. animal crossings or spray from the road) contributed sediment to the river between precipitation events.

The probe deployed upstream of the road crossing in Tributary 2 showed peak turbidity values that were higher than those found upstream of the road crossing in Tributary 1. The probe downstream of the road crossing in Tributary 2, however, showed lower peak turbidity values than at the Tributary 1 downstream site during the August and April events, but not during the March event. This suggests not only do different road sections produce different amounts of sediment but the size of the river that carries it is also important in determining sediment concentrations in stream water.

A clockwise relation between turbidity and discharge was observed at all sites throughout the watershed during all seasons (Figure 3.11). Higher turbidities consistently occurred during the rising limb of storm events, suggesting supply limited conditions and that sediment is flushed from the system during events.

### **3.4.3 Estimated monthly sediment fluxes**

The fall months (September – November) had high sediment fluxes, while the winter and spring months (December, February, April and May) had relatively low

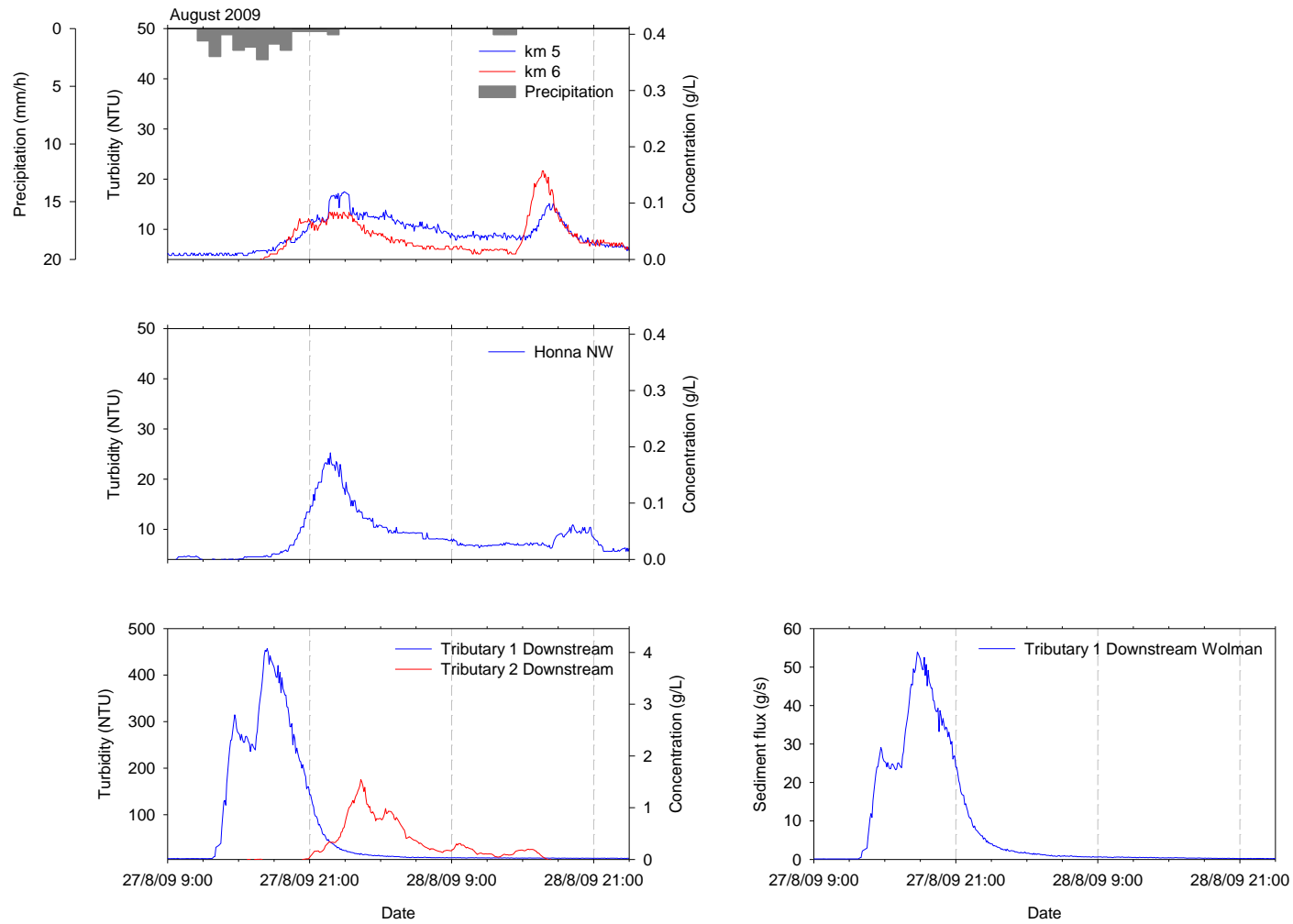


**Figure 3.10 a. August 27, 2009 event**  
**Wolman: sediment flux derived from discharge based on depth-averaged-velocity**

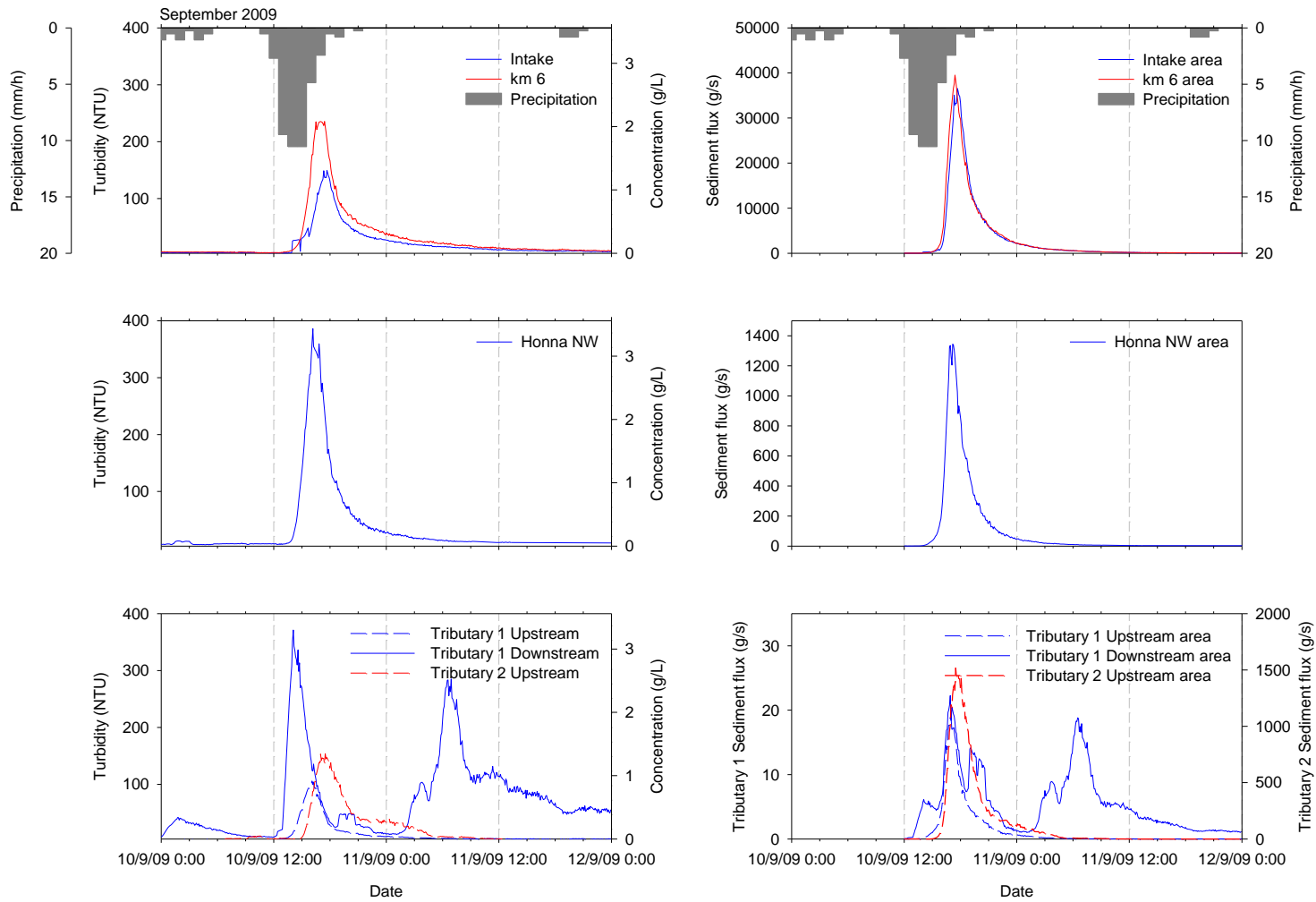


**Figure 3.10 b. September 10, 2009 event**

**Rating:** sediment flux derived from discharge based on rating curve; **Area:** sediment flux derived from discharge based on contributing area-discharge relation; **Wolman:** sediment flux derived from discharge based on depth-averaged-velocity

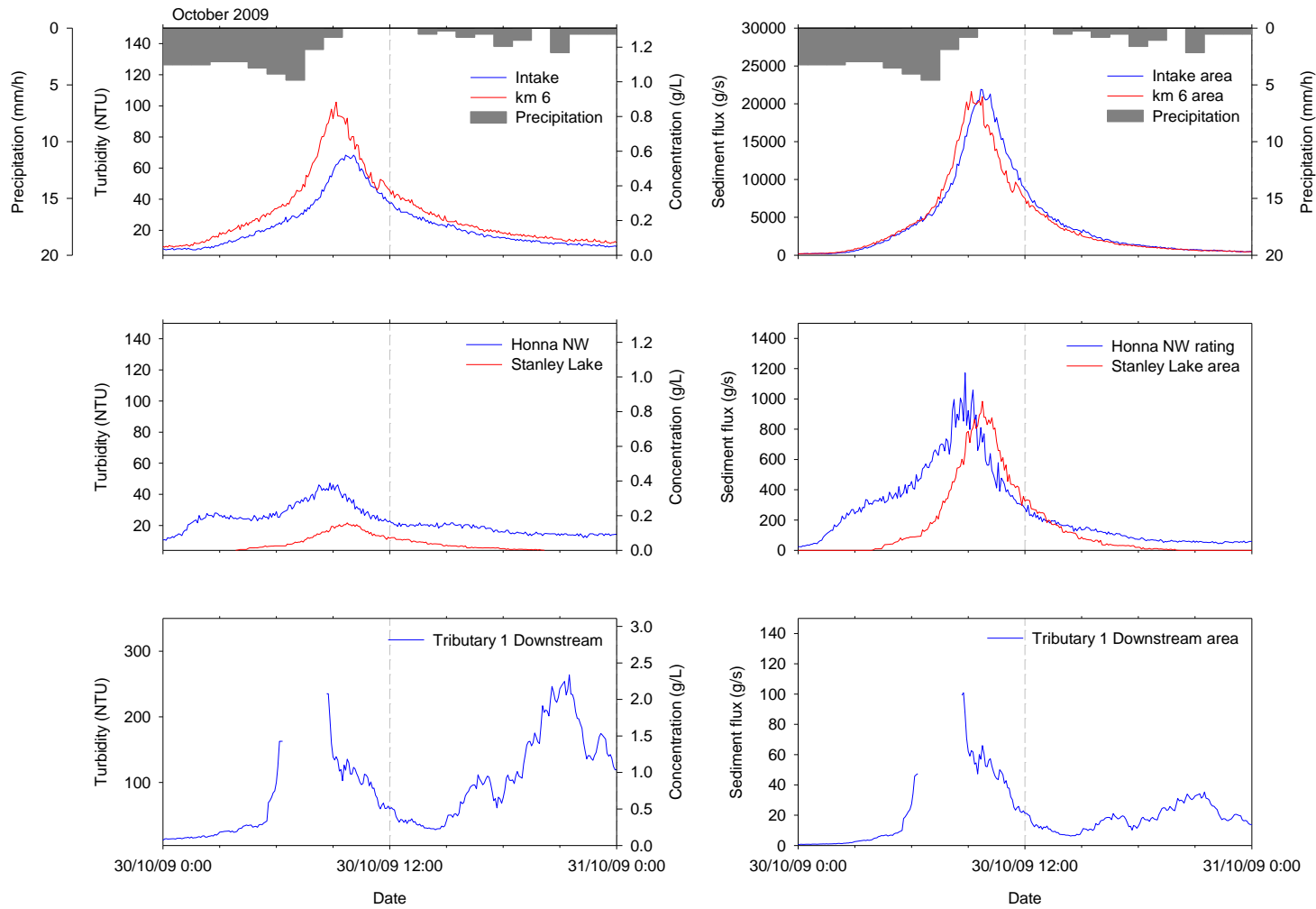


**Figure 3.10 c. October 30, 2009 event**

**Rating:** sediment flux derived from discharge based on rating curve; **Area:** sediment flux derived from discharge based on contributing area-discharge relation



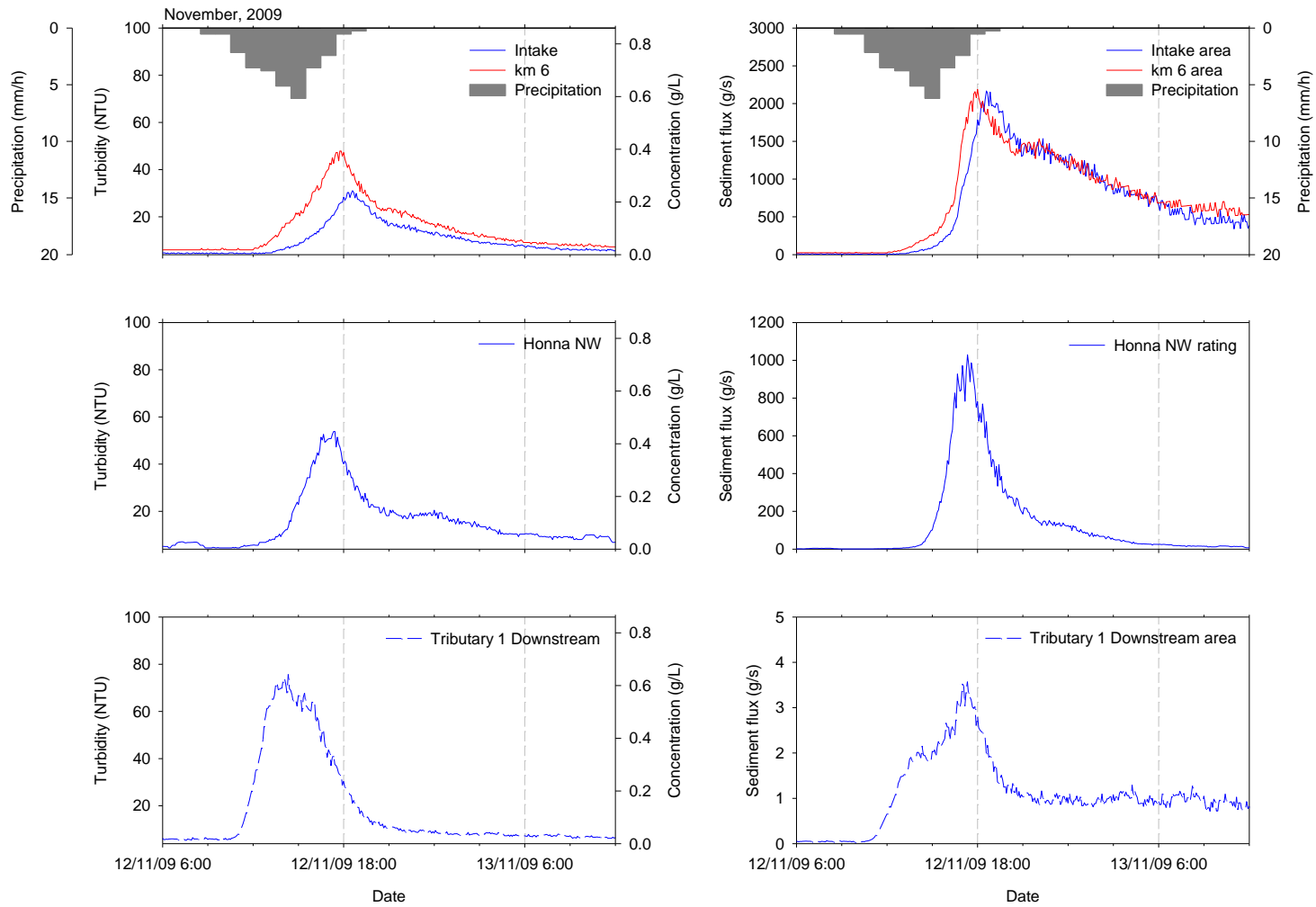


**Figure 3.10 d. November 12, 2009 event**

**Rating:** sediment flux derived from discharge based on rating curve; **Area:** sediment flux derived from discharge based on contributing area-discharge relation

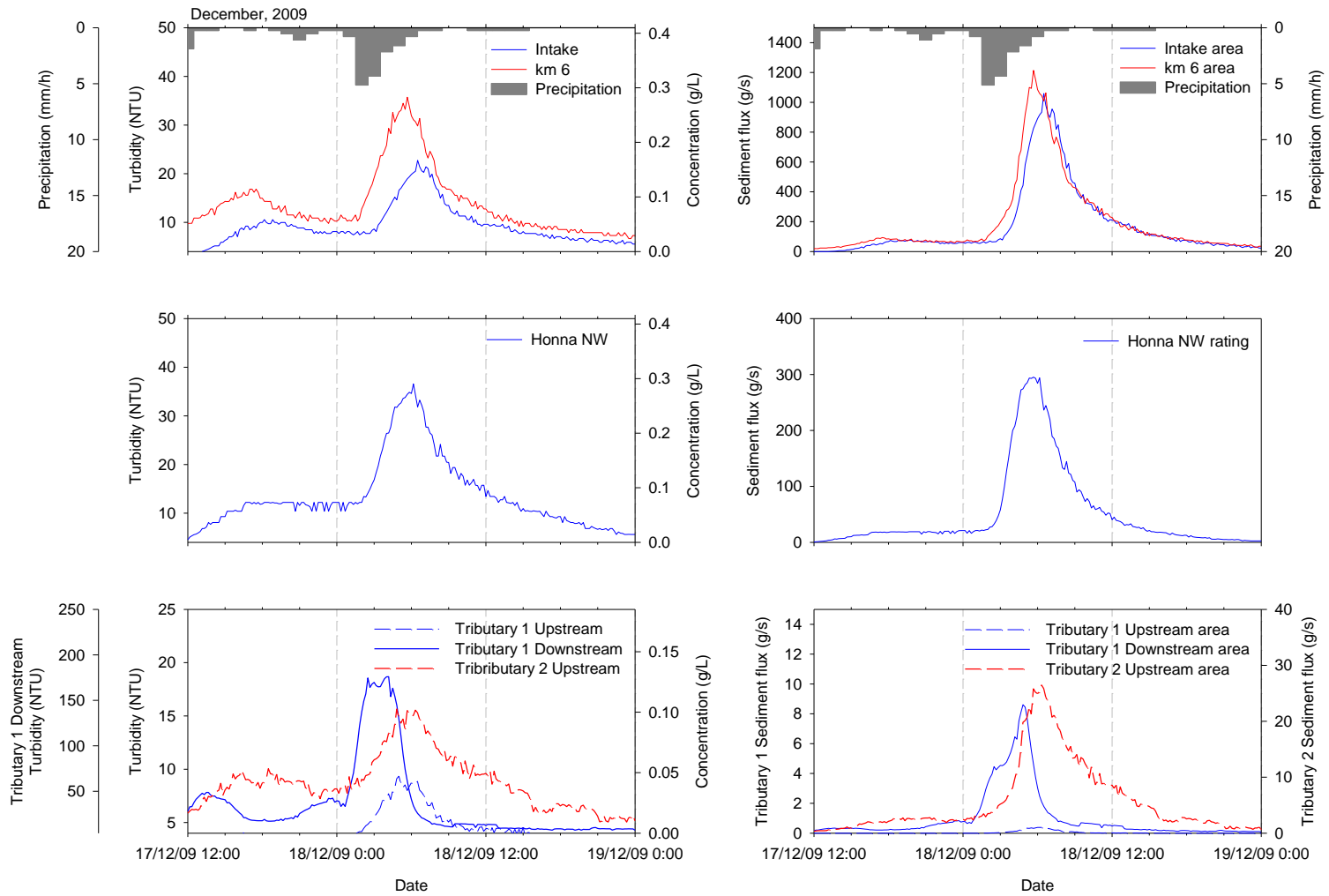


**Figure 3.10 e. December 18, 2009 event**  
**Rating: sediment flux derived from discharge based on rating curve; Area: sediment flux derived from discharge based on contributing area-discharge relation**

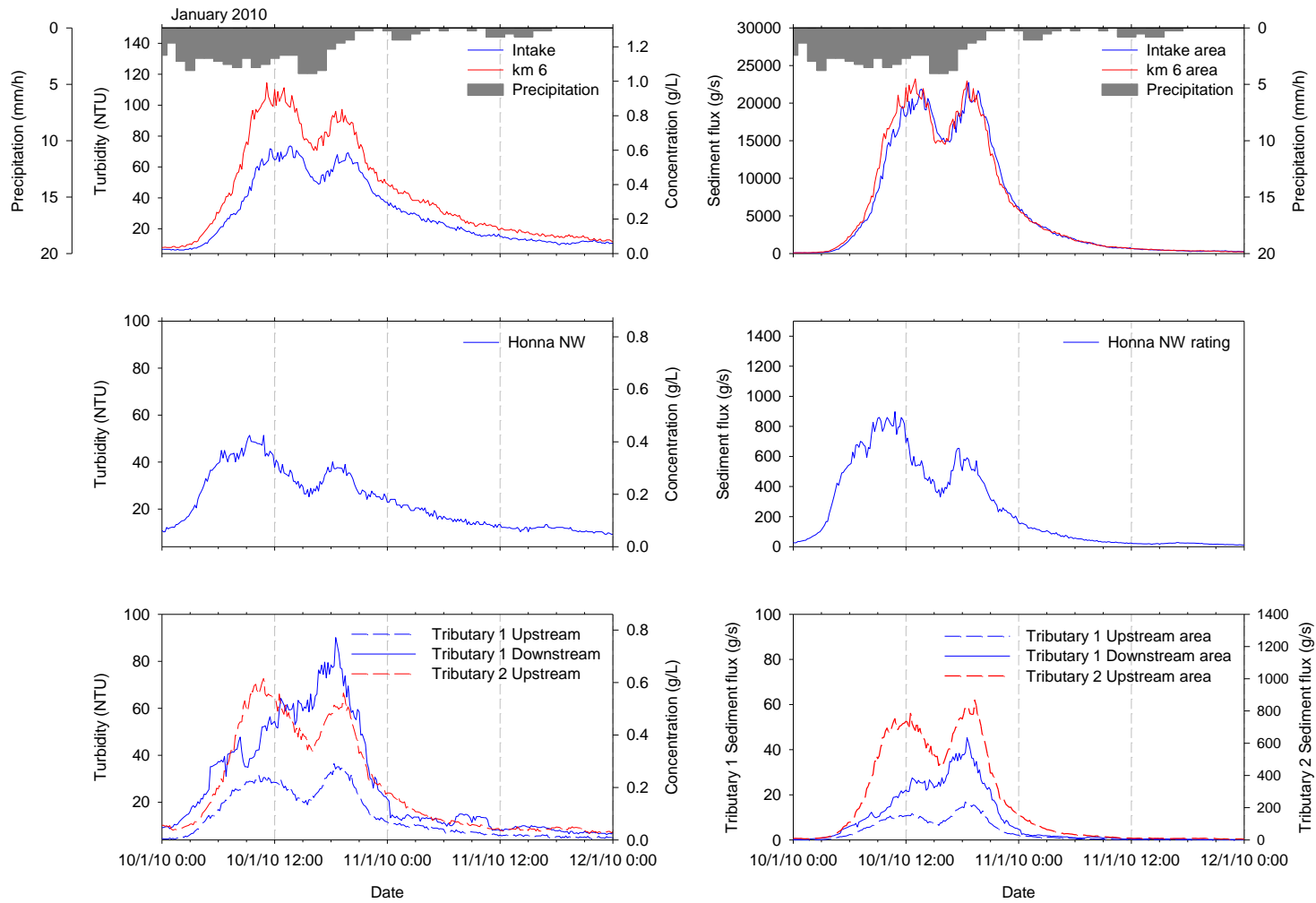


**Figure 3.10 f. January 10, 2010 event**

**Rating: sediment flux derived from discharge based on rating curve; Area: sediment flux derived from discharge based on contributing area-discharge relation**

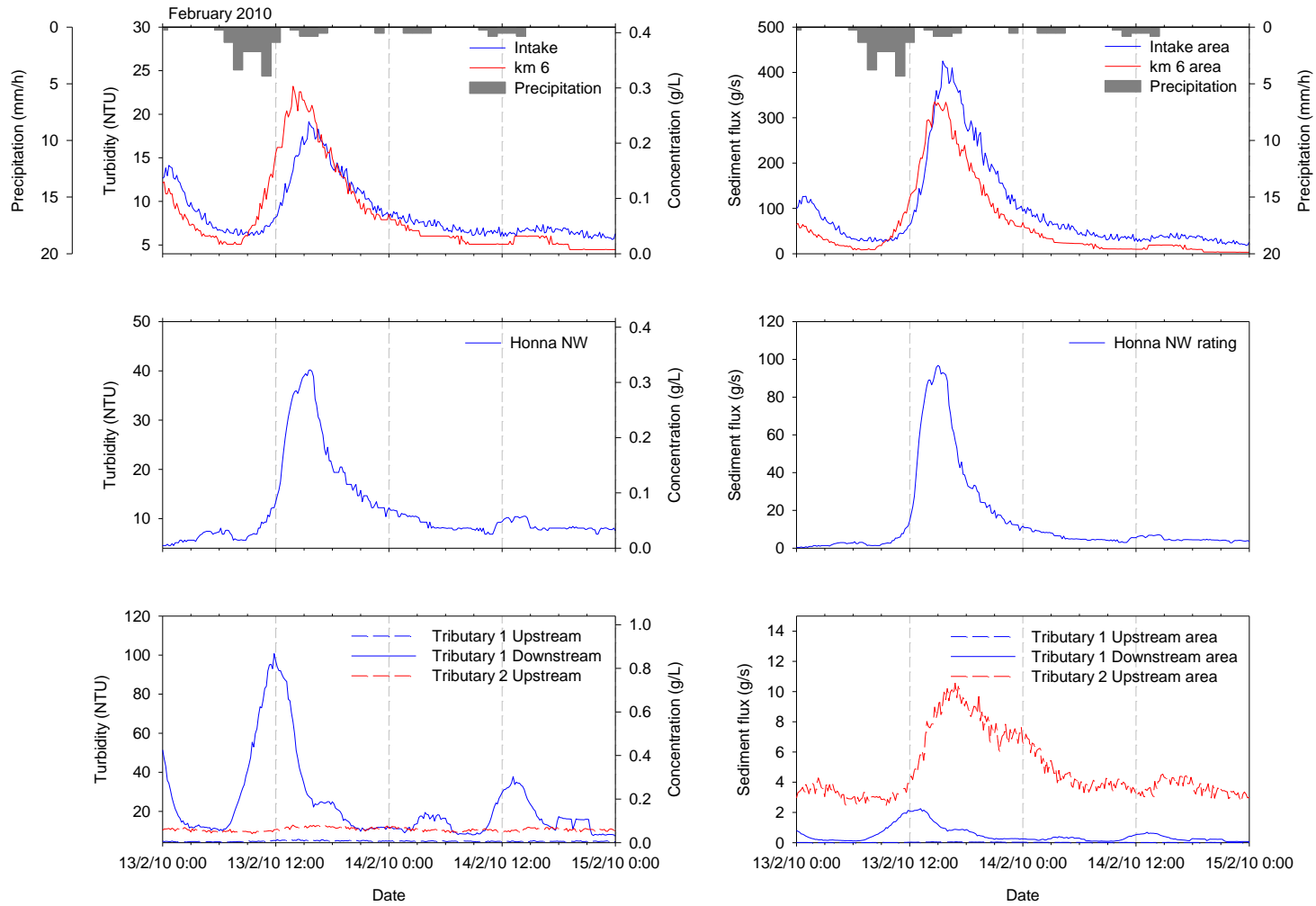


**Figure 3.10 g. February 13, 2010 event**

**Rating: sediment flux derived from discharge based on rating curve; Area: sediment flux derived from discharge based on contributing area-discharge relation**

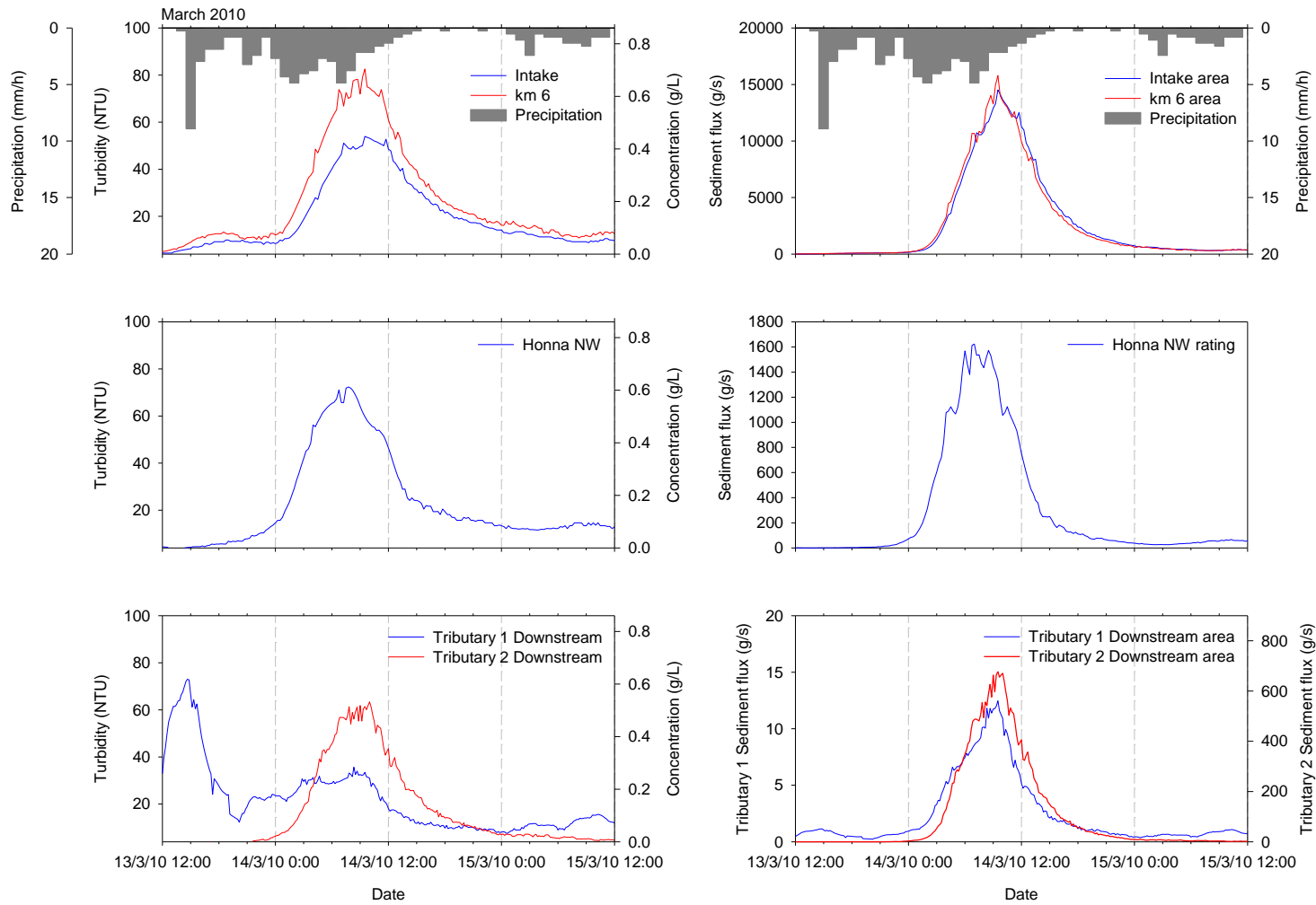


**Figure 3.10 h. March 14, 2010 event**

**Rating: sediment flux derived from discharge based on rating curve; Area: sediment flux derived from discharge based on contributing area-discharge relation**

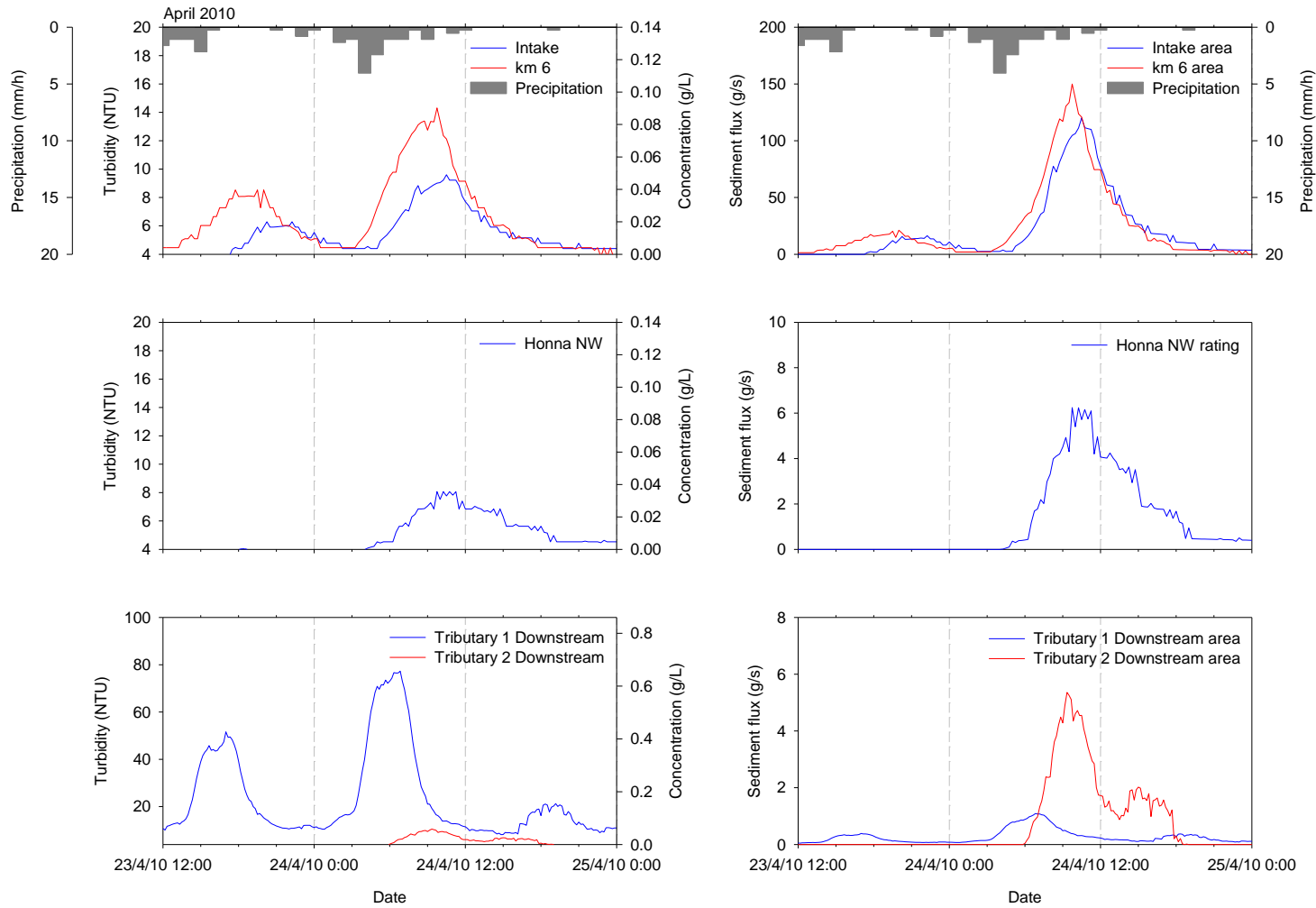


**Figure 3.10 i. April 24, 2010 event**

**Rating: sediment flux derived from discharge based on rating curve; Area: sediment flux derived from discharge based on contributing area-discharge relation**

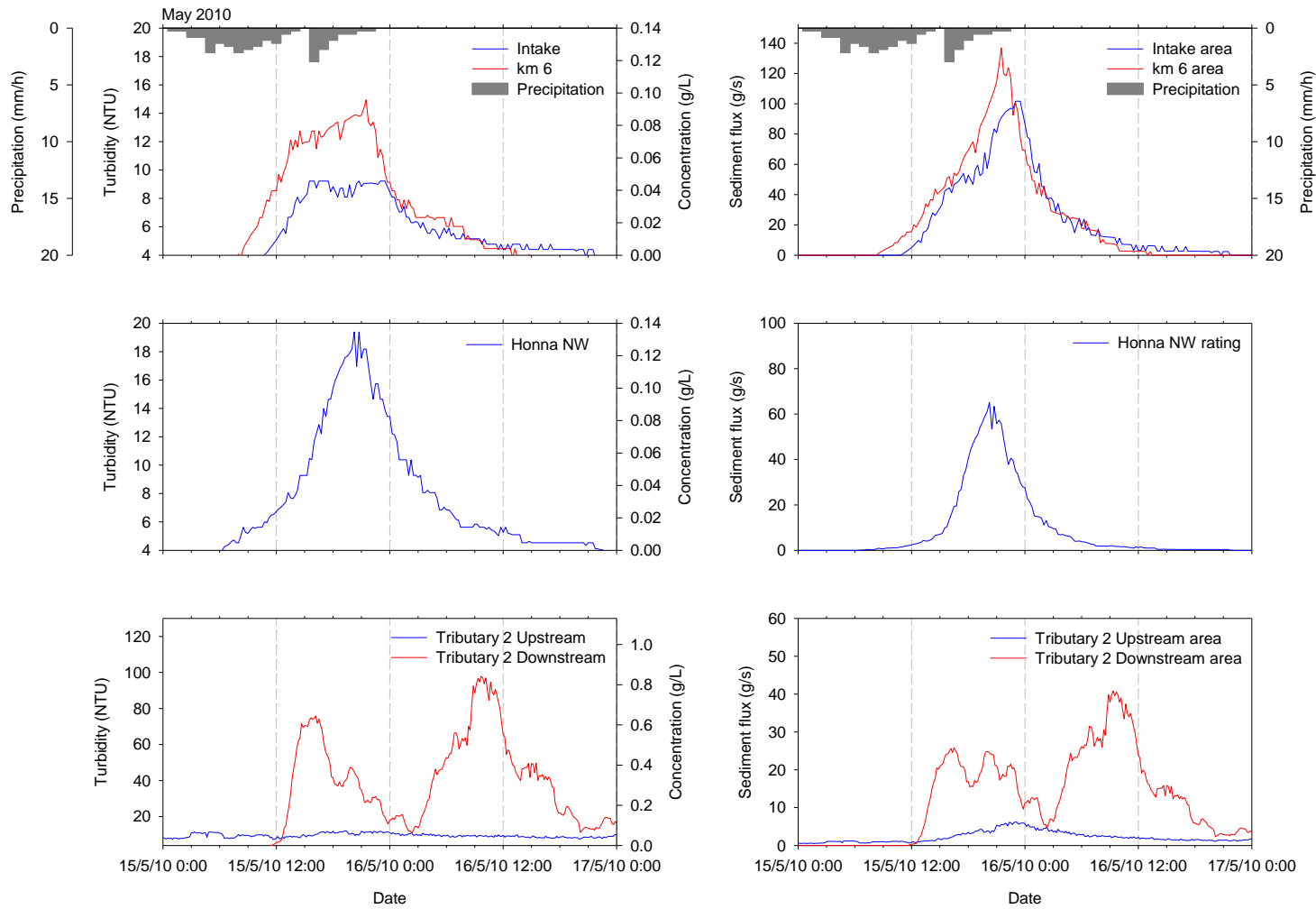


**Figure 3.10 j. May 15, 2010 event**

**Rating: sediment flux derived from discharge based on rating curve; Area: sediment flux derived from discharge based on contributing area-discharge relation**

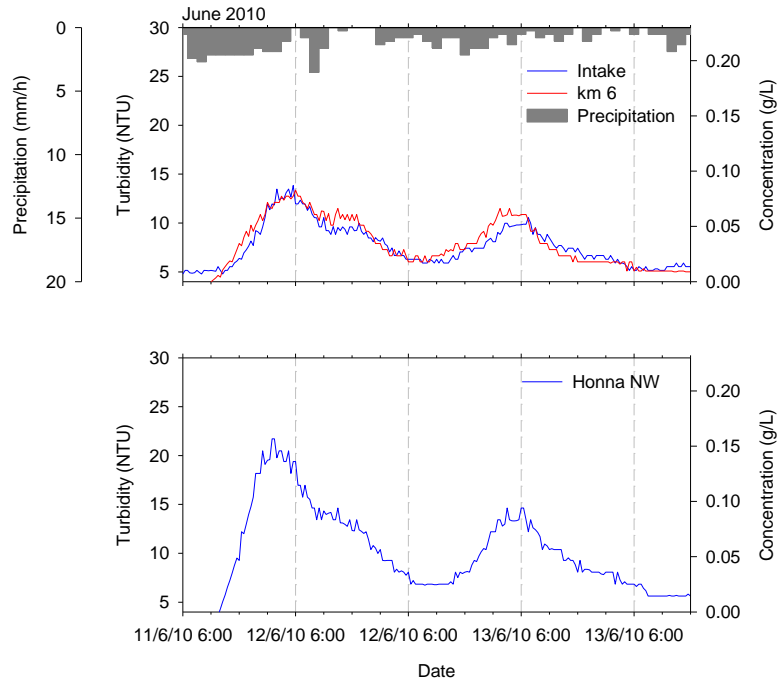


**Figure 3.10 k. June 12, 2010 event**

sediment fluxes along the Honna River and its tributaries (Figure 3.12 a). Although sediment flux data is not available for the summer months, values are expected to be low as precipitation is relatively low during the summer (Figure 1.3). The monthly flux values support the conceptual model of dry summers allowing for the accumulation of sediment within the watershed, which is mobilized and flushed out by several fall storms that lead to high sediment concentrations. High sediment concentrations did not persist throughout the winter of the 2010/2011 season due to lower precipitation and river flow in December and February (Figure 1.3).

The monthly suspended sediment mass flux at km 6 was similar (or slightly higher) than at the Drinking Water Intake for all months with data available except March. In March the suspended sediment flux was significantly (8 times) higher at km 6 (Figure 3.12 a). The much higher flux at km 6 during March matches higher turbidity



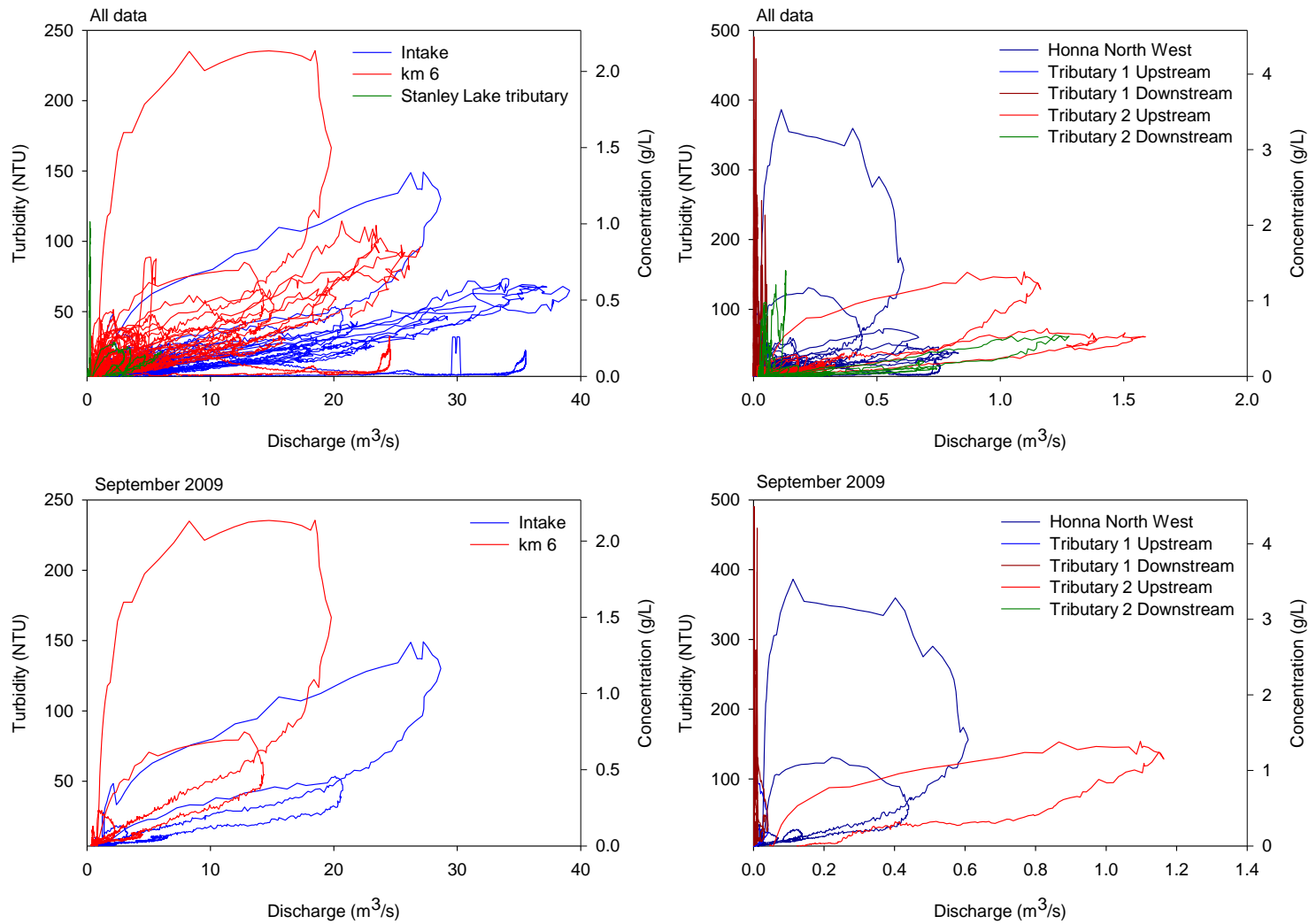


**Figure 3.11 Clockwise hysteretic relation between suspended sediment concentration and discharge**

values recorded in the Honna North West and Tributary 1. The Drinking Water Intake probe has a 10 day data gap during the beginning of March. During this 10 day period km 6 received 16% of its March suspended sediment flux suggesting the data gap does not fully explain the difference in suspended sediment flux at km 6 compared to the Drinking Water Intake. If the March data for the Drinking Water Intake site is ignored then the monthly sediment fluxes at the Drinking Water Intake and km 6 support the results from the individual events discussed above: the sediment flux remains relatively constant as you move downstream along the Honna River, suggesting the major sediment sources are located above km 6 and sediment plumes become diluted as they travel down stream with little sediment being added and potentially some sediment being deposited.

Estimated monthly sediment fluxes for the Honna North West were much smaller than those in the Honna River, although they displayed the same seasonal pattern of high fluxes in fall and low fluxes in winter and spring, with the exception of January and March (Figure 3.12 a). The Honna North West makes up 7% of the contributing area at the Drinking Water Intake site but supplied only 2.5% of the flow and 3.4% of the sediment between September 2009 and May 2010. This suggests that although the Honna North West is a sediment source for the Honna River, other sources, such as roads, other tributaries, or in channel sediment are more important despite the occasionally high suspended sediment concentrations found in the Honna North West. The Whiskey Creek, Skowkona Creek, Honna East, Stanley Lake and Honna North West tributaries all enter the Honna Mainstem above km 6. Due to a lack of appropriate turbidity probe deployment locations in Whiskey Creek, Skowkona Creek and the Honna East, turbidity monitoring was not feasible in these tributaries. Future studies using alternative

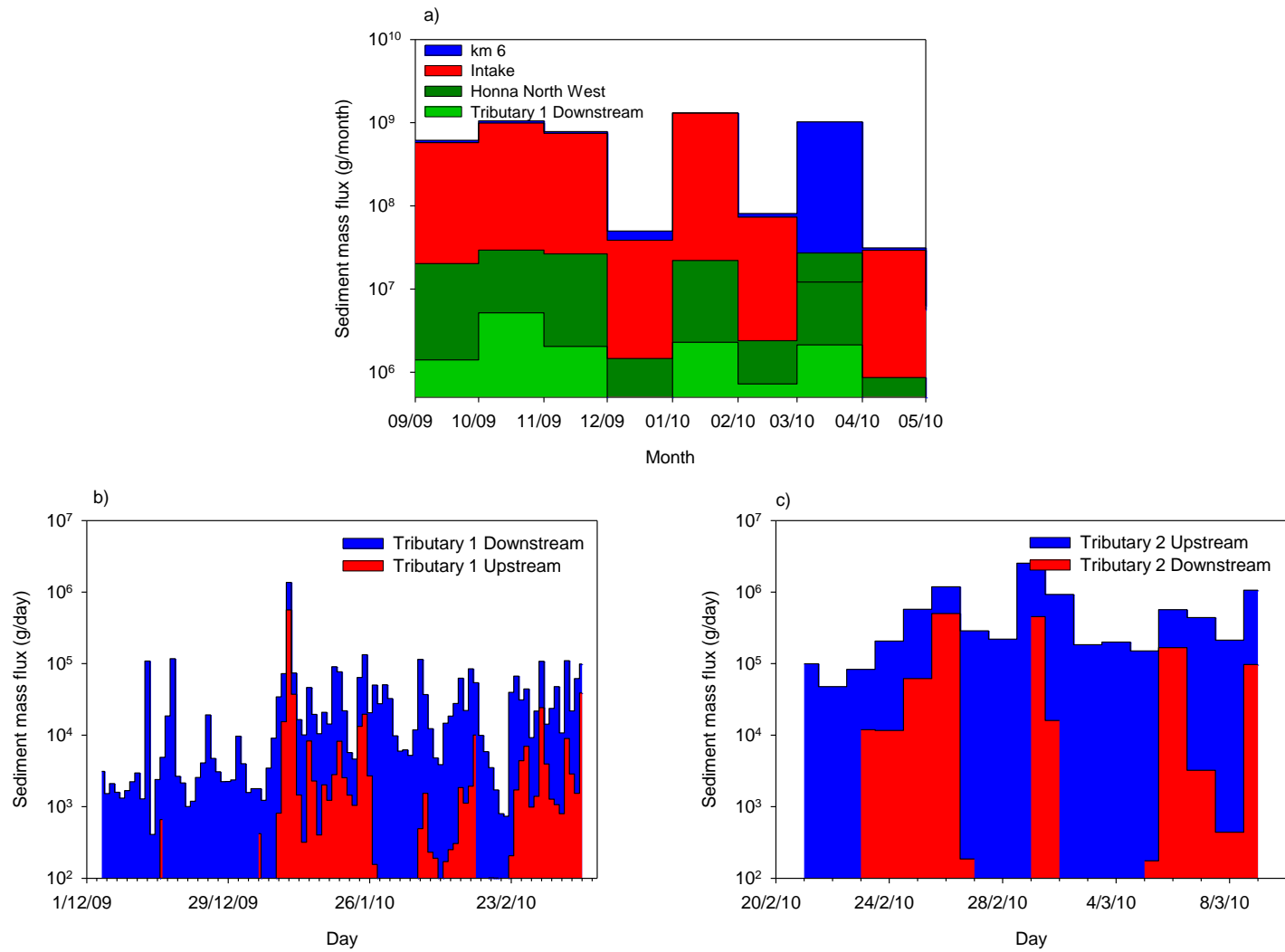


**Figure 3.12 Suspended sediment mass fluxes**

approaches to determine sediment fluxes from these sub-basins are necessary to further isolate the main sediment sources to the Honna Mainstem. Tributary 1 was a small contributor to the Mainstem sediment flux despite frequent high suspended sediment concentrations at the downstream site.

The daily sediment fluxes for January – March 2009 showed the monitoring site downstream from the road crossing at Tributary 1 had consistently higher daily sediment fluxes than the site upstream from the crossing (Figure 3.12 b). On January 5<sup>th</sup> and February 25<sup>th</sup> over 11 kg more sediment more passed the downstream site than the upstream site. An opposite relation was not found at Tributary 2 during the end of February and beginning of March (Figure 3.12 c). The higher sediment fluxes above the road crossing in Tributary 2 during this period suggest the road crossing is only a minor sediment source at this site during this period.

#### **3.4.4 Multiple linear regression**

Multiple linear regression based on the data from the largest event in each month showed the peak turbidity during a rainfall event at the Drinking Water Intake was most influenced by total precipitation and peak discharge and least dependent on antecedent precipitation, antecedent traffic and the calendar day. Peak turbidity during a rainfall event at the Drinking Water Intake can be estimated by:

$$T = 2.5P_{total} + 1.5Q_{peak} \quad AdjustedR^2 = 0.99$$

where  $T$  is the peak turbidity in NTU,  $P_{total}$  is the total depth of precipitation during the event in mm, and  $Q_{peak}$  is the peak discharge during the event in m<sup>3</sup>/s.

The peak turbidity in the Honna North West was most influenced by total precipitation and was least dependent on antecedent precipitation and calendar day. Traffic data for roads in the Honna North West catchment were not available and therefore this variable was not used in the Honna North West regression.. Peak turbidity in the Honna North West can be estimated by:

$$T = 9.1P_{total} \quad AdjustedR^2 = 0.98$$

The September event included in the multiple linear regression had a significantly higher peak turbidity and sediment flux than the other events (Figure 3.13), resulting in high  $R^2$  values despite low significance for each individual variable.

Multiple linear regression showed the total suspended sediment flux at the Drinking Water Intake during a rainfall event was most influenced by peak precipitation and least dependent on antecedent precipitation and traffic. The total sediment flux at the Drinking Water Intake during a rainfall event can be estimated by:

$$\gamma = 4.5 \times 10^7 P_{peak} \quad AdjustedR^2 = 0.21$$

where  $\gamma$  is the total sediment flux in g and  $P_{peak}$  is the peak precipitation intensity. However, this equation explains only 21% of the observed variation in the total sediment flux at the Drinking Water Intake.

The total sediment flux in the Honna North West was most influenced by peak discharge and least dependent on antecedent precipitation. The total sediment flux in the Honna North West during a rainfall event can be estimated by:

$$\gamma = 9.3 \times 10^5 Q_{peak} \quad AdjustedR^2 = 0.52$$

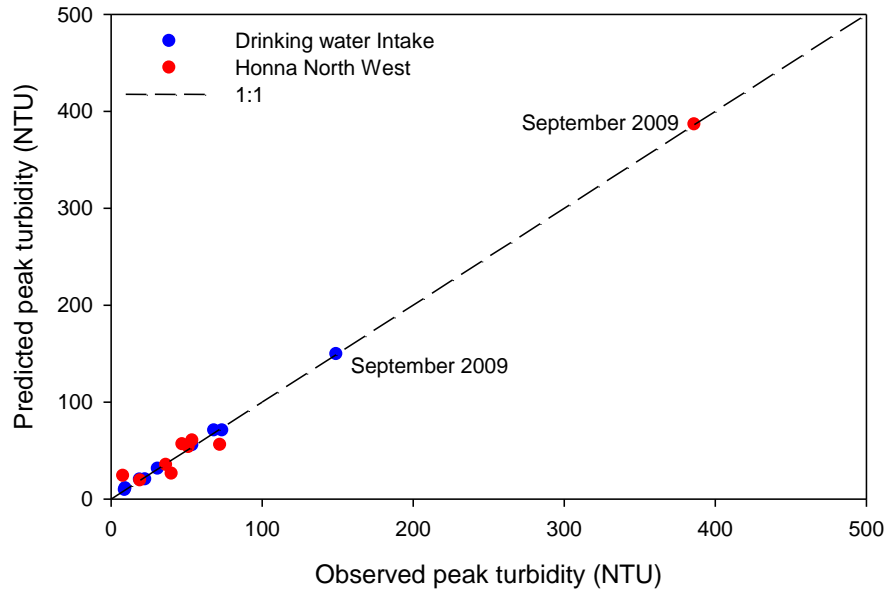


Figure 3.13 Observed and predicted peak turbidity values

### 3.5 Conclusions

Turbidity and suspended sediment concentrations during individual storm events decreased downstream in the Honna River. This resulted in near constant sediment fluxes as you traveled down river for both individual turbidity events and monthly suspended sediment fluxes. These results suggest sediment plumes are diluted (and some deposition of sediment may occur) as the plume travels down the Honna River, and the main sediment sources are located above km 6, either along the Mainstem of the Honna River where the road parallels the river or within its tributaries. The contributions from the Honna North West tributary, however, were small, providing less than 5% of the sediment at the Drinking Water Intake site. More work is needed to identify which tributaries contribute the most sediment to the Honna River. Future road and ditch improvement projects should focus on sections north of km 6 as sections below km 6 can have high suspended sediment concentrations but do not significantly contribute to the

total suspended sediment flux at the Drinking Water Intake. Road sections above km 6 were found to have the highest potential to deliver sediment to the river because of its close proximity to the river and poor quality of the substrate (see Chapter 4).

Smaller tributaries, such as Tributary 1 (and to some degree the Honna North West), tend to have rapid, frequent and large turbidity responses, even during small rainfall events. Small tributaries lack sufficient discharge to dilute sediment and are thus the most sensitive areas for high turbidity if sediment enters these streams from ditches, road crossings or cross drains.

Monthly suspended sediment fluxes were consistently highest during the fall months (September – November). As alternate water reservoirs (e.g. groundwater) may still be strained from summer depletion and usage, high suspended sediment concentrations in fall likely pose the greatest threat to drinking water resources in the Honna River. Relatively low suspended sediment fluxes during the spring months suggest this period is less likely to have high turbidity problems. It is expected that turbidity problems will also be small in summer because of the relatively low rainfall during summer. However large rainfall events during summer may result in very high turbidity because, similar to the fall, sediment hasn't been flushed out of the system and because of the relatively low stream flow the potential for dilution is small.

## **4 SEDIMENT VOLUME**

### **4.1 Introduction**

In 2008 the B.C. Ministry of Forest and Range developed an indicator based water quality assessment methodology called the Water Quality Effectiveness Evaluation (WQEE) (Maloney et al., 2009). The WQEE assesses the contribution of fine sediment to a stream network as a result of forest operations. It is a field based approach to assess stream crossings and other point sources of sediment. Systematic measurements are taken at each crossing within an area of concern, yielding an estimate of the volume of sediment each crossing may deliver to the stream network in a year. The WQEE procedure compares the potential volume of sediment each road crossing contributes to a nearby river (its hazard rating) to the width of the river as an approximation of its ability to dilute the sediment (its risk rating). The WQEE protocol recognizes the absolute volume of sediment calculated by the procedure may be off by up to an order of magnitude (Maloney et al., 2009). However, this error margin is considered acceptable as the risk classes the system employs span several orders of magnitude (Floyd, 2008).

A WQEE assessment of the portion of the Queen Charlotte Mainline Forest Road South with the potential to deliver sediment to the Honna River was completed in fall 2009 to estimate the amount of sediment generated by the road and delivered to the Honna River on an annual basis. This estimate was compared to estimates based on rainfall simulation results (Chapter 2) and turbidity- monitoring results (Chapter 3).

### **4.2 Methods**

All crossings along the Queen Charlotte Mainline Forest Road South with the potential to deliver road derived sediment to the Honna River were evaluated in October



2009. The crossings were located between km 3 and km 10 of the Mainline. South of km 3 the Mainline no longer parallels the Honna River and a wetland adjacent to km 10 prevents transport of any road sediment from moving downstream into the mainstem of the Honna River (Figure 1.2). In total 52 crossings were assessed using the WQEE methodology (as described in Protocol for Evaluating the Potential Impact of Forestry and Range Use on Water Quality (Water Quality Management Routine Effectiveness Evaluation) version 3.0) (Maloney et al., 2009) during or shortly after rain events so the location and extent of overland flow and runoff pathways originating from the road prism could be easily identified.

The area of each component of the road prism, including the road surface, ditch lines, cut slopes and fill slopes draining into each crossing was measured and the slope, amount of exposed soil, and soil texture of each component was noted. The connectivity of each component to the Honna River was estimated by observing flow paths, the extent of overland flow and the degree of ponding of outflow (Table 4.2 and Figure 4.1). The volume of potential sediment generated from each crossing was estimated based on these measurements and the crossing was assigned a corresponding hazard rating (Table 4.1).

<b>Table 4.1 Total fine sediment generation hazard rating (independent of stream size)</b>		
<b>Total volume of fine sediment generated per year</b>	<b>Site sediment generation potential classes (Hazard)</b>	<b>General level of management</b>
< 0.2 m <sup>3</sup>	Very low	Good
0.2 - 1 m <sup>3</sup>	Low	
1 - 5 m <sup>3</sup>	Moderate	
5 - 20 m <sup>3</sup>	High	
> 20 m <sup>3</sup>	Very High	Poor

Table derived from Table 8 in Maloney et al. (2009)

**Table 4.2 Sample form showing required WQEE data gathered for a road crossing**

Form 2. Water Quality Sample Site Field Card												
Sample Site ID:	33		Comments: The culvert is located near the km 7 turbidity probe. The outflow does not flow above ground between the road edge and the Honna River (~10m), but a sediment plume is visible in the Honna River. The RRDu has typar covered blocks but flow is still quite evident.									
Opening ID:	N/A											
District:	Haida Gwaii District											
UTM Zone:	8											
Easting:	0690103											
Northing:	5909098											
Road Ref:	Queen Charlotte Mainline											
Watershed/stream:	Honna River											
Known domestic intake downstream?	Yes											
Stream Channel Width (m):	1											
Date Completed:	26-Oct-09											
Site Type	5											
Components and their Characteristics			Surface Erosion Contribution									
Components	Connectivity	Portion fine sediment	Area (m <sup>2</sup> )	Portion of surface erodible	Net (m <sup>2</sup> )	Slope (%)	Road Use	Surface quality	Depth of erosion (m <sup>3</sup> )	Volume of material (m <sup>3</sup> )	Total sediment contribution (m <sup>3</sup> )	Fine sediment contribution (m <sup>3</sup> )
LRS	-	-	0	-	-	-	-	-	-	-	-	-
RRS	1	1	525	1	525	2-10	Heavy	Average	0.005	2.63	2.63	2.63
Fill	-	-	50	0	0	-	-	-	-	-	-	-
LRDu	-	-	0	-	-	-	-	-	-	-	-	-
LRDd	-	-	0	-	-	-	-	-	-	-	-	-
RRDu	-	-	150	0	0	-	-	-	-	-	-	-
RRDd	-	-	0	-	-	-	-	-	-	-	-	-
LRCu	-	-	0	-	-	-	-	-	-	-	-	-
LRCd	-	-	0	-	-	-	-	-	-	-	-	-
RRCu	0.5	0.5	75	0.05	3.75	>10	-	Good	0.010	0.04	0.02	0.01
RRCd	-	-	0	-	-	-	-	-	-	-	-	-
Total fine sediment generation from surface erosion for site:											2.63	
Rating of total fine sediment generation hazard from site (independent of stream size):											MODERATE	

**Figure 4.1 Sample photos of WQEE assessment at Site 33**



**600mm metal culvert at Site 33**



**Outflow traveling over the forest floor at Site 33**

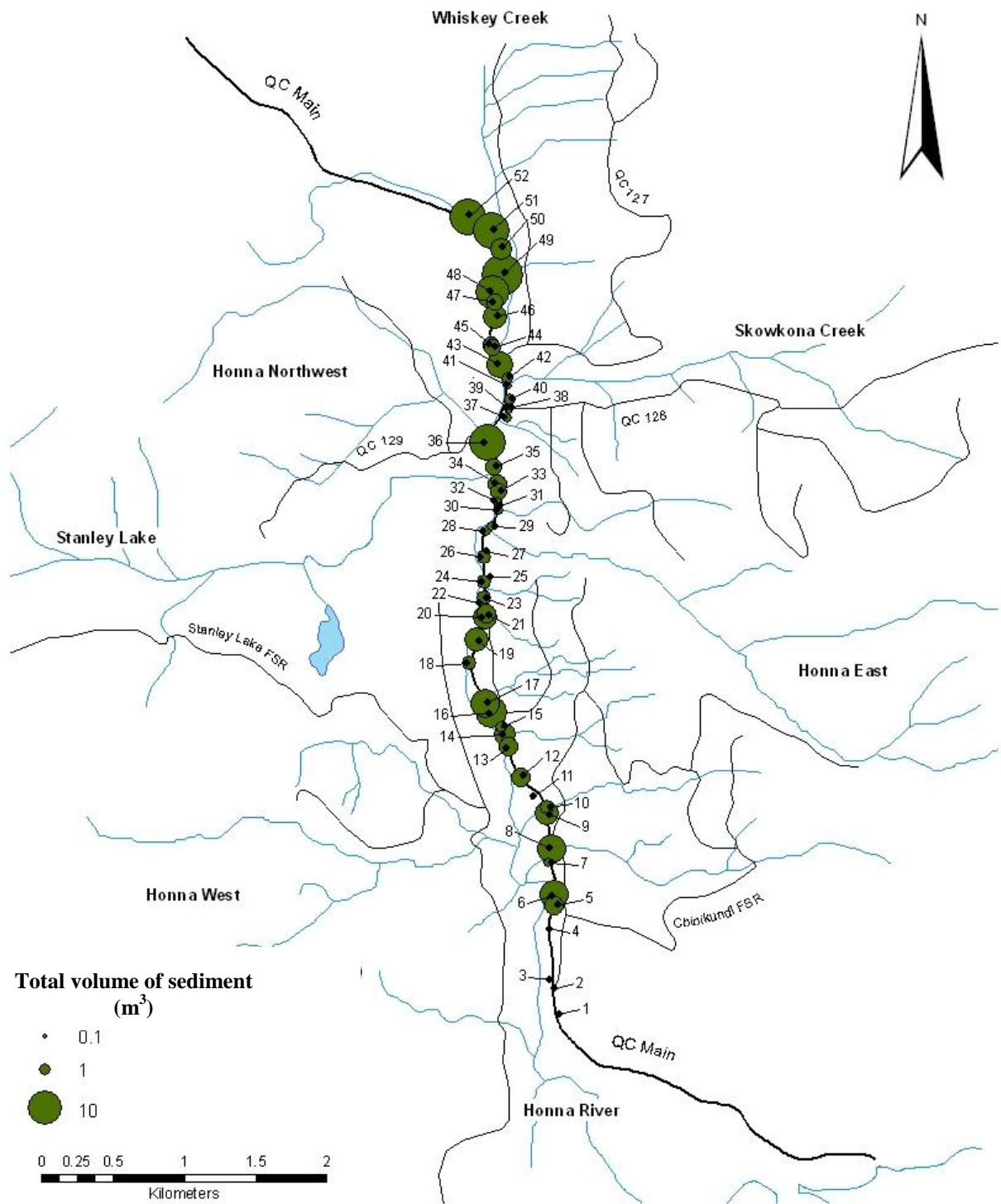


**Figure 4.2** Locations of stream crossings assessed in the Honna Watershed with the hazard score (size of circle) representing the predicted amount of sediment contributed to nearby streams

#### **4.2.1 Road derived sediment**

The rainfall simulation results (Chapter 2) showed the total mass of sediment generated by a 135 m<sup>2</sup> road surface can be estimated based on the rainfall intensity and road use conditions during a precipitation event. Precipitation data for the Honna Watershed from August 2009 to July 2010, measured at Grapple 10 (Figure 2.1), was divided into 75 events. Events were classified as periods with a minimum of 2.5 mm of rain in a 24 hour period, separated by 12 hours of no precipitation. The peak 5 minute precipitation intensity and total number of vehicles (measured near km 3, Figure 2.1) passing during the first 24 hours of each precipitation event were used to estimate the total mass of sediment generated from road surfaces draining into each crossing along the Queen Charlotte Mainline Forest Road South between km 3 and 10 (Table 4.3). These values are an overestimate as the peak precipitation intensity was not sustained throughout an entire event and likely only a few of the total number of recorded vehicles were large (logging) trucks. Precipitation data was not available after July 2, 2010, so the mass of sediment generated during June was used as an estimate for the summer period with missing rainfall data. This also results in an overestimate as July is generally drier than June. On the other hand, small rainfall events and other roads in the Honna watershed were not included in these calculations, which would result in an underestimate of the total amount of sediment produced from forest roads in the Honna Watershed. A particle density of 2650 kg/m<sup>3</sup> and porosity of 20% resulting in a bulk density of 2208 kg/m<sup>3</sup> was used to estimate the volume of sediment from the calculated mass of sediment generated from the entire length of the road at each culvert during one year (August 2009 to July 2010). The 95% confidence interval for the rainfall simulation

multiple linear regression results was used to estimate the range in the calculated volume of sediment.

### **4.3 Results and discussion**

#### **4.3.1 WQEE Results**

The Queen Charlotte Mainline Forest Road South was classified as a heavily used all season road. On average it saw 12 passes of loaded off-highway logging trucks a day during hauling in Fall 2009 and high amounts of local light weight traffic. The WQEE based estimate of the annual total volume of sediment from the Mainline between km 3 and km 10 was 235 m<sup>3</sup>/yr; 74% or 175 m<sup>3</sup>/yr of this volume is expected to reach the Honna River (Table 4.3 and Table 4.4)

Of the 52 crossings assessed, 18 (35%) had a sediment generation hazard rating of low or very low, 22 (42%) had a rating of moderate and 12 (23%) had a rating of high (Figure 4.2 and Figure 4.3). No crossings were assigned a hazard rating of very high. The majority of moderate and high hazard rating culverts were located around km 8 of the Queen Charlotte Mainline Forest Road South where road surface material is of poor quality and the river is very close to the road (Figure 4.2).

The WQEE results showed that the road surface was the primary source of road generated sediment. Ditches, cut slopes and fill slopes were generally well vegetated and rip rap was present in various locations to prevent cut slope erosion in steep areas. Higher hazard ratings were associated with crossings in areas of poor road surface quality. Culverts along the Queen Charlotte Mainline Forest Road South were frequent and well spaced. Higher WQEE hazard ratings were associated with crossings in areas with high connectivity between the road and river. Several ditches contained extensive ditch blocks,

at times covered in geotextile material, to promote pooling of water and to decrease the amount of ditch flow reaching the river. Some of these blocks appeared to be effective during small rainfall events, but during large rainfall events sediment laden water could be seen flowing through the ditch blocks and into the Honna River (Figure 4.4).

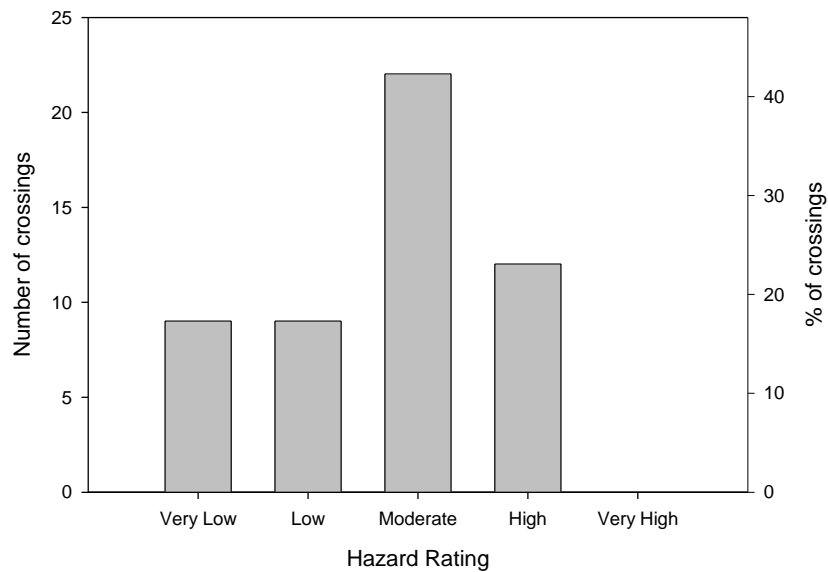


**Figure 4.3 WQEE hazard ratings for stream crossings of the QC Mainline between km 3 and km 10, assessed in October 2009**



**Figure 4.4 Sediment laden road surface runoff passing through ditch blocks along the Queen Charlotte Mainline Forest Road South**

### 4.3.2 Total road derived sediment

The estimated annual road derived sediment volume based on the rainfall simulation results was of the same order of magnitude as those estimated using the WQEE procedure (Figure 4.5). Only a 40% difference was found between the total volume of sediment generated by the entire road in a year based on the two methods (Table 4.3). The rainfall simulation results thus support the WQEE estimated yearly road surface sediment volumes for each road crossing. Compared to sediment volumes based on the rainfall simulation results which do not incorporate any spatial variation in road surface material or slope, the WQEE generally underestimated the sediment volumes at low hazard rating crossings and overestimated those at high hazard rating crossings, however they were generally in good agreement.

Turbidity monitoring above and below road crossing 16 (Tributary 1) supported its high hazard rating. Turbidity measurements taken above and below road crossing 28 (Tributary 2) supported its moderate hazard rating. Sufficient turbidity and discharge data were not available to validate the yearly sediment volume flux estimated by the WQEE procedure at either crossing 16 or 28. However, all evidence suggests the WQEE hazard ratings are a good estimate of the total volume of sediment generated at each road crossing.

According to the WQEE, the Queen Charlotte Mainline Forest Road South produces  $5.8 \times 10^3 \text{ m}^3$  of sediment per  $\text{km}^2$  of road surface and according to rainfall simulation results it produces  $5.0 \times 10^3 \text{ m}^3/\text{km}^2$  (between  $6.5 \times 10^2$  and  $1.1 \times 10^4 \text{ m}^3/\text{km}^2$  at the 95% confidence interval). This is less than the  $1 \times 10^4$  to  $1.5 \times 10^4 \text{ m}^3$  of sediment per



km<sup>2</sup> of used road per year expected by Roberts and Church (1986) for severely disturbed small drainage basins in the Queen Charlotte range.

Ramos-Scharron and MacDonald (2007) measured  $3.6 \times 10^4$  g of sediment generated per m<sup>2</sup> of road surface per year for unpaved roads in St John, US Virgin Islands. Fahey and Coker (1989) measured between  $1.6 \times 10^3$  to  $1.1 \times 10^4$  g/m<sup>2</sup>/year from forest roads in southwest Nelson, New Zealand. These values compare well with the rainfall simulation based flux of  $1.4 \times 10^3$  to  $2.5 \times 10^4$  g/m<sup>2</sup>/year and the WQEE based estimate of  $1.3 \times 10^4$  g/m<sup>2</sup>/year for the Honna Watershed.

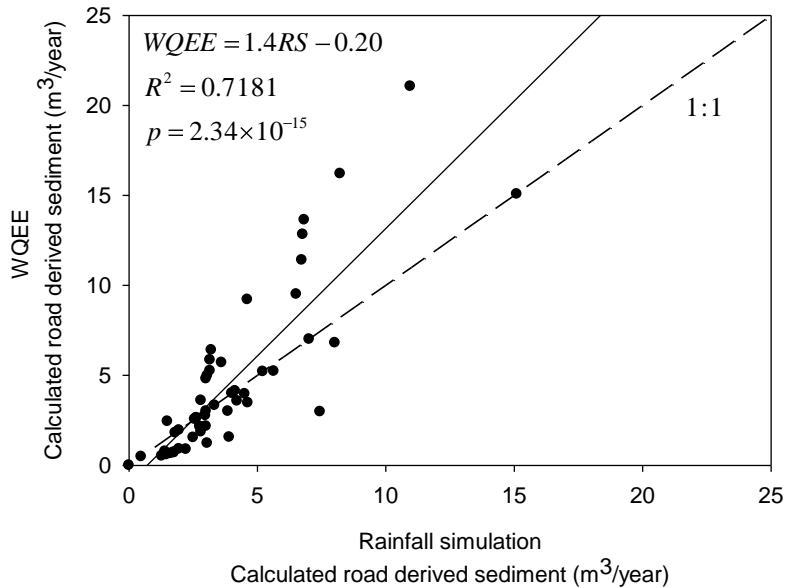


**Figure 4.5 Comparison of WQEE and rainfall simulation (RS) based yearly sediment yield estimates**

### 4.3.3 Comparison to measured sediment flux in the Honna River

The yearly suspended sediment mass flux in the Honna River was estimated by the total mass of sediment passing the Drinking Water Intake between September 1<sup>st</sup> 2009 and May 31<sup>st</sup> 2010, as no discharge data were available for August 2009, or June and July 2010 (See Section 0). The yearly suspended sediment mass flux is therefore

**Table 4.3 Total sediment derived from the road surface for all crossings between km 3 and km 10**

Culvert	Road Surface (m <sup>2</sup> )	WQEE (m <sup>3</sup> /yr)	Road surface sediment Rainfall Simulation based estimate				Culvert	Road Surface (m <sup>2</sup> )	WQEE (m <sup>3</sup> /yr)	Road surface sediment Rainfall Simulation based estimate			
			(g/yr)	(m <sup>3</sup> /yr)	Min. (m <sup>3</sup> /yr)	Max. (m <sup>3</sup> /yr)				(g/yr)	(m <sup>3</sup> /yr)	Min. (m <sup>3</sup> /yr)	Max. (m <sup>3</sup> /yr)
1	550	2	6.1x10 <sup>6</sup>	2.8	0.4	6.1	27	780	2	8.6 x10 <sup>6</sup>	3.9	0.5	8.7
2	600	3	6.6 x10 <sup>6</sup>	3.0	0.4	6.7	28	444	1	4.9 x10 <sup>6</sup>	2.2	0.3	4.9
3	825	4	9.1 x10 <sup>6</sup>	4.1	0.5	9.2	29	280	1	3.1 x10 <sup>6</sup>	1.4	0.2	3.1
4	630	5	7.0 x10 <sup>6</sup>	3.2	0.4	7.0	30	350	1	3.9 x10 <sup>6</sup>	1.8	0.2	3.9
5	924	3	1.0x10 <sup>7</sup>	4.6	0.6	10.2	31	350	1	3.9 x10 <sup>6</sup>	1.8	0.2	3.9
6	1600	7	1.8 x10 <sup>7</sup>	8.0	1.0	17.7	32	324	1	3.6 x10 <sup>6</sup>	1.6	0.2	3.6
7	350	1	3.9 x10 <sup>6</sup>	1.8	0.2	3.9	33	525	3	5.8 x10 <sup>6</sup>	2.6	0.3	5.8
8	1400	7	1.6 x10 <sup>7</sup>	7.0	0.9	15.5	34	665	3	7.4 x10 <sup>6</sup>	3.3	0.4	7.4
9	1125	5	1.2 x10 <sup>7</sup>	5.6	0.7	12.5	35	1485	3	1.6 x10 <sup>7</sup>	7.4	1.0	16.5
10	500	2	5.5 x10 <sup>6</sup>	2.5	0.3	5.5	36	2185	21	2.4 x10 <sup>7</sup>	11.0	1.4	24.2
11	595	3	6.6 x10 <sup>6</sup>	3.0	0.4	6.6	37	293	1	3.2 x10 <sup>6</sup>	1.5	0.2	3.2
12	840	4	9.3 x10 <sup>6</sup>	4.2	0.5	9.3	38	0	0	0.0x10 <sup>0</sup>	0.0	0.0	0.0
13	800	4	8.9 x10 <sup>6</sup>	4.0	0.5	8.9	39	770	3	8.5 x10 <sup>6</sup>	3.9	0.5	8.5
14	900	4	1.0 x10 <sup>7</sup>	4.5	0.6	10.0	40	390	1	4.3 x10 <sup>6</sup>	2.0	0.3	4.3
15	560	2	6.2 x10 <sup>6</sup>	2.8	0.4	6.2	41	256	1	2.8 x10 <sup>6</sup>	1.3	0.2	2.8
16	920	9	1.0 x10 <sup>7</sup>	4.6	0.6	10.2	42	512	3	5.7 x10 <sup>6</sup>	2.6	0.3	5.7
17	1640	16	1.8 x10 <sup>7</sup>	8.2	1.1	18.2	43	640	6	7.1 x10 <sup>6</sup>	3.2	0.4	7.1
18	1300	10	1.4 x10 <sup>7</sup>	6.5	0.8	14.4	44	525	3	5.8 x10 <sup>6</sup>	2.6	0.3	5.8
19	720	6	8.0 x10 <sup>6</sup>	3.6	0.5	8.0	45	1040	5	1.2 x10 <sup>7</sup>	5.2	0.7	11.5
20	630	6	7.0 x10 <sup>6</sup>	3.2	0.4	7.0	46	610	5	6.8 x10 <sup>6</sup>	3.1	0.4	6.8
21	560	4	6.2 x10 <sup>6</sup>	2.8	0.4	6.2	47	300	2	3.3 x10 <sup>6</sup>	1.5	0.2	3.3
22	96	0	1.1 x10 <sup>6</sup>	0.5	0.1	1.1	48	1343	11	1.5 x10 <sup>7</sup>	6.7	0.9	14.9
23	360	2	4.0 x10 <sup>6</sup>	1.8	0.2	4.0	49	1350	13	1.5 x10 <sup>7</sup>	6.8	0.9	15.0
24	390	2	4.3 x10 <sup>6</sup>	2.0	0.3	4.3	50	600	5	6.6 x10 <sup>6</sup>	3.0	0.4	6.7
25	608	1	6.7 x10 <sup>6</sup>	3.0	0.4	6.7	51	1363	14	1.5 x10 <sup>7</sup>	6.8	0.9	15.1
26	600	2	6.6 x10 <sup>6</sup>	3.0	0.4	6.7	52	3013	15	3.3 x10 <sup>7</sup>	15.1	2.0	33.4
<b>Total:</b>								<b>2.35x10<sup>2</sup></b>	<b>4.48x10<sup>8</sup></b>	<b>2.03x10<sup>2</sup></b>	<b>2.63x10<sup>1</sup></b>	<b>4.48x10<sup>2</sup></b>	

an underestimate of the actual suspended sediment mass flux. The yearly mass flux was also converted into a volume using a bulk density of  $2208 \text{ kg/m}^3$ . The yearly sediment volume flux in the Honna River at the Drinking Water Intake was  $1.7 \times 10^3 \text{ m}^3/\text{year}$ . The WQEE based estimate of the annual volume of sediment generated by the Mainline and expected to reach the Honna River was  $1.8 \times 10^2 \text{ m}^3/\text{year}$ , approximately 10% of the measured sediment flux between September 1<sup>st</sup> 2009 and May 31<sup>st</sup> 2010 (Table 4.4). Thus a significantly larger sediment flux was measured in the Honna River than could be attributed to Queen Charlotte Mainline Forest Road South road derived material. This suggests natural sediment sources are important in this watershed. However, road related sediment may make up 10% of the total sediment flux. Roberts and Church (1986) found between 1 and 11% of total sediment delivered to four streams in disturbed watersheds in the Queen Charlotte Ranges with road densities between 0.31 and  $0.93 \text{ km/km}^2$  was derived from forest road surfaces. Sheridan and Noske (2007) found 4.4% of the total suspended sediment load in a forested catchment with a road density of  $1.4 \text{ km/km}^2$  in southeastern Australia was derived from unpaved forest roads. The Honna watershed has a road density of approximately  $1.8 \text{ km/km}^2$ .

If all 92 km of road in the Honna Watershed acted similarly to the Mainline, then between  $3.0 \times 10^2$  and  $5.1 \times 10^3 \text{ m}^3/\text{year}$  of road derived sediment would be generated, or between 20 and 100% of the annual suspended sediment flux based on the 95% confidence interval of the rainfall simulation multiple linear regression equation. However not all road derived sediment would reach the Honna River and most other roads in the Honna Watershed have less traffic than the Mainline.

#### 4.4 Conclusions

The WQEE and rainfall simulation based estimates of the annual volumes of sediment generated by the Queen Charlotte Mainline Forest Road South were similar. The WQEE seems to be an appropriate method for estimating sediment yields in this watershed. The WQEE based estimate of annual road derived sediment flux to the Honna River was 10% of the measured suspended sediment flux; other sediment sources dominate the total suspended sediment flux.

<b>Table 4.4 Total road derived sediment reaching the Honna River</b>					
<b>Culvert</b>	<b>WQEE</b>			<b>Turbidity measurements</b>	
	<b>Sediment volume (m<sup>3</sup>/year)</b>	<b>Culvert</b>	<b>Sediment volume (m<sup>3</sup>/year)</b>	<b>Sediment mass (g/year)</b>	<b>Sediment volume (m<sup>3</sup>/year)</b>
1	0.00	27	0.00		
2	0.00	28	0.89		
3	0.00	29	0.72		
4	0.00	30	0.66		
5	3.49	31	0.47		
6	6.95	32	0.76		
7	0.72	33	2.63		
8	7.01	34	3.36		
9	5.27	35	2.50		
10	1.83	36	11.21		
11	0.00	37	0.59		
12	3.60	38	0.00		
13	3.24	39	0.60		
14	4.05	40	1.39		
15	1.00	41	0.51		
16	9.21	42	1.40		
17	8.10	43	6.40		
18	1.90	44	2.63		
19	4.65	45	2.73		
20	4.77	46	5.22		
21	3.65	47	2.47		
22	0.10	48	9.98		
23	1.62	49	14.96		
24	1.95	50	3.88		
25	0.00	51	12.14		
26	1.73	52	12.20		
<b>Total:</b>			<b>175</b>	<b>3.78x10<sup>9</sup></b>	<b>1426</b>

## **5 SUMMARY AND CONCLUSIONS**

### ***5.1 Rainfall Simulation***

Twenty four large scale rainfall simulation experiments were conducted at km 8 of the Queen Charlotte Mainline Forest Road South. Seven additional small scale rainfall simulation experiments were conducted at various locations between km 3 and km 7 and along a well maintained spur road at km 3. The rainfall simulation experiments were performed to determine the controls on sediment generation from forest roads, in particular the influence of rainfall intensity, rainfall amount, traffic intensity and truck speed. They also determined how long sediment concentrations in road surface runoff remained elevated following truck passage.

The rainfall simulation results showed precipitation intensity was the dominant control on the mass of sediment generated from a forest road. Both precipitation intensity and total precipitation exhibited a linear relation with the total mass of sediment generated from the forest road during an experiment, as did the number of loaded logging trucks passing during a precipitation event. Antecedent precipitation conditions were not important. The large spatial variability in initial sediment concentration demonstrated by the small scale trial results indicate extrapolation from one road section to another must be done cautiously.

Elevated sediment levels in road surface runoff persisted for 30 minutes following the passage of a loaded logging truck during low intensity trials and for shorter times at higher rainfall intensities. The lack of a relation between truck speed and sediment generated by a truck suggests speed restrictions during rainfall events would likely not be an effective way to manage sediment generation due to traffic. The low percent of total

mass due to truck passage (<30% for all but one trial) indicates significant amounts of sediment would be generated during rainfall events even if no trucks were present and suggest closure of roads during rainfall events will not eliminate sediment production from the roads, but may reduce it significantly.

## **5.2 River Monitoring**

Turbidity, converted to a measure of sediment concentration, was monitored at key locations throughout the Honna Watershed between August 2009 and July 2010 in order to obtain information on suspended sediment concentrations during natural rainfall events, the prevalence of high turbidity and to quantify the amount of sediment transported by the Honna River and its tributaries. Three turbidity probes were placed along the Honna River and two in important tributaries. Two small tributaries with road crossings near their confluence with the Honna River were fit with two probes each: one above and one below the crossing.

Peak suspended sediment concentrations decreased and sediment fluxes remained constant as you travel down the Honna River. This suggests the main sediment sources are located above km 6, either along the Mainstem of the Honna River, or within its other tributaries. This also suggests sediment plumes are diluted (and some deposition of sediment may occur) as the plume travels down the Honna River. The Honna North West tributary accounted for less than 3% of the yearly sediment flux at km 6 of the Honna River. More work is needed to identify which tributaries contribute the most sediment to the Honna River.

Suspended sediment concentrations were consistently higher below stream crossings than above stream crossings, showing roads are a source of sediment to the

Honna River. Smaller tributaries tended to have rapid, frequent and large turbidity responses, even during small rainfall events. Small tributaries lack sufficient discharge to dilute sediment that may come from ditches or road crossings but contribute relatively little to the total sediment flux in the Mainstem. Tributary 1 contributed less than 0.5% of the yearly sediment flux at km 6. In order to protect water quality in these streams specific attention should be paid to ditches that drain into small streams.

Monthly sediment fluxes were consistently high during fall months (September – November). As alternative water reservoirs may be strained from summer depletion and usage, high sediment fluxes and turbidity values in fall likely pose the greatest threat to drinking water resources in the Honna River. Relatively low sediment concentrations, associated with low rainfall, suggest spring will not likely result in many sediment related problems. However turbidities larger than 10 NTU still occurred between 2 and 14% of the time during this period.

### ***5.3 Total road derived sediment volume***

A WQEE (Water Quality Effectiveness Evaluation) assessment, which estimates the contribution of fine sediment to a stream network as a result of forest operations on an annual basis, was completed for the portion of the Queen Charlotte Mainline Forest Road South with the potential to deliver sediment to the Honna River. This estimate was compared to estimates based on the rainfall simulation and river monitoring results.

The WQEE estimated volume of sediment generated from the Mainline was 1.4 times the estimated volume of sediment based on the rainfall simulation results. The yearly sediment flux in the Honna River was an order of magnitude larger than the estimated volume of sediment generated by the Queen Charlotte Mainline Forest Road

South that is expected to reach the Honna River. Although the Mainline contributed significant amounts of sediment to the Honna River, other sediment sources were dominant in the Honna River.

WQEE results and river monitoring results both show the dominant sediment sources are located above km 6 of the Queen Charlotte Mainline Forest Road South. Future road and ditch improvement projects should focus on sections north of km 6 because this section of the road may deliver a significant amount of sediment to the Honna River. These results are in agreement with Bruce and Chatwin (1987, 1988) who also found the main sediment sources along the Queen Charlotte Mainline Forest Road South were above km 6, specifically around km 7.5.



## WORKS CITED

- Akay, A.E., Erdas, O., Reis, M., Yuksel, A., 2008. Estimating sediment yield from a forest road network by using a sediment prediction model and GIS techniques. *Building and Environment* 43, 687-695.
- Amman, J.R., 2004. Sediment production from forest roads in the upper Oak Creek Watershed of the Oregon Coast Range. MSc. Thesis, Oregon State University.
- Arnaez, J., Larrea, V., Ortigosa, L., 2004. Surface runoff and soil erosion on unpaved forest roads from rainfall simulation tests in northeastern Spain. *Catena* 57, 1-14.
- Beschta, R.L., 1978. Long-term patterns of sediment production following road construction and logging in the Oregon Coast Range. *Water Resources Research* 14, 1011-1016.
- Bilby, R.E., 1985. Contributions of road surface sediment to a western Washington stream. *Forest Science* 31, 827-838.
- Bilby, R.E., Sullivan, K., Duncan, S.H., 1989. The generation and fate of road-surface sediment in forested watersheds in southwestern Washington. *Forest Science* 35, 453-468.
- Blanchard, D.D., 1953. Raindrop size distribution in Hawaiian rains. *Journal of Meteorology* 10, 457-473
- Bruce, P.G., Chatwin, S.C., 1988. Honna River - Mainline sediment yield study II. Land Use Planning Advisory Team, MacMillan Bloedel Limited, Nanaimo.
- Bruce, P.G., Chatwin, S.C., 1987. Honna River - Mainline sediment yield study. Land Use Planning Advisory Team, MacMillan Bloedel Limited, Nanaimo.
- Croke, J.C., Mockler, S., Hairsine, P.B., Fogarty, P., 2006. Relative contributions of runoff and sediment from sources within a road prism and implications for total sediment delivery. *Earth Surface Processes and Landforms* 31, 457-468.
- Croke, J.C., Mockler, S., Fogarty, P., Takken, I., 2005. Sediment concentration changes in runoff pathways from a forest road network and the resultant spatial pattern of catchment connectivity. *Geomorphology* 68, 257-268.
- DeBoer, D.W., Monnens, M.J., Kincaid, D.C., 2001. Measurement of sprinkler droplet size. *Applied Engineering in Agriculture* 17, 11-15.
- Dingman, S.L., 2009. *Suspended-sediment concentration and load. Fluvial Hydraulics*, Oxford University Press Inc. New York, p. 492.
- Dobson Engineering Ltd., 1996. Honna River Watershed, results of the coastal watershed assessment procedure. Kelowna, 550-604.

- Egan, B., Izard, D., Fergusson, S., 1999. The ecology of the Coastal Western Hemlock zone. B.C. Ministry of Forests, Research Branch, Victoria.
- Eigel, J.D., Moore, I.D., 1983. A simplified technique for measuring raindrop size and distribution. *Transaction of the American Society of Agricultural Engineers* 26, 1079-1084.
- Fahey, B.D., Coker, R.J., 1992. Sediment production from forest roads in Queen Charlotte Forest and potential impact on marine water-quality, Marlborough Sounds, New-Zealand. *New Zealand Journal of Marine and Freshwater Research* 26, 187-195.
- Fahey, B.D., Coker, R.J., 1989. Forest road erosion in the granite terrain of Southwest Nelson, New Zealand. *Journal of Hydrology (N.Z.)* 28, 123.
- Fernandez-Raga, M., Fraile, R., Keizer, J.J., Varela Teijeiro, M.E., Castro, A., Palencia, C., et al., 2010. The kinetic energy of rain measured with an optical disdrometer: An application to splash erosion. *Atmospheric Research* 96, 225-240.
- Floyd, W., 2008. Stream crossing sediment delivery assessments in Russell Creek Watershed: the development of a coastal water quality indicator. BC Ministry of Forest and Range, Nanaimo.
- Foltz, R.B., 1996. Traffic and no-traffic on an aggregate surfaced road: sediment production differences. *Proceedings of the Seiman on Environmentally Sound Forest Roads and Wood Transport*, 17-22 June, 1996, Sinaia, Romania.
- Fransen, P.J.B., Phillips, C.J., Fahey, B.D., 2001. Forest road erosion in New Zealand: Overview. *Earth Surface Processes and Landforms* 26, 165-174.
- Gippel, C.J., 1995. Potential of turbidity monitoring for measuring the transport of suspended-solids in streams. *Hydrological Processes* 9, 83-97.
- Haggart, J.W., 2004. Geology, Queen Charlotte Islands, British Columbia. Geological Survey of Canada, Open File 4681.
- Hairsine, P.B., Rose, C.W., 1992. Modeling water erosion due to overland-flow using physical principles 1. Sheet flow. *Water Resources Research* 28, 237-243.
- Harikumar, R., Sampath, S., Kumar, V.S., 2010. Variation of rain drop size distribution with rain rate at a few coastal and high altitude stations in southern peninsular India. *Advances in Space Research* 45, 576-586.
- Harrison, K., Perry, C., 2007. Evaluating and interpreting application uniformity of center pivot irrigation systems. The University of Georgia, College of Agriculture and Environmental Science, Circular.
- Hudson, N.W., 1993. Field measurement of soil erosion and runoff. Silsoe Associates, Ampthill, Bedford.
- Hudson, R.H., 2001. Interpreting turbidity and suspended sediment measurements in high-energy streams in coastal British Columbia. BC Ministry of Forests, Nanaimo, B.C. Vancouver Forest Region Technical Report TR-08.

- Luce, C.H., 2002. Hydrological processes and pathways affected by forest roads: what do we still need to learn? *Hydrological Processes* 16, 2901-2904.
- Luce, C.H., Black, T.A., 2001. Effects of traffic and ditch maintenance on forest road sediment production. 2001. Proceedings of the Seventh Federal Interagency Sedimentation Conference, March 25-29, 2001, Reno Nevada.
- Luce, C.H., Black TA, 1999. Sediment production from forest roads in western Oregon. *Water Resources Research* 35, 2561-2570.
- Maloney, D., Chatwin, S., Carver, M., Carson, B., Beaudry, P., 2009. Protocol for evaluating the potential impact of forestry and range use on water quality (water quality routine effectiveness evaluation). Forest and Range Evaluation Program, B.C., Ministry of Forest and Range and B.C. Ministry of Environment, Victoria, BC.
- Marquis, P., 2008. Watershed measurement methods and data limitations: Physical water quality. in: Pike, R.G., editor. *Compendium of forest hydrology and geomorphology in British Columbia*. B.C. Ministry of Forests and Range Research Branch, Victoria, BC, 553-638.
- Marquis, P., 2005. Turbidity and suspended sediment as measures of water quality. *Watershed Management Bulletin* 9, 21.
- Mason, B.J., Andrews, J.B., 1960. Drop-size distributions from various types of rain. *Quarterly Journal of the Royal Meteorological Society* 86, 346-353.
- Meidinger, D., Pojar, J., 1991. *Ecosystems of British Columbia*, special report series 6. Ministry of Forest, Research Branch, Victoria, BC.
- Meyer, L.D., 1994. Rainfall simulators for soil erosion research. in: Lal, R., editor. *Soil erosion research methods*. second ed., Soil and Water Conservation Society. Ankeny, IA p. 83-104.
- Murray, W.A., 1964. Rainfall intensity-duration-frequency maps for British Columbia. Department of transport, Meteorological Branch.
- Niu, S., Jia, X., Sang, J., Liu, X., Lu, C., Liu, Y., 2010. Distributions of raindrop sizes and fall velocities in a semiarid plateau climate: Convective versus stratiform rains. *Journal of Applied Meteorology and Climatology* 49, 632-645.
- Phillips, R.W., Lantz, R.L., Claire, E.W., Moring, J.R., 1975. Some effects of gravel mixtures on emergence of coho salmon and steelhead trout fry. *Transactions of the American Fisheries Society* 104, 461-466.
- Pike, R.G., Feller, M.C., Stednik, J.D., Rieberger, K.J., Carver, M., 2010. Water quality and forest management. in: Pike, R.G., Redding, T.E., Moore, R.D., Winker, R.D., Bladon, K.D., editors. *Compendium of forest hydrology and geomorphology in British Columbia*. B.C. Ministry of Forest and Range, Forest Science Program. Victoria, B.C, p. 401-440.
- Proffitt, A.P.B., Rose, C.W., 1991. Soil-erosion processes 1. the relative importance of rainfall detachment and runoff entrainment. *Australian Journal of Soil Research* 29, 671-683.

- Ramos-Scharron, C.E., MacDonald, L.H., 2007. Runoff and suspended sediment yields from an unpaved road segment, St John, US Virgin Islands. *Hydrological Processes* 21, 35-50.
- Reid, L.M., Dunne, T., 1984. Sediment production from forest road surfaces. *Water Resources Research* 20, 1753-1761.
- Renard, K.G., 1985. Rainfall simulation and USDA erosion research: History, perspective, and future. in: *Proceedings of the Rainfall simulator workshop*, Jan. 14-15, 1985. Tucson, Arizona. Society for Range Management.
- Roberts, R.G., Church, M., 1986. The sediment budget in severely disturbed watersheds, Queen Charlotte Ranges, British Columbia. *Canadian Journal of Forest Research* 16, 1092-1106.
- Rodgers, M., Hayes, G., Healy, M.G., 2009. Cyclic loading tests on sandstone and limestone shale aggregates used in unbound forest roads. *Construction and Building Materials* 23, 2421-2427.
- Sheridan, G.J., Noske, P.J., 2007. Catchment-scale contribution of forest roads to stream exports of sediment, phosphorus and nitrogen. *Hydrological Processes* 21, 3107-3122.
- Smith, J.A., Hui, E., Steiner, M., Baeck, M.L., Krajewski, W.F., Ntelekos, A.A., 2009. Variability of rainfall rate and raindrop size distributions in heavy rain. *Water Resources Research* 45, W04430, doi:10.1029/2008WR006840.
- Spinelli, R., Marchi, E., 1996. A literature review of the environmental impacts of forest road construction. *Proceedings of the Seiman on Environmentally Sound Forest Roads and Wood Transport*, 17-22 June, 1996, Sinaia, Romania.
- Tappel, P.D., Bjornn, T.C., 1983. A new method of relating size of spawning gravel to salmonid embryo survival. *North American Journal of Fisheries Management* 3, 123-135.
- Tokay, A., Bashor, P.G., Habib, E., Kasparis, T., 2008. Raindrop size distribution measurements in tropical cyclones. *Monthly Weather Review* 136, 1669-1685.
- van Rijn, L.C., 1994. *Principles of fluid flow and surface waves in rivers, estuaries, seas, and oceans*. second ed. Aqua Publications, pp. 400, Netherlands.
- Whiting, P.J., Dietrich, W.E., 1990. Boundary shear-stress and roughness over mobile alluvial beds. *Journal of Hydraulic Engineering – ASCE* 116, 1495-1511.